October 2020 Volume 3, Issue 1
www.pmf.ni.ac.rs/chemianaissensis

Chemia Naissensis

ISSN 2620-1895

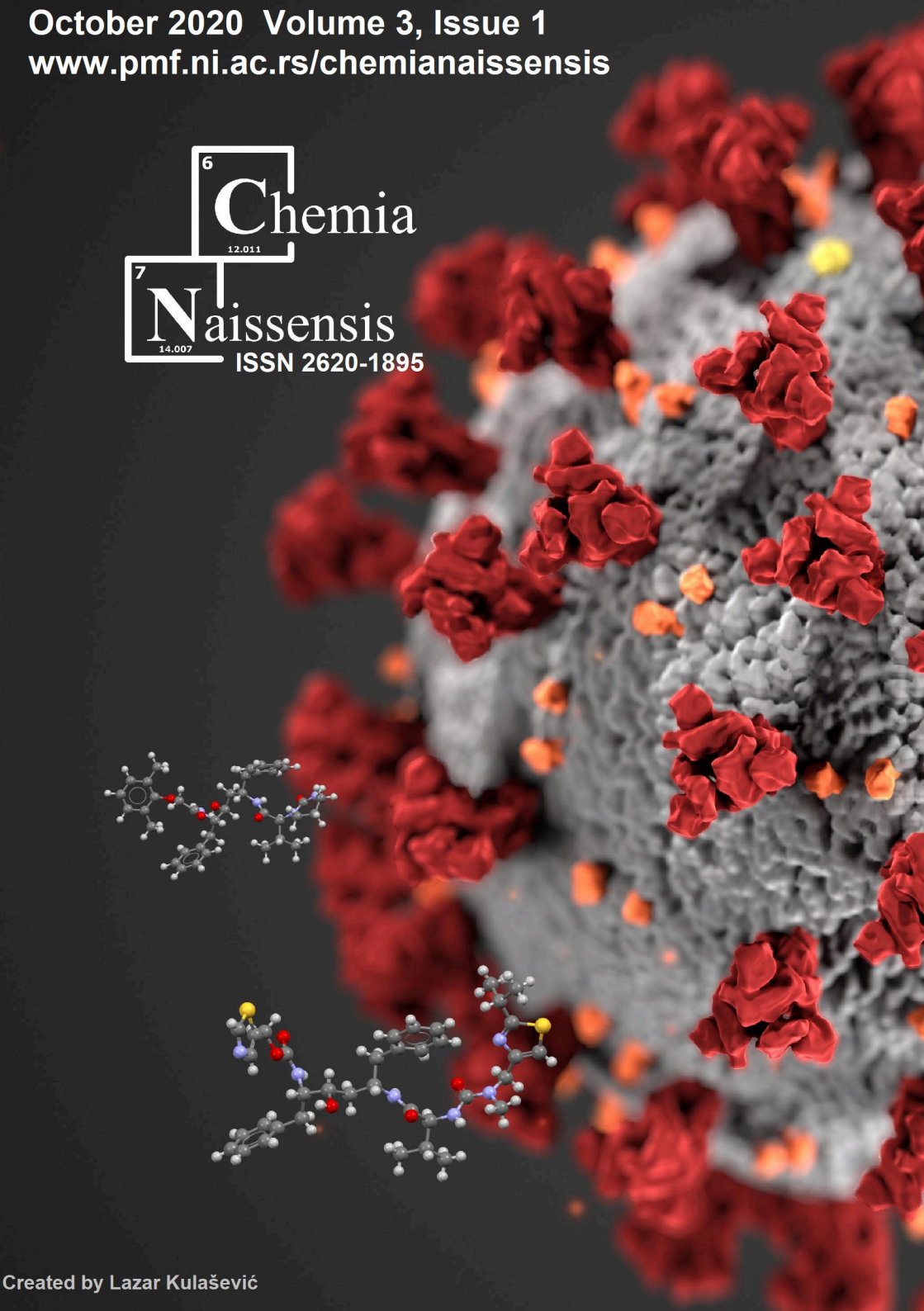

Created by Lazar Kulašević

CONTENT

Reviews

Research articles

Azhar Abbas, Hatem M. A. Amin, Muhammad Akhtar, Muhammad A. Hussain, Christopher Batchelor-McAuley, Richard G. Compton

Popular Scientific Article

Violeta Ivanović, Miroslav Rančić, Biljana Arsić, Aleksandra Pavlović

Android applications as an additional tool in inorganic chemistry teaching: A short-review

Marina V. Blagojević[1], Danijela A. Kostić[1*], Maja N. Stanković[1], Dragan M. Đorđević[1], Vladimir D. Dimitrijević[1], Milica G. Nikolić[1], Nenad S. Krstić[1]

1-University of Nis, Faculty of Sciences and Mathematics, Department of Chemistry, Visegradska 33, 18000 Nis, Serbia

Marina V. Blagojević: marina.blagojevic2631@gmail.com

Danijela A. Kostić: danijelaaakostic@yahoo.com

Maja N. Stanković: majastan@gmail.com

Dragan M. Đorđević: dragance73@yahoo.com

Vladimir D. Dimitrijević: vladimir15041987@gmail.com

Milica G. Nikolić: milica.nikolic.1990@gmail.com

Nenad S. Krstić: nenad.krstic84@yahoo.com

ABSTRACT

The concept of mobile access to information is present in all aspects of society today and it constitutes the digital need of the individual. The aim of this paper is to provide a brief overview and systematization of various easily accessible android applications for mobile phones and tablets that would promote proper understanding of chemical concepts, as well as facilitate the acquisition of knowledge in chemistry by students in both primary and secondary schools. Mobile learning has many advantages such as diversity, entertainment, communication, interactivity, but also learning completely adjusted to the needs of the individual regardless of place and time. The use of these tools has a great impact on a different approach in teaching chemistry and contributes to improving of the final learning outcomes. That is why it is important for every teacher to integrate technology into pedagogy and use it to promote student-centered learning.

Keywords: android applications, mobile learning, teaching tools, interactivity

* Corresponding author: Danijela Kostic - danijelaaakostic@yahoo.com
University of Nis, Faculty of Sciences and Mathematics, Department of Chemistry, Visegradska 33, 18000 Nis, Serbia

INTRODUCTION

Chemistry is largely an abstract science. Years back, this subject was not a favorite among students, and there are numerous factors for that: abstractiveness, excessive curricula, inadequate textbooks, non-existence or poor equipment of the chemistry cabinet, poor motivation and engagement of teachers and disinterest of students (Ristić and Milošević, 2019).

Previously, classes were traditionally realized through chalk, blackboard and oral lectures.

Science today follows the trends of modern information technologies. Therefore, it is necessary to keep up trends in the field of teaching and knowledge transfer. In order for teaching to be more efficient, a multidisciplinary approach is introduced in its realization. Multimedia teaching tools satisfy modern didactic-methodical principles of teaching.

A form of learning that implies that part of the activities, in addition to the traditional classroom, also takes place on the Internet, is called combined or hybrid teaching. If the teaching material is modified and a learning tool or platform is chosen, students can receive exceptional support during learning. They can access teaching materials and study them further, practice or check the degree of mastery of teaching contents, progressing at their own pace and in accordance with their own abilities. With the help of the Internet, communication and cooperation skills, creativity and knowledge exchange are developed (Priručnik, 2014). This form of e-learning serves as a supplement to classical teaching, not as its substitute.

In the 21st century, the application of PPt in teaching has become widespread. Many studies show that this method has significant advantages over traditional teaching, but also a number of disadvantages (Kostic et al., 2018; Kostic et al., 2011; Zarubica et al., 2012; Nikolic et al., 2014).

In this paper, we will focus only on the application of mobile devices (mobile phones, tablets) in the learning process, the so-called mobile learning (m-learning). This form of learning has advantages, because it does not limit people who learn to sit, for example, in front of a computer, but it is possible to learn anywhere and anytime. This approach was adopted as A3 (abbreviation for "Anywhere, Anytime, Anyplace") (https://en.wikipedia.org/wiki/Android_(operating_system) Access: 20/3/2017).

How much the appearance of mobile devices has affected society positively or negatively in general remains for each individual to conclude. Opinions of teachers and attitudes also differ (O'Bannon and Thomas, 2014).

It is inevitable that the younger generations are increasingly using mobile devices in their daily activities, whether they are used for communication, entertainment or learning. This leads to a number of negative phenomena such as physical inactivity, loss of concentration, non-acceptance in society if the mobile phone is not of a newer generation, *etc*. However, there are also positive aspects of the proper use of mobile devices, such as: adoption of new technologies, learning new contents or good information (Heflin et al., 2017).

At the moment, the most widespread phones in the world are with the Android operating system (Figure 1). With the appearance of the Android OS in 2010, the representation grew from 33.2% in 2011 to 86.8% in 2016 (İlhan, 2016). iOS is the mobile operating system of Apple. It was originally developed for the iPhone, and later for the iPod, iTouch, iPad and Apple TV. The market for Apple devices fluctuated between 15% and 12.5%. Apple does not allow the iOS operating system to be run on the third-party hardware. From September 1, 2010, Apple's App Store service contains more than 250,000 iOS applications, which have been downloaded more than 6.5 billion times (https://prezi.com/p/ekhzkjtnuyg5/aplikacije-za-iphone/).

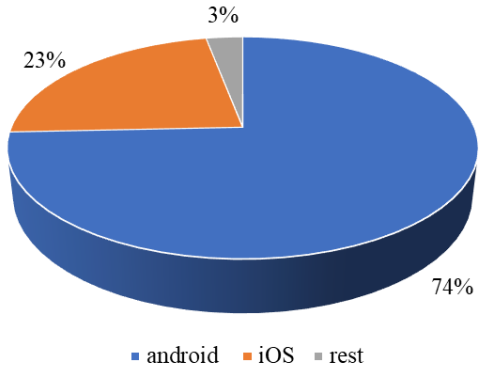

Figure 1. The share of operating systems in mobile phones in the world

As the android operating system is more represented in this paper, we provide an overview of selected applications that can be used as additional (interactive) tools in the teaching of inorganic chemistry. By using omnipresent and easily accessible android applications as additional tools in teaching chemistry, the acquisition of knowledge in chemistry by pupils in both primary and secondary schools can be facilitated and improved.

As corresponding applications are not always available (free of charge), teachers experiences difficulties to assess their characteristics solely on the basis of reviews. Therefore, there is a need to create specific mobile learning applications, and in addition, empowering educators to create their own mobile applications is likely to lead to the integration of mobile technology into teaching.

With the appearance of the Internet and the evolution of smartphones and tablets, pupils /students have instant access to a wealth of information. Of course, adopting integrative technology-based technology strategies is a major challenge for both teachers and students(Williams et al., 2011).

Hew and Brush (2007) pointed out that the lack of resources and knowledge and skills on how to make the best use of these technologies are some of the main obstacles. However, continuous education in this area, activity of educators and engagement of students can lead to significant results.

Data collected during several semesters of using mobile applications in teaching showed that the interest of students in chemistry has increased significantly which has led to better results in terms of knowledge and its application (Naik et al., 2015).

Android applications as educational tool

Technology such as iOS and Android based mobile apps can be used as an interactive educational tool, which allows a dynamic learning experience that directly benefits students. The mobile apps can be used in a General Chemistry course to teach the subjects of atoms, elements and the periodic table. Because these apps are interactive, they enhance student engagement and spark interesting learning of these fundamental concepts (Libmanet and Huang, 2013).

Google play store offers many interesting apps in chemistry, but here it will be presented selected apps that can be used in teaching of inorganic chemistry. They could be grouped into a dozen categories based on the content they offer and they are: Periodic table of elements, complete applications, applications with video content, chemical reactions, 3D display, minerals, electronic configuration, equalization of equations of chemical reactions, solutions, notes. This is not a sharp division of applications, because they enable a large number of functions, but there is one representative from each.

The described applications can be accessed easily *via* a mobile phone from the Google Play Store or using the QR codes given at the end of the description of each application.

Periodic table of elements: Merck PTE

The "Merck PTE" application enables the user to understand the complex science of chemistry and provides quick access to all the necessary information. Whether it is a pupil or a teacher, a student or a professor, an amateur or an expert, a hobbyist or a technician, "Merck PTE" provides broader information about each element of the Periodic Table. The periodic table of elements is shown in a digital form, which can be seen in Figure 2a, where information about each element can be found immediately, calculations can be made, such as calculating the molar mass of any compound, comparing elements in terms of atomic gradation, electronegativity and many other features. The app also contains historical facts and that is why it can be very entertaining.

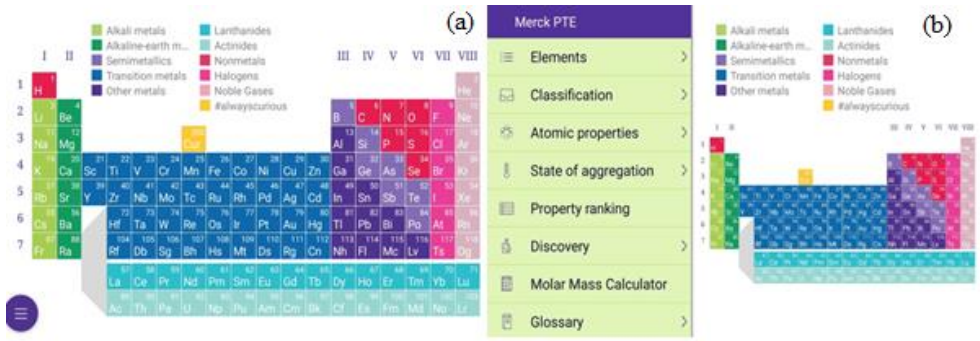

Figure 2. (a) The initial interface of the "Merck PTE" application and (b) the appearance of the application menu

By clicking on any element of the Periodic Table, an image of that element appears with general information about it. The application menu (Figure 2b) is quite simple, clear and provides a large number of options:

1) *the possibility of classification according to different criteria.* With this application it is possible to classify elements according to which group they belong to (metals, non-metals, *etc.*) (Figure 3a), according to radioactivity or percentage share in the Earth's crust;
2) *displaying the properties of atoms.* We can get information about the atomic radii of the elements (Figure 3b), values for electronegativity (according to the Allred-Rochow and Pauling scale), ionization energy and relative atomic mass;
3) *state of aggregation of the elements.* This application provides information about the state of aggregation of the element at a certain temperature, which is adjusted by moving the cursor (with a finger) on the temperature scale (Figure 3c);
4) *historical data about the element.* Merck PTE provides data on when an element was discovered as well as which scientist discovered it (Figure 3d);
5) *calculating the molar mass of the compound* (Figure 3e);
6) *explanation of chemical terms.* This application also offers a list of terms in alphabetical order that occur using the same, as well as an explanation for each of them (Figure 3f).

The internet is not required for this application to work; it works in offline mode, which can be an advantage in some situations. It has dynamic design, economical handling access rights, an interactive operating system, as well as smart controls and numerous choices.

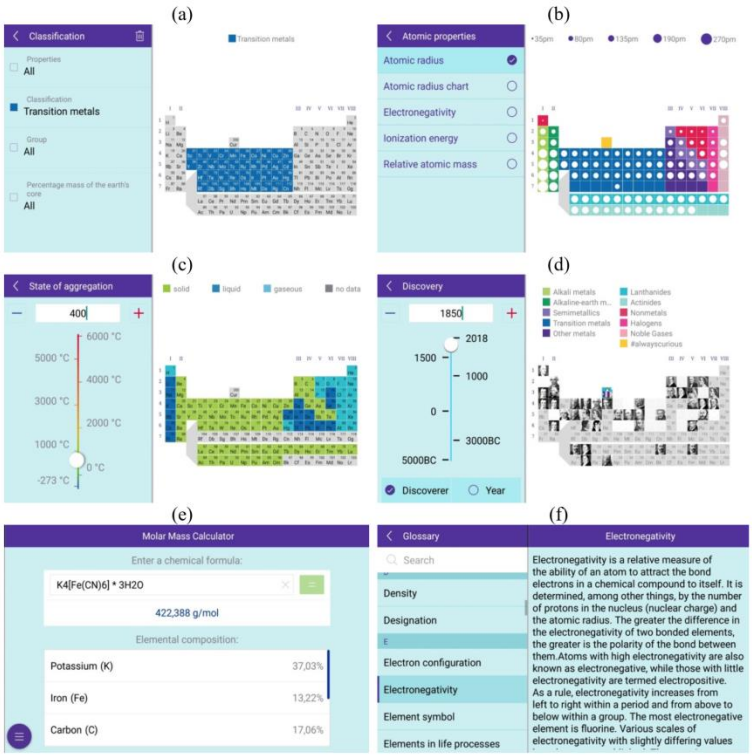

Figure 3. Examples of user interface: (a) transitional metals, (b) relation of atomic radius of atoms, (c) state of aggregation of elements at a temperature of 400℃, (d) elements discovered until 1850, (e) calculating the molar mass of the compound, (f) explanation of the term electronegativity. The Merck PTE application can be easily accessed by scanning the QR code from Figure 4.

Figure 4. QR code for Merck PTE app

Complete apps: Chemical suite free

The initial interface of this application is the Periodic Table of the Elements (Figure 5).

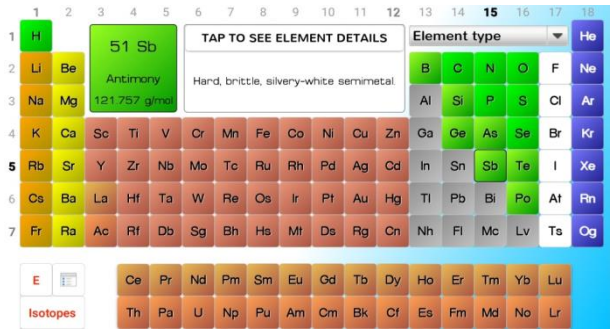

Figure 5. The initial interface of the app Chemical suite free

Each element is described with more than 30 characteristics, including general and physical properties (Figure 6a), history, *etc*. This application also provides information on the isotopes (natural, radioactive) that are characteristic of each element.

In an easy and simple way, this application allows the calculation of the molecular weight of the compound (Figure 6b), then it has a list of chemical and physical constants that can be searched using the search option (Figure 6c) and they are divided by scientific fields. Each constant is defined by a numerical value and the unit in which it is expressed, with the existence of a unit converter (Figure 6d). Through this application chemical reactions can be equalized, the search of elements in a given range of values of relative atomic mass can be performed (Figure 6e), you can apply the equation of state of an ideal gas with conversion (pV = nRT) and the trend of changing a certain element property can be graphically displayed (relative atomic mass, ionization energy density, atomic, ionic, covalent radius) (Figure 6f).

Figure 6. Overview of application functions: (a) characteristics of phosphorus atoms, (b) calculating the molecular weight of the compound P_2O_5, (c) Planck's constant, (d) unit conversion, (e) elements of relative atomic masses in the range from 5 to 10 and (f) graphical representation of the first ionization energy of the elements of the Periodic Table

Chemical Suite free application can be easily accessed by scanning the QR code from Figure 7.

Figure 7. QR code for Chemical Suite free app

Video: MEL chemistry

"MEL Chemistry" provides an amazing experience of performing experiments. Namely, there is a large number of experiments here the conduct of which was recorded by a camera.

The experiments are listed on the initial interface where each of them has an appropriate creative name. By clicking on one of them, the application offers new possibilities such as information on safety, expected result, waste disposal, as well as a scientific explanation of a given experiment.

Each experiment was characterized by a certain degree of difficulty, danger and duration (Figure 8a). The application can become a personal assistant to the user in performing experiments because it leads them step by step towards the ultimate goal of the experiment and also provides help in solving problems. This application can be used at home because children actually want real chemistry, not toys- "plastic accessories" to play with. Real chemistry means real opportunity, real responsibility, but also real danger. There is the possibility of ordering sets with utensils and dishes on the *MEL Science* website.

The Mel Science kit is organized into several packages. The first package is a starter kit that contains all the equipment needed for future experiments. The set includes a cardboard set with VR glasses, glass instruments, telephone stand, goggles and much more. The second and third packages are systematized according to the topics they deal with. Each package has enough material to do (and repeat) several experiments on the same topic. The kits are marked with warning labels and safety instructions for security reasons.

In addition, the application offers the ability to detect the real structure of substances found in the environment and visualization of molecules in 3D (Figure 8b). *What does kitchen salt actually look like at the molecular level?* "MEL Chemistry" will show the structure of these and hundreds of other molecules including, for example, sulfuric acid, hydrochloric acid, sodium carbonate, sodium bisulfate, potassium permanganate, calcium hydroxide, *etc*. In addition, the molecules of new compounds are constantly updated on this list.

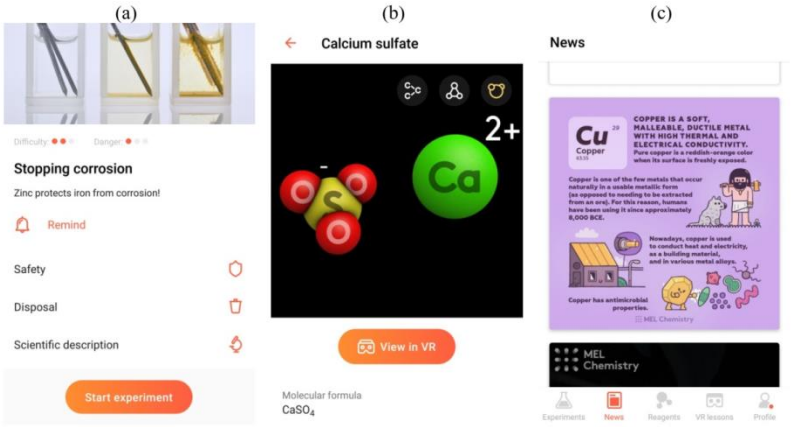

Figure 8. Overview of application functions: (a) properties of the corrosion inhibition experiment, (b) 3D structure of CaSO4 molecules and (c) interesting information about copper

This application also offers other options such as "news" with many interesting facts from the world of chemistry (Figure 8c); MEL code reader by scanning the substance bottle, using the phone to detect the

molecules it contains; VR experiences that gain a new level of understanding science. There are over 80 different VR classes and tests that cover the standard school chemistry curriculum. The only deficiency of this application can be the lack of search option for experiments, which can make it a little difficult to use. MEL application can be easily accessed by scanning the QR code from Figure 9.

Figure 9. QR code for MEL chemistry app

Beaker mix chemicals

The "Beaker" application has the role of a virtual chemical laboratory, where everyone can try themselves in the role of a scientist. A mobile phone becomes a glass that can be held, shaken, heated, covered, and it can contain various substances. You can do experiments with more than 150 chemicals. The app offers acids, salts, bases as well as atoms and molecules of elements in the appropriate state of aggregation, arranged in alphabetical order (Figure 10a).

This app offers interactive options during the experiments as well:

1) adding: clicking on any of the chemicals, they go to the beaker. If there are more, in addition to the visual and sound experience, their reaction is accompanied by chemical equations, molecular formulae of the product and the current temperature (° C) of the reaction in the beaker (Figure 10b);
2) heating (burner): dragging a finger from the lower right to the lower left corner of the screen turns on the burner;
3) shaking: to speed up the reaction (Figure 10c);
4) covering the beaker (lid): dragging a finger from the upper right to the upper left corner of the screen covers the beaker;

The application also provides information about the density, molar mass, mass concentration of all offered substances represented by both the molecular formula and the name. The Air Mick option requires internet connection and geolocation services, while other possible options (cooling, mixing, and separation) need to be paid for, so unfortunately the application is not completely free.

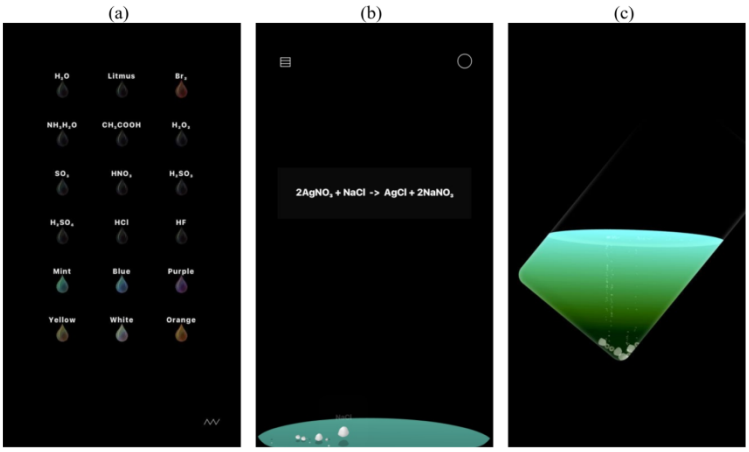

Figure 10. Examples of application user interface: (a) some of the substances to use, (b) sedimentation of AgCl and (c) mobile phone manipulation

The dark background of the application makes it easier to monitor the course of reactions, as well as all chemical and physical phenomena, but it can also be changed by the color of your choice. By using this application, real work with toxic and dangerous substances is excluded, but the same or even better effect of students' acquiring new concepts and knowledge is achieved. There are no more worries about rough reactions because they are happening on the screen. This app is a solution for schools which have no laboratories or whose laboratories are not equipped well enough. As the safety and health of the participants in the laboratory is a priority, this app can be an extremely useful teaching tool in schools and colleges. Beakers Mix Chemicals application can be easily accessed by scanning the QR code from Figure 11.

Figure 11. QR code for Beakers Mix Chemicals app

3D: Virtual orbitals 3D chemistry

It is very difficult to understand atomic orbitals drawn on the blackboard or a piece of paper (2D view). The "Virtual Orbitals" app provides better orbital visualization in three-dimensional (3D) form and helps to understand them (Figure 12a). This app provides interactive manipulation with selected atomic orbitals "finger touch and move"; the way the orbital can be seen from all aspects (3D view) enables students' visual understanding of the concept and appearance of the orbital.

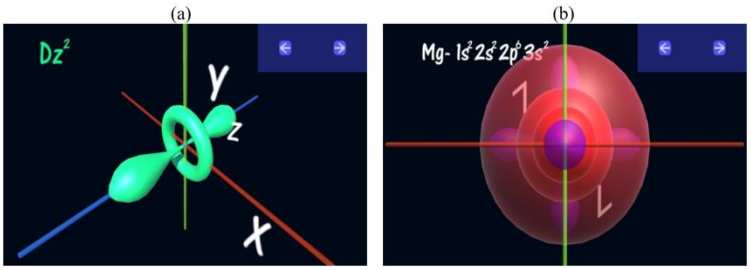

Figure 12. Examples of user interface: **(**a) orbital d_{z2} and (b) atomic orbitals of magnesium

This application includes the following atoms with their electronic configuration: hydrogen, helium, lithium, boron, carbon, oxygen, neon, sodium, magnesium (Figure 12b), silicium, potassium, argon, calcium, zinc, iron, *etc*. The Virtual orbitals 3D chemistry app can be easily accessed by scanning the QR code from Figure 13.

Figure 13. QR code for Virtual orbitals 3D chemistry app

Minerals

As its name suggests, the app presents basic concepts about minerals. The application also offers instructions for macroscopic and microscopic determination of some minerals.

This application provides a spreadsheet of the most important information about each mineral: group, cristal system, the class of symmetry, the mode of appearance, firmness, solidity, colour, genesis, the use, the deposits (Figure 14a).

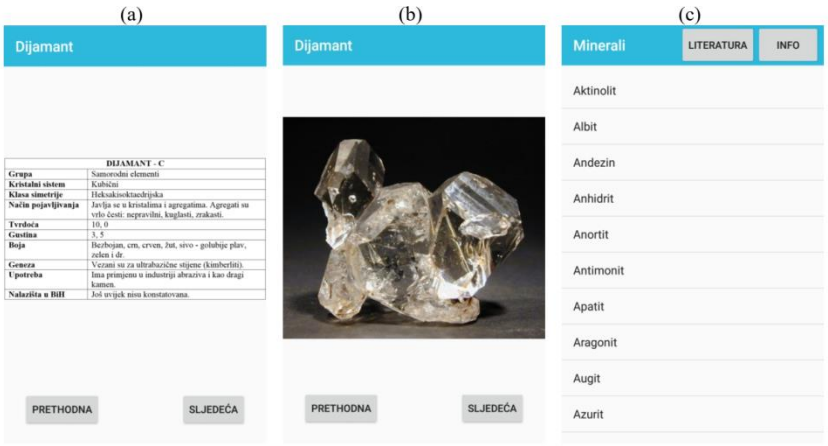

Figure 14. Examples of user interface: (a) characteristics of the diamond, (b) the appearance of a diamond and (c) the list of offered minerals

The app is in Serbian which highly facilitates its use. The defect of the app is that there are not so many images and their quality is not at high level (Figure 14b). There is no search option either but all the minerals are listed in alphabetical order (Figure 14c). The Minerals app can be easily accessed by scanning the QR code from Figure 15.

Figure 15. QR code for Minerals app

Electron configuration

Writing an electronic configuration of elements is often an unsolvable problem for students. However, using this application can make it much easier.

"Electron configuration" is an application designed for students, but it is also useful for enthusiasts in chemistry, because it is very easy to use it, it provides help as well as checkout in learning. It is based on a simple and nice user interface. The app can be used in two ways: selecting elements from a ready-made list (Figure 16a) or selecting one specific element in the search (Figure 16b). Further information about the element is available *via* the “Google” icon which leads to Google search engine (Figure 16c).

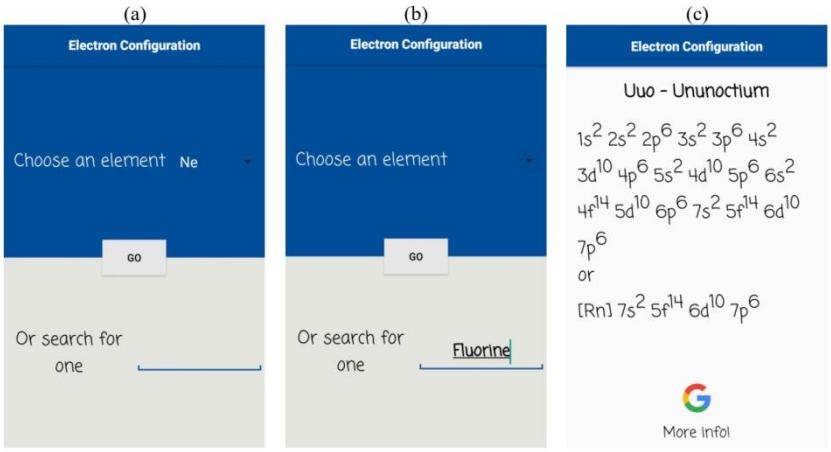

Figure 16. Examples of user interface: (a) selecting elements from the list, (b) search for a specific element and (c) user interface

The Electron configuration app can be easily accessed by scanning the QR code from Figure 17.

Figure 17. QR code for Electron configuration app

Chemical balancer

The "Chemical Balancer" application enables the equalization of chemical reaction equations. The use involves entering the molecular formulae of the reactants and products and then by clicking on "balance" the equalization process is performed. The result is displayed in a very short time (Figure 18a). It is suitable for any chemical equation, as long as it is not written in ionic form.

It is a very useful tool for chemistry students, as well as for teachers, researchers, analysts and pharmacists. "Chemical Balancer" is a free and very easy to use application. This application can be used to check the accuracy of the examples done during the exercise. The Electron configuration app can be easily accessed by scanning the QR code from Figure 18b.

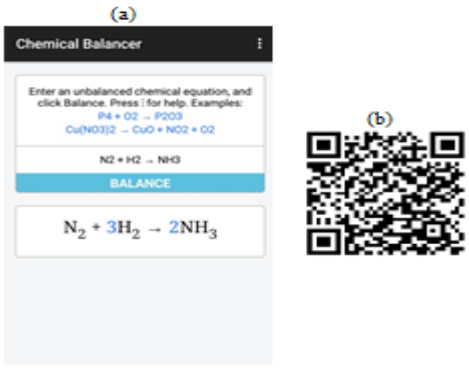

Figure 18. (a) User interface layout (b) QR code for Electron configuration app

Solution calculator lite

"Solution calculator lite" is a practical and very simple app for both chemistry students and researchers/ scientists working in the laboratory for chemistry, biochemistry or biology.

This application offers the following features:

1) *suitable calculator for making chemical solutions.* In the "Make" section, it is necessary to enter the required concentration, volume of solution and molar mass of the compound. Clicking on the "calculate" option, the result is obtained, *i.e.*, the mass of the compound necessary for the required concentration of a solution. The app remembers all previous calculations that are easily visible. Each value can be expressed in a pair of offered units (Figure 19a). It is also possible to calculate the dilution of the solution using the stock solution in the "dilute" section. The app helps to quickly determine how much chemical / stock solution is needed (Figure 19b). This way there is no waste of time and all attention is focused on working in the laboratory.
2) *calculating the molecular weight (MW) of common chemicals in the laboratory.* This is done by entering the molecular formula of the compound (Figure 19c), while for some substances listed in alphabetical order, molar masses (ATP, EDTA) have already been introduced.
3) *provides detailed information about each of the 118 elements,* such as: atomic and mass number, position determined by a group and period, original name and the year of discovery, density, melting point, electronic configuration, but also a suitable description of that element.

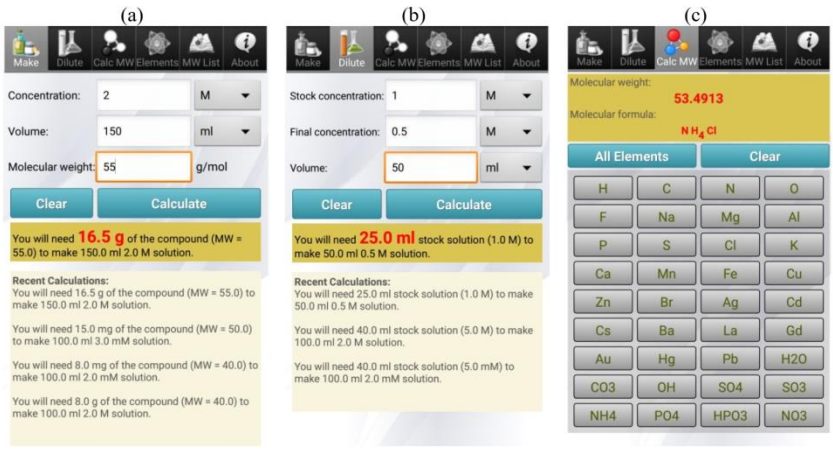

Figure 19. Functions of the app: (a) making a solution, (b) dilution of the solution, (c) calculating the molecular weight

The Solution calculator lite app can be easily accessed by scanning the QR code from Figure 20.

Figure 20. QR code for Solution calculator lite app

CHEMISTRY NOTES Offline

Chemistry Notes

The "Chemistry Notes" application is specially designed for high school students and can be used for practice and preparation of control tasks. This app contains notes that are grouped into 45 chapters and some of them are: atoms and molecules, the structure of atoms, acids, bases and salts, metals, *etc*. A graphic representation of some of the chapters can be seen in Figure 21.

Irregular order of chapters as well as the lack of search option can be suggested as disadvantages, but this is compensated by very concise notes, accompanied by Figures and examples. The app is easy to use and does not take up much memory space on a mobile phone and it can be used in an offline mode. This application is a good IT tool and repetitorium.

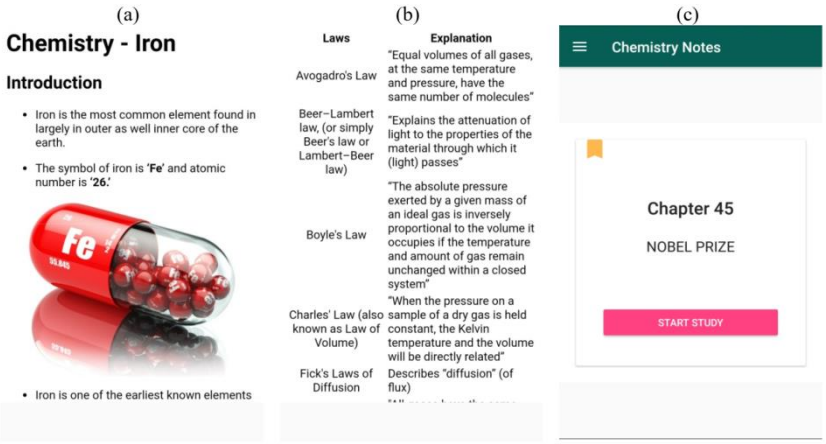

Figure 21. Chapter: (a) Iron, (b) Chemical laws and (c) Nobel Prizes

The Chemistry notes app can be easily accessed by scanning the QR code from Figure 22.

Figure 22. QR code for Chemistry notes app

The following applications are not free of charge and that is why the scope of reviews has been reduced. However, they can make a significant contribution as additional tools in teaching inorganic chemistry.

Chemist virtual lab

The "Chemist virtual lab" application is a virtual chemical laboratory. It is great for various experiments, research, learning or just for playing.

Laboratory utensils and accessories are on a virtual shelf; 17 basic laboratory elements that are sufficient for all manipulations in the laboratory: glasses, Erlenmeyer flasks, round bottom flasks, a test tube, a reagent bottle, a ring stand, a tripod, an alcohol burner, a porcelain cup, a watch glass, a funnel, extensions and a plug. Equipment also includes a paper indicator, a thermometer, a glass rod, a pipette and matches and they can be selected from the drop-down menu. Clicking on a selected dish, it moves to the desktop where a large number of dishes can be found at the same time with an arrangement that suits the user (Figure 23a).

The application offers more than 200 inorganic and about 60 organic chemical reagents. This way, the needs of both primary and secondary school students, but also students at the faculty are included. Chemicals are grouped into 4 categories: mixtures, solids, liquids, gases and all of them are on the virtual

shelf in reagent bottles, displayed in the appropriate state of aggregation and color. The "search" option will speed up finding the required reagent.

In order to see the physical and chemical properties: molecular weight, volume, temperature, concentration, reactions with other substances, you can click on a chemical substance (Figure 23b). By dragging the reagent bottle with the substance to the container, a window appears showing the mass and amount of the substance poured into the container. This way you can see what is happening in the beaker, not only visually, but also in the exact ratio of the reactants.

The course of the experiment is followed by the equation of the chemical reaction that appears in the upper part of the screen (Figure 23c). 6 practical application options can be tried out with one touch and dragging (change of laboratory temperature, adjustment of air composition, time acceleration ...). The experiment can be saved with all the steps that have been done.

Experimenting with different substances is a fun, but sometimes not so safe. However, the application provides the possibility of complete freedom, without fear of cracking the dishes due to some untested reaction or possible injuries. It will make for all the necessary chemicals to be at your fingertips, without previous purchasing; there will never be a mess and possible "explosions" can be stopped at any time. This application helps you gain real experience, like in a real laboratory, because it goes through the whole experimental process, to which excellent visual and sound effects also make a contribution.

The application has passed the security test for viruses and other malicious attacks and contains no threats, so the security of the mobile phone and personal data is ensured. It should be emphasized that the application is not free of charge.

Figure 23. Examples of user interface: (a) working area with laboratory utensils, (b) solid-state substances with characteristics and (c) chemical reaction process

The Chemist virtual lab app can be easily accessed by scanning the QR code from Figure 24.

Figure 24. QR code for Chemist virtual lab app

The following applications are made by "Ajax media tech" on the same principle. Each contains learning, practice and quiz options.

Mole concept in chemistry

"Mole concept" is an interactive application with the help of which students can learn the meaning of the term mole in chemistry in a simple and comprehensive way, as well as formulae for calculating numerical values. It is intended for lower grade students.

The app “Mole concept” is simple to use and it offers three functions:

1) learning- mastering knowledge in an interesting way (Figure 25a),
2) exercising- checking learnt concepts (Figure 25b),
3) quiz- application of acquired knowledge (Figure 25c).

The application contains 3D simulations and videos to make learning the concept of the mole more understandable and easier to learn with minimal effort and long-term memory.

Figure 25. Application functions overview: (a) learning, (b) practice and (c) quiz

The Mole concept in chemistry app can be easily accessed by scanning the QR code from Figure 26.

Figure 26. QR code for Mole concept in chemistry app

Reactivity series of metals

The "Reactivity Series of Metals" application helps students learn all about the reactivity of metals and the various changes that occur during reactions. This application shows a series of reactivity of metals and the most reactive metals, but also chemical reactivity trends in a simple way with interesting "do-it-yourself" activities. Students can research and practice what they have learnt through interesting examples. The application will make learning more interesting through interactive activities, 3D simulations and videos for better understanding of the concepts (Figure 27).

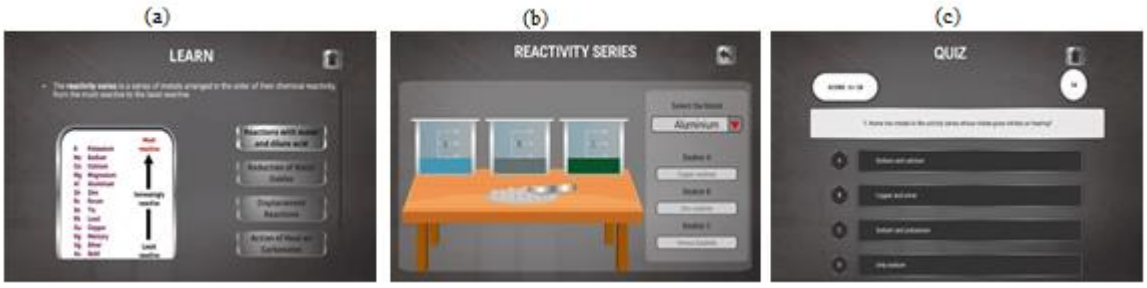

Figure 27. Application functions overview: (a) learning, (b) practice and (c) quiz

The Reactivity series of metals app can be easily accessed by scanning the QR code from Figure 28.

Figure 28. QR code for Reactivity series of metals app

Acids and Bases in Chemistry

The application is based on the concept of acids and bases and their properties, especially chemical ones. It describes in more details the reactions of metals with acids or bases. All differences are in the spreadsheet in order to be better noticed and remembered (Figure 29).

Figure 29. Application functions overview: (a) learning, (b) practice and (c) quiz

The Acid and Bases in Chemistry app can be easily accessed by scanning the QR code from Figure 30.

Figure 30. QR code for Acid and Bases in Chemistry app

Ammonia Structure & Properties

The application describes the structure of ammonia and its properties. The geometry of NH_3 molecules, its physical and chemical properties, as well as the entire procedure of the Haber-Bosch process shown in a Figuresque way are considered (Figure 31). The questions in the "quiz" section are not trivial, but they encourage the user to think.

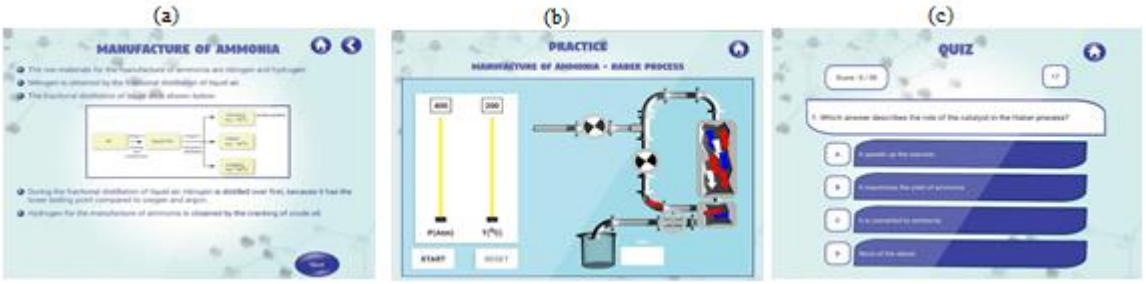

Figure 31. Application functions overview: (a) learning, (b) practice and (c) quiz

The Ammonia structure & properties app can be easily accessed by scanning the QR code from Figure 32.

Figure 32. QR code for Ammonia structure & properties app

Salts in Chemistry

The application is excellent for the teaching unit "Salts". It describes the reaction of salt formation, types of salts (acidic, basic) and NaCl is taken as an example. It is intended for lower grade students who encounter this term for the first time. Spreadsheets, animations and creative illustrations of the structure of salt contribute to better understanding of the new concept (Figure 33).

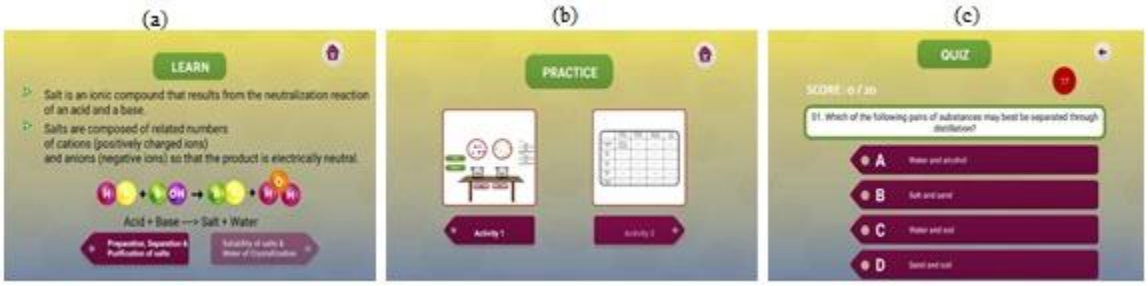

Figure 33. Application functions overview: (a) learning, (b) practice and (c) quiz

The Salts in chemistry app can be easily accessed by scanning the QR code from Figure 34.

Figure 34. QR code for Salts in chemistry app

Redox Reaction – Chemistry

This application includes oxidation and reduction reactions. As they can be very problematic for students, the application will help them master the reactions faster. With very simple but useful explanations of the terms of reduction and oxidation, the app offers users the possibility to equalize redox reactions, which is great for exercise (Figure 35).

Figure 35. Application functions overview: (a) learning, (b) practice and (c) quiz

The Redox Reactions - Chemistry app can be easily accessed by scanning the QR code from Figure 36.

Figure 36. QR code for Redox Reactions – Chemistry app

Water Treatment Plant Process

Water, a compound that is irreplaceable for the functioning of the organism, is shown in this application from the chemical side. Namely, the application, in addition to chemical and physical properties, also describes water pollution, as well as the process of its purification. Very suitable content (Figure 37), in addition to providing scientific knowledge, pays attention to raising users' awareness of the importance of water, which is now neglected. That is why it is necessary to show younger students what are the negative actions that can endanger the survival of the human species, so as not to be repeated.

Figure 37. Application functions overview: (a) learning, (b) practice and (c) quiz

The Water treatment plant process app can be easily accessed by scanning the QR code from Figure 38.

Figure 38. QR code for Water treatment plant process app

DISSCUSION

Visualization is a convenient method in teaching. In chemistry, visual representations have several important functions: to make the connections visible, to present the dynamic and interactive nature of chemistry, to provoke the transformation from two-dimensional to three-dimensional ways of thinking and to determine how much time a student needs to remember that information (Vavra et al., 2011). Pedagogical experiments implemented in primary and secondary schools have shown that a multidisciplinary approach (visualization, ppt presentations with video and audio recordings, performing experiments in front of students) in teaching inorganic chemistry significantly increases students' interest in chemistry and science and better knowledge acquisition by students from processed teaching units (Nikolic et al., 2014; Nikolic et al., 2018).

The student can actively participate in the lessons *via* their mobile phone or tablet. Practicing tasks through online tests, reading books in electronic form, learning and research provide greater motivation for the work of each child and create a desire for better results. The essence of multimedia is interactivity as the main feature of the media.

Teachers are always there for all questions, advice and problems of their students, they can communicate with them, consult them for everything that is not clear to them whenever they want. All this is the credit of many important and tempting applications. With popular applications, learning on tablets becomes easier and more interesting, students are more imaginative, more active in class and motivated to explore and learn, they progress faster and become more successful.

Mobile learning, known as "m-learning", refers, as the name suggests, to learning on the go. What makes m-learning special is the simple and fast access to the necessary information in different locations using mobile devices that are adapted in size and shape to easy portability (Krmek, 2017). The most widespread phones in the world are those with the Android operating system at the moment.

The advantages of m-learning are reflected in the following: introduction of new technologies in teaching processes; mobile devices are easier to manipulate (transfer) than PCs and books; they are important for students with special needs; they are cheaper than laptops or computers, and can also be used as means of communication; multimedia content has a greater impact on perception and memory; reducing costs of training; support for continuously learning in any situation.

According to the literature, m-learning has also some disadvantages: limited power supply of mobile devices; monitor and key size; different mobile devices have different screen sizes and different operating systems; additional work is necessary to transfer existing electronic learning materials to mobile platforms; limited memory; safety; high costs of buying the latest models of mobile devices (Ristić and Milošević, 2017).

However, considering that the development of science and technology is going at a high speed, some of these shortcomings can be overcome. For example, using a power bank as an additional power source for mobile phones; using the "screen mirroring" option when the display of the phone or tablet is copied on a monitor (TV, video beam, PC monitor, *etc.*). Lack of memory can be compensated by using the cloud and external memory which is now more affordable. And finally, the purchase of the latest phones as one of the disadvantages makes no sense, because cheaper phones of the newer generation can also be used.

CONCLUSION

In a traditional school, the teacher was the mediator between the teaching content and the students. The teacher was the exclusive organizer of the educational work, and the relations between the teacher and the student were based on hierarchical principles. The student was in a subordinate position.

A modern school is also looking for a modern teacher who should be new, unrepeatable, up-to- date. The modern approach to teaching chemistry is based on the strategy of learning by discovery. This enabled the students to no longer be passive listeners sitting in the desks, but active participants in the learning process. Students learn best when they are helped to discover the principles on which phenomena are based. The teacher only becomes the moderator who guides the student.

Research shows that the use of information technology and educational software enables better control and management of the teaching and learning process through constant feedback, which has a strong stimulating and motivating role. Their use favors the development of abstract thinking and enables planned progress in the process of acquiring knowledge. The concept of mobile access to information and social networks that are present in all aspects of society today constitute the digital need of the individual. In addition, the availability of mobile technology allows students today to use that technology in education as well.

Recommendations for using the applications are as follows:

1) improving students' attention in class, increasing both motivation and engagement,
2) focusing on important learning goals,
3) showing movement or a better explanation of a concept by presenting it in three dimensions,
4) fulfilling the request of visualization,

5) short, simple and clear representation of the teaching unit,
6) combining with other forms of teaching, and not as a substitute for good teaching,
7) adjusting the content with the level of knowledge that students possess as well as their abilities,
8) planning a suitable date for the use of application in teaching, because students, who are at the beginning of learning, are not able to distinguish between important and less important segments,
9) explaining concepts that cannot be seen (such as atomic collisions).

The introduction of mobile phones and tablets in teaching represents a real revolution in education. It is now necessary to enable digital education of teachers who will not avoid technology, but will use all its advantages and provide students with exciting and modern teaching suitable for new, net- generations. Present research provides evidence that visualization has an important place in teaching and learning science. Nevertheless, chemistry teachers must be careful in choosing the facilities and activities that can be realized *via* mobile phones, so that they justify the teaching purpose and are adapted to each student individually.

This work represents a good basis for the realization of a new pedagogical experiment in primary and secondary schools for monitoring the improvement of the teaching of inorganic chemistry, which will be the subject of our future research.

Acknowledgement

This work was supported by the Ministry of Education, Science and Technological Development of the Republic of Serbia, Contract No. 451-03-68/2020-14/200124.

Conflict-of-Interest Statement

Authors declare no conflict of interest.

REFERENCE

Heflin, H., Shewmaker, J., & Nguyen, J. (2017). Impact of mobile technology on student attitudes, engagement, and learning. Computers & Education, 107, 91-99.

Hew, K. F., & Brush, T. (2007). Integrating technology into K-12 teaching and learning: Current knowledge gaps and recommendations for future research. Educational Technology Research and Development, 55, 223–252.

https://prezi.com/p/ekhzkjtnuyg5/aplikacije-za-iphone/, access 23/07/2020

İlhan, I. (2016). Mobile device based test tool for optimization algorithms. Computer Applications in Engineering Education, 24, 744–754.

Kostić, D. A., Mitić, S. S., Gošnjić-Ignjatović, A. J., Ranđelović, J., & Zarubica, A. R. (2011). A correlation between traditional and computer-based interactive teaching method in the presentation of the lesson Proteins. The New Educational Review, 25, 172 -182.

Kostić, D. A., Nikolić, R. S., Krstić, N. S., Nikolić, M. G., Dimitrijević, V. D., & Simić, S. (2018). Multidisciplinary approach to teaching inorganic chemistry in high school: an example of the topic of metals. Current Science, 115, 268–273.

Krmek, M. (2017). Mobilne tehnologije u nastavi (B.Sc. Thesis). Učiteljski fakultet. Zagreb. https://urn.nsk.hr/urn:nbn:hr:147:246288 (in Croatian)

Libman, D., & Huang, L. (2013). Chemistry on the go: Review of chemistry apps on smartphones. Journal of Chemical Education, 90, 320–325.

Naik, G., & Ramirez, M. (2015). Integrating audio-visual materials and mobile app technologies into chemistry course curriculum. Selected papers from the 26th International Conference on College Teaching and Learning, 154−161.

Nikolić, R. S., Kostić, D. A., Krstić, N. S., Trajković, A., & Stojanović, N. (2014). A Multidisciplinary Approach to Teaching Metals as Part of the Elementary School Curriculum in Serbia: a review. The New Educational Review, 36, 95-103.

O'Bannon, B. W., & Thomas, K. (2014). Teacher perceptions of using mobile phones in the classroom: Age matters!. Computers & Education, 74, 15–25.

Priručnik 2014 – Primena informaciono-komunikacionih tehnologija u nastavi, Zavod za unapređivanje obrazovanja i vaspitanja, Beograd, 2014 (in Serbian).

Ristić, O., & Milošević, M. (2017). Primena android aplikacija u obrazovanju, Selected papers from National conference with international participation about information technologies, education and entrepreneurship, http://www.ftn.kg.ac.rs/konferencije/ITOP17/Radovi/Olga%20Ristic,%20Marjan%20Milosevic.pdf, accessed 23/07/2020

Vavra, K., Janjic-Watrich, V., Loerke, K., Phillips, M. L., Norris, P. S., Macnab, J. (2011). Vizualisation in science education: a review. Alberta science education journal, 41, 22-30.

Williams, A. J., & Pence, H. E. (2011). Smart phones, a powerful tool in the chemistry classroom. Journal of Chemistry Education, 88, 683–686.

Zarubica, A., Kostić, D., Rančić, S., Popović, Z., Vasić, M., Radulović, N. (2012). An Improvement of the Eighth Grade Pupils` Organic Chemistry Knowledge with the Use of a Combination of Educational Tools: An Evaluation Study - Expectations and Effects. The New Educational Review, 30, 93–102.

Android aplikacije kao dodatni alat u predavanju neorganske hemije: kratak prikaz

Marina V. Blagojević[1], Danijela A. Kostić[1], Maja N. Stanković[1], Dragan M. Đorđević[1], Vladimir D. Dimitrijević[1], Milica G. Nikolić[1], Nenad S. Krstić[1]

1-Univerzitet u Nišu, Prirodno-matematički fakultet, Departman za hemiju, Visegradska 33, 18000 Nis, Srbija

Sažetak

Koncept mobilnog prilaza informaciji prisutan je u svim aspektima društva danas i čini digitalnu potrebu individue. Cilj ovog rada je pružanje pregleda i sistematizacije različitih lako dostupnih android-aplikacija za mobilne telefone i tablete koje bi trebalo da promovišu potpuno razumevanje hemijskih koncepata i, takođe, da olakšaju sticanje znanja u hemiji od strane učenika, kako u osnovnim tako i u srednjim školama. Mobilno učenje ima mnoge prednosti kao što su raznolikost, zabava, komunikacija, interaktivnost, kao i učenje potpuno prilagođeno individui nezavisno od prostora i vremena. Korišćenje ovih alata ima veliki uticaj na različite prilaze u predavanju hemije i doprinosi poboljšanju krajnjih ishoda učenja. Stoga je važno za svakog nastavnika da integriše tehnologiju u pedagogiju i iskoristi ih za promociju učenja zasnovanog na potrebama i mogućnostima studenta.

*Ključne reči**:** android-aplikacije, mobilno učenje, nastavnički alati, interaktivnost*

Des applications Android comme outil supplémentaire dans l'enseignement de la chimie inorganique : une brève revue

Marina V. Blagojević[1], Danijela A. Kostić[1], Maja N. Stanković[1], Dragan M. Đorđević[1], Vladimir D. Dimitrijević[1], Milica G. Nikolić[1], Nenad S. Krstić[1]

1-Université de Nis, Faculté des sciences naturelles et des mathématiques, Département de chimie, Višegradska 33, 18000 Niš, Serbie

Résumé

Aujourd'hui, le concept d'accès mobile à l'information est présent dans tous les aspects de la société et il représente le besoin numérique de l'individu. L'objectif de cet article est de donner un bref aperçu et une systématisation de diverses applications Android facilement accessibles et destinées aux téléphones portables et aux tablettes. Elles devraient favoriser la compréhension complète des concepts chimiques et faciliter l'acquisition des connaissances en chimie de la part des élèves, tant dans des écoles primaires que dans des écoles secondaires. L'apprentissage mobile possède de nombreux avantages, tels que : la diversité, le divertissement, la communication, l'interactivité, mais aussi un apprentissage entièrement adapté aux besoins de l'individu indépendamment de l'espace et du temps. L'utilisation de ces outils a un grand impact sur des différentes approches à l'enseignement de la chimie et contribue à l'amélioration des résultats finaux de l'apprentissage. Pour chaque enseignant, il est important dès lors d'intégrer la technologie dans la pédagogie et de l'utiliser pour promouvoir un apprentissage concentré sur l'élève.

Mots-clés: applications Android, apprentissage mobile, outils pédagogiques, interactivité

Андроид приложения в качестве дополнительного инструмента в преподавании неорганической химии: краткий обзор

Марина В. Благоевич[1], Даниела А. Костич[1], Майя Н. Станкович[1], Драган М. Джорджевич[1], Владимир Д. Димитриевич[1], Милица Г. Николич[1], Ненад С. Крстич[1]

1-Университет в Нише, Естественно-математический факультет, Кафедра химии, Вишеградска 33, 18000 Ниш, Сербия

Аннотация

Концепция мобильного доступа к информации присутствует сегодня во всех сферах жизни общества и представляет собой цифровую потребность человека. Цель данной статьи – провести краткий обзор и систематизацию различных легкодоступных приложений платформы Андроид для мобильных телефонов и планшетов, которые могут способствовать правильному пониманию химических концепций, а также могут облегчить учебу в области химии учащимся как начальных, так и средних школ. Мобильное обучение имеет много преимуществ, таких как разнообразие, развлечение, общение, интерактивность, а также и возможность приспособить обучение потребностям человека независимо от места и времени. Использование этих инструментов оказывает большое влияние на различные подходы к преподаванию химии и способствует улучшению итоговых результатов обучения. Вот почему для каждого преподавателя важно интегрировать технологии в педагогику и использовать их в качестве поддержки обучения, ориентированного на учащихся.

Ключевые слова: приложения платформы Андроид, мобильное обучение, учебно-методические средства, интерактивность

Android-Anwendungen als zusätzliches Werkzeug im Unterricht in der anorganischen Chemie: Ein kurzer Überblick

Marina V. Blagojević[1], Danijela A. Kostić[1], Maja N. Stanković[1], Dragan M. Đorđević[1], Vladimir D. Dimitrijević[1], Milica G. Nikolić[1], Nenad S. Krstić[1]

1-Universität Niš, Fakultät für Naturwissenschaften und Mathematik, Department für Chemie, Višegradska 33, 18000 Niš, Serbien

ABSTRAKT

Das Konzept des mobilen Zugangs zu Informationen ist heute in allen Bereichen der Gesellschaft präsent und stellt das digitale Bedürfnis des Einzelnen dar. Das Ziel dieses Beitrags ist es, einen kurzen Überblick und eine Systematisierung verschiedener leicht zugänglicher Android-Anwendungsprogramme für Mobiltelefone und Tablets zu geben, die das vollständige Verständnis chemischer Konzepte fördern und den Erwerb chemischer Kenntnisse von Schülern der Grund- und Mittelschulen erleichtern sollten. Mobiles Lernen bietet viele Vorteile wie Vielfalt, Spaß, Kommunikation, Interaktivität, aber auch Lernen, das unabhängig von Ort und Zeit vollständig an die Bedürfnisse des Einzelnen angepasst ist. Die Verwendung dieser Tools hat einen großen Einfluss auf unterschiedliche Ansätze im Chemieunterricht und trägt zur Verbesserung der endgültigen Lernergebnisse bei. Deshalb ist es für jeden Lehrer wichtig, Technologie in die Pädagogik zu integrieren und sie zur Förderung des schülerzentrierten Lernens zu nutzen.

Schlüsselwörter: *Android-Anwendungen, mobiles Lernen, Lehrmittel, Interaktivität*

Betalains-natural pigments for healthy food

Dusan Paunovic[1], Branka Stojanovic[1], Danica Dimitrijevic[1], Jovana Krstic[1], Danijela Kostic[2,*]

1-Union Nikola Tesla University of Belgrade, Faculty of Applied Sciences, Serbia

2-University of Nis, Faculty of Sciences and Mathematics, Department of Chemistry, Visegradska 33, 18000 Nis, Serbia

Dusan Paunovic: dpaunovic3@gmail.com
Branka Stojanovic: brankastojanovic81@gmail.com
Danica Dimitrijevic: danicadimitrijevic7@gmail.com
Jovana Krstic: jovanaveljkovic81@gmail.com
Danijela Kostic: danijelaaakostic@yahoo.com

ABSTRACT

The application of artificial colors in practice has shown many negative effects on food safety and human health. Allergic reactions to artificial colors are very common, especially in children. Some research suggests that prolonged use of artificial colors can be the cause of cancer. Betaine is one of the most widespread groups of plant pigments, which is increasingly being researched in recent times. Therefore, the use of cheap plant pigments such as betaine is important. They are safe for use in food and have good biological and pharmacological properties. Some of them have an antioxidant, antimicrobial, antilipidemic, anticancer role. They can be used in food instead of anthocyanins. Some properties are beneficial to our health due to which they can be used to enhance the flavor and color of ice-cream, jellies, jams, desserts, sauces, sweets, tomato paste, breakfast cereals.

Keywords: betalains, isolation, identification, stability, application, health benefit

Introduction

The development of synthetic chemistry has led to the production of numerous artificial colors, which were widely used in the food industry after the Second World War. The prolonged use of artificial colors has caused numerous adverse effects on human health. Allergic reactions in children to artificial colors were particularly pronounced. Some colors have been found to have a carcinogenic effect. All this has directed scientists to research natural colors, which provide bright coloration to fruits, flowers, and roots of plants, and do not have negative effects on health; on the contrary, they have many beneficial effects.

So far, betalains have been much less studied than other natural plant pigments: chlorophylls, carotenoids and anthocyanins. Betalains are water-soluble and nitrogen-containing pigments, divided into betacyanins and betaxanthins. Red and violet tonalities result from different substitution patterns in betacyanins, while different amino acid or amine side chains determine the color of betaxanthins (Figure 1).

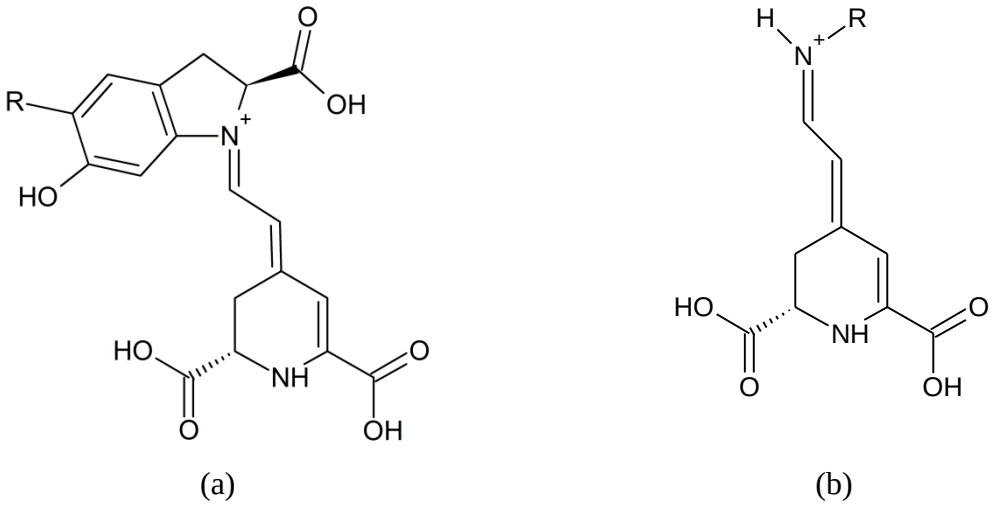

(a) (b)

Figure 1. Structures of (a) betacyanins and (b) betaxanthins.

Glycosylation and acylation result in a diversity of betacyanin structures. The betanidin aglycone is usually linked with glucose, occasionally with glucuronic acid, sophorose, rhamnose, and apiose, at the C-5 or C-6 position. Further modification occurs by aliphatic or aromatic acid esterificationof the sugar moiety. Malonic, 3-hydroxy-3-methyl-glutaric, caffeic, *p*-coumaric, cinnamic, and ferulic acids are typical acid substituents (Strack et al., 2003).

Betalains are found in numerous sources (flowers, fruits, roots, leaves, stalks, seeds, grains) in the plant kingdom. In food, however, their occurrence is limited, the red beet is being regarded for a long time as practically the sole source of betacyanin. Betalaines are found in various plant organs and accumulate in cellular vacuoles, mainly in the epidermal and subepidermal tissues. However, they are

sometimes accumulated in plant stems, such as subterranean parts, seeds, flowers and leaves (Delgado-Vargaset al., 2000).

About 75 betalains have been structurally identified from plants of about 17 families out of 34 families under the order Caryophyllales, such as Aizoaceae, Amaranthaceae, Basellaceae, Cactaceae, Chenopodiaceae, Didiereaceae, Holophytaceae, Nyctaginaceae, Phytolaccaceae, and Portulacaceae families, to name a few. Betalains have also been found in mushrooms in the genera Amanita, Hygrocybe, and Hygrophorus. Only a few fruits and vegetables contain betalains and the best known is beet roots (*Beta vulgaris*) that produces betanin ($C_{24}H_{27}N_2O_{13}$), an important natural food colorant (Slimen et al., 2017).

The other edible sources known to contain betalains are fruits of *Opuntia* spp. (*e.g.*, *O. ficus-indica*, commonly known as prickly pear), Swiss chard (*Beta vulgaris* subsp. *vulgaris*, Cicla-Group and Flavescens-Group), grains or leaves of amaranth (*Amaranthus* spp.), pitahaya (*Hylocereus* spp.), also known as dragonfruit, ulluco (*Ullucus tuberosus*), djulis (*Chenopodium fromosanum*, a native cereal in Taiwan), and bilberry cactus (*Myrtillocactus geometrizans)*, an endemic plant locally consumed in Mexico, which contains 233 mg/kg of total betalains in its fruit pulp (Delgado-Vargas et al., 2000).

Betanin was discovered around 1920, while the crystalline form of betanin was produced in the 1960s (Nottingham, 2004).

At the root of beetroot, betanin is normally found in a much higher amount than other betacyanin pigments. Like all betacyanins, betanin is metabolically derived from a molecule known as 3,4-dihydroxyphenylalanine (L-DOPA) (Gandía-Herrero and García-Carmona, 2012).

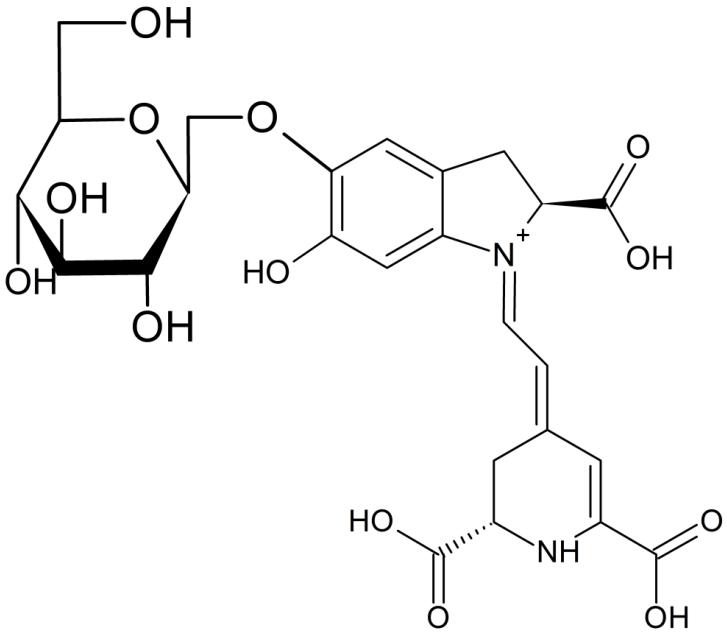

Figure 2. Structure of betanin

The biosynthesis of betalains is discussed in detail in a review article (Khan and Giridhar, 2015). Betanin is formed from two L-DOPA molecules. One molecule undergoes a change to the form of betalamic acid. Another molecule of L-DOPA is changed to cyclo-DOPA glucoside (CDG), which condenses with betalamic acid and builds betanin (Hussain et al., 2018b).

A small change in structure translates betanidin into betanin. Other small biochemical modifications yield other betacyanin pigment. The most important factors affecting the synthesis of beetroot pigments are temperature, soil fertility, soil moisture, irrigation and harvesting time (Jackman and Smith, 1996).

After betanin, yellow betaxanthins, vulgaxanthin-I and vulgaxanthin-II are the most significant beetroot pigments. These pigments were first described by Mario Piattelli with collaborators in the 1960s in Naples (Piattelli and Minale, 1964).

In the cultures under study (Piatta d'Egitto), they found at least six betaxanthins, all of which were in small quantities. In total, they listed sixteen different betalains, including indicaxanthin, isobetanin, neobetanin, and prebetanin. The characteristic color of the beetroot is due to variations in the betalain pigments, especially the relative concentrations of betanin and yellow betaxanthin. Species with a dark purple-red color have a high ratio of betanin to betaxanthin, while yellow and gold species such as Burpee's Golden have relatively large amounts of betaxanthin and have very little or no betanin at all. Species with white carrots, including Albina Verduna and Blankoma, have extremely low amounts of both betacyanin and betaxanthin (Nottingham, 2004).

Extremely dark and light rings are usually visible when the beetroot is crossed. This is due to the different amounts of pigments in the vascular system and the storage tissue of the root. The vascular system is seen as dark rings due to the large amount of pigments, while the storage tissue looks like brighter rings. In some dark red species such as Boltardy and Red Ace, these color differences are barely noticeable. The color difference is most evident in the Chioggia species, with concentric patterns (as targets) pinkish-red (vascular system) and white (storage tissue).

The content of betacyanin in beets is 75-95% and yellow betaxanthin vulgaxanthin I is the most abundant. In the other parts of the beet (shell), the highest concentration of betanin is present. Betacyanins are more stable than betaxanthin at 25^{o}C (Kujala et al., 2002).

Beetroot contains about 130 mg of betanin/100g of raw material. New selections can contain up to 450-500 mg betanin/100g. Betanin is the most prevalent among the betacyanins and the most significant. In addition to betanin, there are isobetanin, betanidin and isobetanidin (Kujala et al., 2002).

The betalains are generally arranged according to the outer parts of the beet root. However, they are not limited to the root, but give a red color that can be observed on leaves, stems and flowers. Of the yellow betaxanthins, vulgaxanthin I is the most abundant.

Isolation and identification of betalains

Betalains are generally extracted from ground plant material by maceration with water, at differents temperatures or Soxhlet extraction. For a complete extraction, it is preferable to use methanol or ethanol solutions (20–50%, v/v). Before extraction, a short heat treatment (70 °C, 20 min) can be made for inactivating degradative enzymes, despite the possible destruction of some pigments. A slight acidification with HCl or citric acid or acidified ethanol can be used for the precipitation of betacyanins. The addition of aqueous ethanol (95%) will give betaxanthins (Celli and Brooks, 2017). However, other techniques have been assayed to extract betalains, particularly from red beet: diffusion extraction, ultrafiltration and reverse osmosis and loose reverse osmosis (LRO), cryogenic freezing, aqueous two-phase extraction, pulsed electric fields and gamma irradiation, microwave(Bastos and Gonçalves, 2017) and ultrasound-assisted extractions (Cardoso-Ugarte et al., 2014).

Purification and isolation of betalains is needed before their qualitative and quantitative analysis for eliminating possible interfering compounds. Chromatographic and electrophoretic procedures have been used to separate and/or purify betalains. For the separation of these pigments, ion chromatography on cation exchange resins followed by adsorption chromatography on polyamide column or a sequential chromatography on a series of Sephadex ion exchangers can be used (Piattelli et al., 1964).

There are several chemical tests for the characterisation of betalains and distinguishing (recognizing) anthocyanins from betalains. In order to characterize betalains, some other important determinations can be made. Betalains, as pigments, have a maximum absorbance in the visible part of the spectrum, which characterizes them; it is clear that structural modifications can be monitored using UV-VIS spectroscopy.

Red betacyanins absorb at λ_{max} = 540 nm, and yellow betaxanthins at λ_{max} = 480 nm. Acetylated betalains show a second (secondary) absorbance maximum in the UV spectrum of 260 to 320 nm and the ratio of the maximum in the visible spectrum to the maximum in the UV spectrum is used as a measure of the number of acyl groups in the structure (Hussain et al., 2018a).

Separation, identification and quantification of betalains have been carried through high performance liquid chromatography (HPLC) coupled to ultraviolet-visible (UV-Vis) (Faridah et al., 2015), photodiode array (PDA), mass spectrometry (MS) and nuclear magnetic resonance detection (NMR) by using reversed phase columns and binary gradient dilutions (acidified water with formic acid 2–5%, v/v) and acetonitrile or methanol (Stintzing and Carle, 2004; Stintzing et al., 2004). As betaxanthins are fluorescent pigments, the detection of these pigments may be done using fluorescence methods (Gandía-Herrero et al., 2005).

By refining the methodological approach, the HPLC method can be coupled to DAD, MS and NMR (Castellanos-Santiago and Yahia, 2008). In this way, separation and identification can be performed simultaneously. In addition, several chemical tests have been introduced to characterize betalains, and many of them are based on the changes in pH (Delgado-Vargas, 2002).

Stability of betalains

Betalains are an alternative to synthetic colorants, having stability over a wide pH range and a high molar extinction coefficient and being neither toxic nor allergens. Degradation after processing or storage includes reactions such as isomerization, deglycosylation, hydrolysis, decarboxylation, and dehydrogenation, involving color alterations and absorption changes. Factors affecting the stability of betalains include chemical structure, pigment content, matrix, additives, enzymes, pH, thermal treatment, water activity, exposure to oxygen and light during storage, and storage temperatures (Herbach et al, 2006).

In order to retain the coloring strength and chromatic characteristics of betalains, reduced thermal exposure is recommended during processing, together with the inactivation of deleterious enzymes, avoidance of light and oxygen, and the addition of antioxidants and/or chelating additives.

In the food industry, betalaines represent an important natural color. The basic source of betalains is beetroot. During commercial extraction, the beetroot is first ground, the colored juice is collected and concentrated. Betalaine is sold to the food industry as a juice concentrate or powder. The juice is concentrated in vacuum until 60-65% of the total dry matter is reached. In the manufacture of powder (which usually contains 0.3-1.0% of pigments), lyophilization is applied (Chikara et al., 2019).

In juices and powdered products, a high concentration of pigments is achieved by fermentation. Beet juice soluble fermenters can be removed in the biofermenter, using yeasts such as *Candida utilis* and *Saccharomyces cerevisiae*, to remain a more concentrated (relative to pigments) product. Powders obtained after fermentation of beet juice contain 5-7 times the amount of betacyanin than powders obtained from unfermented juice (Hadipour et al., 2020).

Betalaine extracts can have a wide variety of colors, depending on the relative ratio of betacyanin to betaxanthin present. Dye products are usually odorless and tasteless, but can affect the aroma and flavor of foods. The most important coloring agent is pure betanin, E-162 (beet red), which is used to color a wide range of processed foods (Khan, 2016).

The biggest problem with the use of betalains in foods is stability, which limits their use. Betalains extracts must be carefully manipulated as they are sensitive to environmental influences, especially pH, heat, light, moisture and oxygen. Environmental influences have an interactive effect and pigments can quickly discolor under adverse conditions. Red pigment betanin degrades to a light

brown color when exposed to air, bright light, and high temperatures. This discoloration is partly reversible, if the adverse conditions are only temporary (Azeredo, 2009).

Betalains remain unchanged in the pH range of 3.5 to 7.0. Beetroot extracts in most foods will therefore not discolour as a direct consequence of pH. The optimal pH for the color of betacyanin and betaxanthin is in a poorly acidic medium, in the range of 5.0-6.0. The color of beetroot extract changes from red to blue with a pH change over 7.0. The beet tissue exposed to high or alkaline pH (7.5-8.5) becomes discolored. Chopped beetroot retains its purple-red color well in acidic solutions such as acetic acid (Azeredo, 2009).

Betalain heating can cause discoloration. Red pigment betanin, for example, can turn light brown if gradually heated, especially if elevated temperatures are associated with an alkaline pH (Pedreño and Escribano, 2001).

According to the current legisalation in Republic of Serbia (Official Gazette SCG 56/2003 as amended 4/2004, 5/2004, 16/2005), the use of betanin, as the main pigment of beetroot, as a natural food color E162, is allowed. The FAO and WHO expert team recommends the application of beetroot products in dairy products, fresh fruits and vegetables, pastas, fresh meat, fresh eggs, baby food, fruit juices, nectars and wines, *etc*. They are best suited for use in food products that undergo minimal heat treatment, short durability, packaged in dried form with reduced oxygen, light and moisture.

As a result, red beet is well accepted as red food colourant, specially betanin, denoted as E-162 in the European Union (Downham and Collins, 2000) and 73.40 in the chapter 21 of the Code of Federal Regulations (CFR) section of the Food and Drug Administration (FDA) in the USA.

The stability of betalain is the greatest in low-moisture foods. High humidity increases the rate of degradation of pigments. Over time, oxygen exposure accelerates the darkening or discoloration of pigments in food products. Betalains react with air oxygen, but discoloration is partially reversible if oxygen levels decrease immediately (Martins et al., 2017).

Despite the relative lack of stability when compared to synthetic food colors, betalains are widely used in the food industry (Peschel et al., 2006).

Exposure of a solution of betanin to light at 25^{o}C significantly affects its stability, while degradation due to heat is so pronounced at 55^{o}C. Also, the degradation of betanin in solution is a partially reversible process (Pedreño and Escribano, 2001).

In general, high betalains content, high degree of glucosylation and acylation, antioxidant, chelation agents, low T, elimination of light, N_2 increases stability of betalains. The presence of metal ions, enzymes, light, high T and O_2 decreases the stability of betalains (Esatbeyoglu et al., 2015).

The betalain pigment is usually extracted from fruit pulp or pieces of other raw material (*e.g.*, red beet) with a solvent (water, ethanol, or methanol), with or without heat treatment or acidification, to improve the pigment yield. The stability of betanin can be affected by pH, water activity, exposure to light, oxygen, enzymatic activities, metal, and temperature. Temperature is the most important factor in pigment degradation during the separation and concentration processes (Vergara et al.,

2015). Despite their coloring capacity and superior antiradical activity, betalains have not been considered by the food industry as potential additives. This is in part due to their instability, which prevents long-term storage (Gokhale and Lele, 2014). The susceptibility of betalains restricts their use as food colorants (Ravichandran et al., 2014). Thus, the stability of betalains could be improved by using microencapsulation technologies such as spray drying (Janiszewska, 2014).

Potential health benefit of betalains

Beetroot pigments exhibit antioxidant properties. In various model systems, betacyanins have been shown to be potent antioxidants. Their positive electrostatic charge increases their affinity for biological membranes, which are major targets of oxidation. The antioxidant activity of betalains can be verified through different chemical and biological methods; anti-cancer, antiviral, and anti-oxidant activity has been attributed to betalain pigments. Due to their powerful anti-oxidant ability and their capacity to absorb free radicals, betalains can be used in the treatment of inflammatory and cardiovascular diseases, cancer, asthma, arthritis, oxidative stress, intestinal inflammation, diabetes, and other diseases associated with aging (Khan, 2016). The anti-oxidant properties of betalains can be related to structural features. In betaxanthins, an increasing number of hydroxy and imino residues improves free radical scavenging. In betacyanins, glycosylation reduces activity, while acylation generally raises the anti-oxidant potential (Stintzing and Carle, 2004).

- Free radical scavenging of reactive oxygen species (Escribano et al., 1998; Esatbeyoglu et al., 2014; Kanner, et al., 2001; Livrea and Tesoriere, 2004; Tesoriere et al., 2004;);
- Protection of LDL against oxidation (Neelwarne, 2012; Reddy et al., 2005; Siriwardhana et al., 2006; Tesoriere et al., 2003; Tesoriere et al., 2004);
- Prevention of DNA-damage (Zielińska-Przyjemska et al., 2012);
- Induction of antioxidant: paraoxonase 1 (Schrader et al., 2011), heme oxygenase 1 (Kikuchi et al., 2005) and phase II detoxifying enzymes (Krajka-Kuźniak et al., 2013; Saw and Kong, 2011);
- Gene regulatory activity (*e.g.* Nrf2-dependent signal transduction pathway) (Na and Surh, 2014; Schrader and Rimbach, 2011);
- Anti-inflammatory activity (*e.g.* inhibition of cyclooxygenase-2) (Reddy et al., 2005; Ruiz et al., 2013; Zielińska-Przyjemska et al., 2016; ;
- Anticancer activity (Govind et al., 2011; Kapadia et al., 1996).

Application of betalains as a natural pigment in food

Stability of betalains goes over a broad pH range from 3 to 7, which makes them particularly suitable for use in a broad array of low-acid and neutral foods. Their exploitation started in the 1970s, when *B. vulgaris* was proposed for use in low-acid foods such as meat and dairy products (Elbe and Maing, 1973).

The colourant is commercialized as a liquid concentrate and spray-dried powder with a colour strength or tinctorial power (at 535 nm/1 % solution) ranging between 2 and 5. It is mainly used in dairy products, yogurt, puddings, ice creams, frozen fruit desserts, gelatins, beverages, confectioneries, candies and baked foods (Obón et al., 2009).

In different geographical regions, other plants may be used to provide colourants, such as Amaranthus pigments, which are added to beverages, bread, and other foods in the southwestern United States, Mexico, Bolivia, Ecuador, Argentina and China (Cai and Corke, 1999). Recently, a successful industrial process for juice production from *Opuntia ficus-indica* (L.) Mill. has been established, opening up the possibility of commercial use of this plant species from semi-arid areas (Mosshammer et al., 2006; Mosshammer et al., 2007).

Conclusion

The color of food is a significant factor in industry. However, to ensure the food safety, it is important to add up safe and healthy ingredients into the food products. The artificial colors may cause some allergic reactions; their long-term use is considered to be a cause of carcinogenesis. Therefore, the possibility of using inexpensive, natural plant pigments of betalains is significant. Betalain stability is affected by long term exposure to oxygen/air, light in the presence of oxygen, high temperature and water activity (wa) but it is highly stable in the presence of low moisture. Its pigments show more stability towards pH and temperature and are suitable for those foods in which anthocyanin cannot be used as a coloring agent. Betalains can enhance the flavor and color of icecream, jellies, jams, desserts, sauces, sweets, tomato paste and breakfast cereals. They have some properties which are beneficial to our health. Betalains exibit antioxidant, antimicrobial, antilipidemic and anticancer activity.

Acknowledgements

The authors acknowledge the Ministry of Education, Science and Technological Development of Serbia for the financial support (451-03-68/200124).

Conflict-of-Interest Statement:

Authors declare no conflict of interest.

Reference

Azeredo, H.M.C. (2009). Betalains: properties, sources, applications, and stability - a review. International Journal of Food Science & Technology, 44, 2365–2376. doi: 10.1111/j.1365-2621.2007.01668.x.

Bastos, E.L., & Gonçalves, L.C.P. (2017). Microwave-assisted extraction of betalains. Water Extraction of Bioactive Compounds, 245–268. doi: 10.1016/B978-0-12-809380-1.00009-7.

Cardoso-Ugarte, G.A., Sosa-Morales, M.E., Ballard, T., Liceaga, A., & San-Martin-Gonzalez, M.F. (2014). Microwave-assisted extraction of betalains from red beet (*Beta vulgaris*). LWT - Food Science and Technology, 59, 276–282. doi: 10.1016/j.lwt.2014.05.025.

Castellanos-Santiago, E. & Yahia, E.M. (2008). Identification and quantification of betalains from the fruits of 10 mexican prickly pear cultivars by high-performance liquid chromatography and electrospray ionization mass spectrometry.Journal of Agricultural and Food Chemistry, 56, 5758–5764.

Cai,Y., & Corke, H. (1999). *Amaranthus* betacyanin pigments applied in model food systems.
Journal of Food Science, 64, 869–873.

Celli, G.B., & Brooks, M.S.-L. (2017). Impact of extraction and processing conditions on betalains and comparison of properties with anthocyanins — A current review. Food Research International, 100, 501–509. doi: 10.1016/j.foodres.2016.08.034.

Chhikara, N., Kushwaha, K., Sharma, P., Gat, Y. & Panghal, A. (2019). Bioactive compounds of beetroot and utilization in food processing industry: A critical review. Food Chemistry, 272, 192–200.

Delgado-Vargas, F., & Paredes-Lopez, O. (2002). Natural colorants for food and nutraceutical uses. (1st ed.). CRC Press.

Delgado-Vargas, F., Jiménez, A.R., & Paredes-López, O. (2000). Natural pigments: carotenoids, anthocyanins, and betalains--characteristics, biosynthesis, processing, and stability. Critical Reviews in Food Science and Nutrition, 40, 173–289.

Downham, A., & Collins, P. (2000). Colouring our foods in the last and next millennium. International Journal of Food Science & Technology, 35, 5–22. doi: 10.1046/j.1365-2621.2000.00373.x.

von Elbe, J.H. & Maing, I.-Y. (1973). Betalains as possible food colorants of meat substitutes. Cereal Science Today, 18, 263– 264, 316-317.

Esatbeyoglu, T., Wagner, A.E., Motafakkerazad, R., Nakajima, Y., Matsugo, S., & Rimbach, G. (2014). Free radical scavenging and antioxidant activity of betanin: Electron spin resonance spectroscopy studies and studies in cultured cells. Food and Chemical Toxicology, 73, 119–126. doi: 10.1016/j.fct.2014.08.007.

Esatbeyoglu, T., Wagner, A.E., Schini-Kerth ,V.B., & Rimbach, G. (2015). Betanin-a food colorant with biological activity. Molecular Nutrition &Food Research, 59, 36–47.

Escribano, J. Pedreño, M.A., García-Carmona, F., & Muñoz, R. (1998). Characterization of the antiradical activity of betalains from *Beta vulgaris* L. roots. Phytochemical Analysis, 9, 124–127.

Faridah, A., Holinesti, R., & Syukri, D. (2015). Betalains from red pitaya peel (*Hylocereus polyrhizus*): extraction, spectrophotometric and HPLC-DAD identification, bioactivity and toxicity screening. Pakistan Journal of Nutrition, 14, 976–982. doi: 10.3923/pjn.2015.976.982.

Gandía-Herrero, F., & García-Carmona, F. (2012). Characterization of recombinant Beta vulgaris 4,5-DOPA-extradiol-dioxygenase active in the biosynthesis of betalains. Planta, 236, 91–100. doi: 10.1007/s00425-012-1593-2.

Gokhale, S.V., & Lele, S.S. (2014). Betalain content and antioxidant activity of *Beta vulgaris*: effect of hot air convective drying and storage. Journal of Food Processing and Preservation, 38, 585–590. doi: 10.1111/jfpp.12006.

Kapadia, G.J., Azuine, M.A., Rao, G.S., Arai, T., Iida, A. & Tokuda, H. (2011). Cytotoxic effect of the red beetroot (*Beta vulgaris* L.) extract compared to doxorubicin (adriamycin) in the human prostate (PC-3) and breast (MCF-7) cancer cell lines. Anti-Cancer Agents in Medicinal Chemistry, 11, 280–284.

Hadipour, E., Taleghani, A., Tayarani-Najaran, N., &Tayarani-Najaran, Z. (2020). Biological effects of red beetroot and betalains: A review. Phytotherapy Research, doi: 10.1002/ptr.6653.

Herbach, K.M., Stintzing, F.C., & Carle, R. (2006). Betalain Stability and Degradation—Structural and Chromatic Aspects. Journal of Food Science, 71(4), R41-R50.

Hussain, E.A., Sadiq, Z., & Zia-Ul-Haq, M. (2018a). Betalains as Colorants and Pigments. In Betalains: Biomolecular Aspects, Springer, Cham., 125–137. doi: 10.1007/978-3-319-95624-4_7.

Hussain, E.A., Sadiq, Z., & Zia-Ul-Haq, M. (2018b). Biosynthesis of Betalains. In Betalains: Biomolecular Aspects, Springer, Cham., 57–95. doi: 10.1007/978-3-319-95624-4_4.

Jackman, R.L., & Smith, J.L. (1996). Anthocyanins and betalains. Natural Food Colorants. Springer, Boston, MA, 244–309. doi: 10.1007/978-1-4615-2155-6_8.

Janiszewska, E. (2014). Microencapsulated beetroot juice as a potential source of betalain. Powder Technology, 264, 190–196. doi: 10.1016/j.powtec.2014.05.032.

Kapadia, G.J., Tokuda, H., Konoshima, T., & Nishino H. (1996). Chemoprevention of lung and skin cancer by *Beta vulgaris* (beet) root extract. Cancer Letters, 100, 211–214.-doi.org/10.1016/0304-3835(95)04087-0

Kanner, J., Harel, S.,& Granit, R. (2001). Betalains-a new class of dietary cationized antioxidants. Journal of Agricultural and Food Chemistry, 49, 5178–5185.

Khan, M.I. (2016). Plant betalains: safety, antioxidant activity, clinical efficacy, and bioavailability. Comprehensive Reviews in Food Science and Food Safety, 15, 316–330. doi: 10.1111/1541-4337.12185.

Khan, M.I., & Giridhar, P. (2015). Plant betalains: Chemistry and biochemistry. Phytochemistry, 117, 267–295. doi: 10.1016/j.phytochem.2015.06.008.

Kikuchi, G., Yoshida, T., & Noguchi, M. (2005). Heme oxygenase and heme degradation. Biochemical and Biophysical Research Communications, 338, 558–567. doi: 10.1016/j.bbrc.2005.08.020.

Krajka-Kuźniak, V., Paluszczak, J., Szaefer, H., & Baer-Dubowska, W. (2013). Betanin, a beetroot component, induces nuclear factor erythroid-2-related factor 2-mediated expression of

detoxifying/antioxidant enzymes in human liver cell lines. The British Journal of Nutrition, 110, 2138–2149. doi: 10.1017/s0007114513001645.

Kujala, T.S., Vienola, M.S, Klika K.D., Loponen J.M., & Pihlaja K. (2002). Betalain and phenolic compositions of four beetroot (*Beta vulgaris*) cultivars. European Food Research and Technology, 214, 505–510. doi: 10.1007/s00217-001-0478-6.

Livrea, M.A., & Tesoriere, L. (2004). Antioxidant activities of prickly pear (*Opuntia ficus indica*) fruit and its betalains: betanin and indicaxanthin. In: Herbal and Traditional Medicines: Biomolecular and Clinical Aspects, CRC Press, doi: 10.1201/9780203025901.ch24.

Martins, N., Roriz, C.L., Morales, P., Barros, L., & Ferreira, I.C.F.R. (2017). Coloring attributes of betalains: a key emphasis on stability and future applications. Food & Function, 8, 1357–1372. doi: 10.1039/C7FO00144D.

Mosshammer, M.R., Stintzing, F., & Carle, R. (2006). Cactus pear fruits (*Opuntia spp*.): A review of processing technologies and current uses. Journal of Professional Association for Cactus Development, 8, 1–25.

Mosshammer, M.R., Rohe, M., Stintzing, F.C., & Carle, R. (2007). Stability of yellow-orange cactus pear (*Opuntia ficus-indica* [L.] Mill. cv. 'Gialla') betalains as affected by the juice matrix and selected food additives. European Food Ressearch Technology, 225, 21–32.

Na, H.-K., & Surh, Y.-J. (2014). Oncogenic potential of Nrf2 and its principal target protein heme oxygenase-1. Free Radical Biology and Medicine, 67, 353–365. doi: 10.1016/j.freeradbiomed.2013.10.819.

Neelwarne, B. (2012). Red beet biotechnology: food and pharmaceutical applications. Springer.

Nottingham, S. (2004). Beetroot, Academia edu(e-book)

Obón, J.M., Castellar, M.R., Alacid M., & Fernández-López, J.A. (2009). Production of a red-purple food colorant from *Opuntia stricta* fruits by spray drying and its application in food model systems. Journal of Food Engineering, 90 ,471–479.

Pedreño, M.A., & Escribano, J. (2001). Correlation between antiradical activity and stability of betanine from *Beta vulgaris* L. roots under different pH, temperature and light conditions. Journal of the Science of Food and Agriculture, 81, 627–631. doi: 10.1002/jsfa.851.

Peschel, W., Sánchez-Rabaneda, F., Diekmann, W., Plescher, A., Gartzía, I., Jimenez, D., Lamuela-Raventós, D., Buxaderas,S., & Codina C. (2006). An industrial approach in the search of natural antioxidants from vegetable and fruit wastes. Food Chemistry, 97, 137–150. doi: 10.1016/j.foodchem.2005.03.033.

Piattelli, M., & Minale, L. (1964). Pigments of centrospermae—II.: distribution of betacyanins. Phytochemistry, 3, 547–557. doi: 10.1016/S0031-9422(00)82927-1.

Piattelli, M., Minale, L., & Prota, G. (1964). Isolation, structure and absolute configuration of indicaxanthin. Tetrahedron, 20, 2325–2329. doi: 10.1016/S0040-4020(01)97621-5.

Reddy, M.K., Alexander-Lindo, R.L., & Nair, M.G. (2005). Relative inhibition of lipid peroxidation, cyclooxygenase enzymes, and human tumor cell proliferation by natural food colors. Journal of Agricultural and Food Chemistry, 53, 9268–9273.

Ruiz, S., Pergola, P.E., Zager, R.A. & Vaziri, N.D. (2013). Targeting the transcription factor Nrf2 to ameliorate oxidative stress and inflammation in chronic kidney disease. Kidney International, 83, 1029–1041. doi: 10.1038/ki.2012.439.

Saw, C.L.L., & Kong, A.-N.T. (2011). Nuclear factor-erythroid 2-related factor 2 as a chemopreventive target in colorectal cancer. Expert Opinion on Therapeutic Targets, 15, 281–295.

Schrader, C., & Rimbach, G. (2011). Determinants of paraoxonase 1 status: genes, drugs and nutrition. Current Medicinal Chemistry, 18, 5624–5643.

Siriwardhana, N., Shahidi, F., & Jeon, Y.-J. (2006). Potential antioxidative effects of cactus pear fruit (*Opuntia ficus-indica*) extract on radical scavenging and dna damage reduction in human peripheral lymphocytes. Journal of Food Lipids, 13, 445–458. doi: 10.1111/j.1745-4522.2006.00065.x.

Slimen, I.B., Najar, T., & Abderrabba, M. (2017). Chemical and antioxidant properties of betalains. Journal of Agricultural and Food Chemistry, 65, 675–689. doi: 10.1021/acs.jafc.6b04208.

Stintzing, F.C., Conrad, J., Klaiber, I., Beifuss, U., & Carle, R. (2004). Structural investigations on betacyanin pigments by LC NMR and 2D NMR spectroscopy. Phytochemistry, 65, 415–422. doi: 10.1016/j.phytochem.2003.10.029.

Stintzing, F.C., & Carle, R. (2004). Functional properties of anthocyanins and betalains in plants, food, and in human nutrition. Trends in Food Science & Technology, 15, 19–38. doi: 10.1016/j.tifs.2003.07.004.

Strack, D., Vogt, T., & Schliemann, W. (2003). Recent advances in betalain research. Phytochemistry, 62, 247–269.

Tesoriere, L., Butera,D., D'Arpa, D., Di Gaudio, F., Allegra, M., Gentile, C. & Livrea, M.A. (2003). Increased resistance to oxidation of betalain-enriched human low density lipoproteins. Free Radical Research, 37, 689–696.

Tesoriere, L., Allegra, M., Butera, D.,& Livrea,M.A.(2004). Absorption, excretion, and distribution of dietary antioxidant betalains in LDLs: potential health effects of betalains in humans. The American Journal of Clinical Nutrition, 80, 941–945.

Tesoriere, L., Butera, D., Pintaudi, A.M., Allegra, M., & Livrea, M.A. (2004). Supplementation with cactus pear (*Opuntia ficus-indica*) fruit decreases oxidative stress in healthy humans: a comparative study with vitamin C. The American Journal of Clinical Nutrition, 80, 391–395.

Vergara, C., Cancino-Madariaga, B., Ramírez-Salvo, A., Sáenz, H., Robert, P., & Lutz, M. (2015). Clarification of purple cactus pear juice using microfiltration membranes to obtain a solution of betalain pigments. Brazilian Journal of Food Technology, 18, 220–230. doi: 10.1590/1981-6723.5014.

Zielińska-Przyjemska, M., Olejnik, A., Kostrzewa, A., Łuczak, M., Jagodziński, P.P., & Baer-Dubowska, W.(2012). The beetroot component betanin modulates ROS production, DNA damage and apoptosis in human polymorphonuclear neutrophils. Phytotherapy research: PTR, 26, 845–852.

Zielińska-Przyjemska, M., Olejnik, A., Dobrowolska-Zachwieja, A., Łuczak, M., Baer-Dubowska, W. (2016). DNA damage and apoptosis in blood neutrophils of inflammatory bowel disease patients and in Caco-2 cells *in vitro* exposed to betanin. Postępy Higieny i Medycyny Doświadczalnej, 70, 265–271. doi: 10.5604/17322693.1198989.

Betalaini-prirodni pigmenti za zdravu hranu

Dusan Paunovic[1], Branka Stojanovic[1], Danica Dimitrijevic[1], Jovana Krstic[1], Danijela Kostic[2]

1-Union Nikola Tesla Univerzitet u Beogradu, Fakultet primenjenih nauka, Srbija
2-Univerzitet u Nišu, Prirodno-matematički fakultet, Departman za hemiju, Visegradska 33, 18000 Nis, Serbia

Sažetak

Primena veštačkih boja u praksi pokazala je mnoge negativne efekte na bezbednost hrane i zdravlje ljudi. Veštačke boje vrlo često izazivaju alergijske reakcije, posebno kod dece. Neka istraživanja ukazuju da dugotrajna upotreba veštačkih boja može biti uzrok kancera. Betalaini su jedna od najrasprostranjenijih grupa biljnih pigmenata, koja se u poslednje vreme sve više istražuje zbog čega je upotreba jeftinih biljnih pigmenata kao što su betalaini važna. Bezbedni su za upotrebu u hrani i imaju dobra biološka i farmakološka svojstva. Neki od njih imaju antioksidativna, antimikrobna, antlipidemijska, antikancerogena svojstva. Mogu se koristiti u hrani umesto antocijanina. Zahvaljujući tome se mogu koristiti za poboljšanje ukusa i boje sladoleda, želea, džema, deserta, soseva, slatkiša, paste od paradajza, žitarica za doručak.

Ključne reči: betalaini, izolovanje, identifikacija, stabilnost, zdravstvena korist, primena

Pigments naturels à la base de bétalaïnes pour une alimentation saine

Dusan Paunović[1], Branka Stojanović[1], Danica Dimitrijević[1], Jovana Krstić[1], Danijela Kostić[2]

1-Université Union Nikola Tesla de Belgrade, Faculté des sciences appliquées, Serbie
2-Université de Niš, Faculté des sciences naturelles et des mathématiques, Département de chimie, Višegradska 33, 18000 Niš, Serbie

Résumé

L'application des colorants artificiels dans la pratique a montré de nombreux effets négatifs concernant la sécurité alimentaire et la santé humaine. Des réactions allergiques aux colorants artificiels sont très fréquentes, en particulier chez les enfants. Certaines recherches démontrent que l'utilisation prolongée de couleurs artificielles peut être la cause du cancer. Des bétalaïnes représentent l'un des groupes de pigments végétaux les plus répandus, qui fait de plus en plus l'objet de recherches ces derniers temps. C'est pourquoi l'utilisation des pigments végétaux coûtant moins cher, tels que les bétalaïnes, est importante. Ils sont sûrs à utiliser dans les aliments et ont de bonnes propriétés biologiques et pharmacologiques. Certains d'entre eux ont des qualités antioxidantes, antimicrobiennes, antiépidémiques et anticancéreuses. Ils peuvent être employés dans les aliments au lieu des anthocyanes. Grace à cela, ils peuvent être utilisés pour rehausser la saveur et la couleur des glaces, gelées, confitures, desserts, sauces, sucreries, pâte de tomates, céréales pour le petit déjeuner.

Mots-clés: bétalaïnes, isolement, identification, stabilité, bénéfice sanitaire, application

Беталаины - натуральные пигменты для здорового питания

Душан Паунович[1], Бранка Стоянович[1], Даница Димитриевич[1], Йована Крстич[1], Даниела Костич[2]

1-Университет «Юнион Никола Тесла» в Белграде, Факультет прикладных наук, Сербия
2-Университет в Нише, Естественно-математический факультет, Кафедра химии, Вишеградска 33, 18000 Ниш, Сербия

Аннотация

Применение искусственных красителей на практике показало множество отрицательных последствий для безопасности пищевых продуктов и здоровья человека. Аллергические реакции на искусственные красители очень распространены, особенно у детей. Некоторые исследования показывают, что длительное использование искусственных красителей может стать причиной рака. Беталаины является одной из наиболее распространенных групп растительных пигментов, исследования которых ведутся в последнее время все активнее. Поэтому важно использовать дешевые растительные пигменты, такие как беталаин. Они безопасны для употребления в пищу и обладают хорошими биологическими и фармакологическими свойствами. Некоторые из них обладают антиоксидантным, противомикробным, антипидемическим, противораковым действием. Их можно употреблять в пищу вместо антоцианов. Некоторые свойства полезны для нашего здоровья, благодаря чему их можно использовать для улучшения вкуса и цвета мороженого, желе, джемов, десертов, соусов, сладостей, томатной пасты, сухих завтраков.

Ключевые слова: беталаины, изоляция, идентификация, стабильность, применение, польза для здоровья

Betalaine - natürliche Pigmente für gesunde Ernährung

Dusan Paunović[1], Branka Stojanović[1], Danica Dimitrijević[1], Jovana Krstić[1], Danijela Kostić[2]

1-Union Nikola Tesla Universität Belgrad, Fakultät für Angewandte Wissenschaften, Serbien
2-Universität Niš, Fakultät für Naturwissenschaften und Mathematik, Department für Chemie, Višegradska 33, 18000 Niš, Serbien

ABSTRAKT

Die Anwendung künstlicher Farbstoffe in der Praxis hat viele negative Auswirkungen auf die Lebensmittelsicherheit und die menschliche Gesundheit gezeigt. Allergische Reaktionen auf künstliche Farbstoffe sind sehr häufig, insbesondere bei Kindern. Einige Untersuchungen weisen darauf hin, dass eine längere Verwendung künstlicher Farbstoffe die Ursache für Krebs sein kann. Betalaine sind eine der am weitesten verbreiteten Gruppen von Pflanzenpigmenten, die in jüngster Zeit zunehmend erforscht wird. Daher ist die Verwendung billiger Pflanzenpigmente wie Betalaine wichtig. Sie sind sicher für die Verwendung in Lebensmitteln und haben gute biologische und pharmakologische Eigenschaften. Einige von ihnen haben antioxidative, antimikrobielle, antlipidemische und krebsbekämpfende Eigenschaften. Sie können in Lebensmitteln anstelle von Anthocyanen verwendet werden. Einige Eigenschaften sind für unsere Gesundheit von Vorteil, dank dessen sie dafür verwendet werden können, um den Geschmack und die Farbe von Eis, Gelees, Marmeladen, Desserts, Saucen, Süßigkeiten, Tomatenmark und Frühstückszerealien zu verbessern.

Schlüsselwörter: *Betalaine, Isolation, Identifizierung, Stabilität, Anwendung, Nutzen für die Gesundheit*

Eco-friendly polymer succinate capping on silver nano-particles for enhanced stability: a UV-Vis and electrochemical particle impact study

Azhar Abbas [1,2,*], Hatem M. A. Amin [1,5], Muhammad Akhtar [3,4], Muhammad A. Hussain[2], Christopher Batchelor-McAuley[1], Richard G. Compton [1]

1- Oxford University, Department of Chemistry, Physical and Theoretical Chemistry Laboratory, South Parks Road, Oxford, OX1 3QZ, United Kingdom

2- University of Sargodha, Department of Chemistry, Ibne Sina Block, Sargodha 40100, Pakistan

3- Islamia University of Bahawalpur, Faculty of Pharmacy and Alternative Medicine, Department of Pharmacy, Bahawalpur 63100, Pakistan.

4- King's College London, Faculty of Life Sciences & Medicine, School of Cancer and Pharmaceutical Sciences, London, SE1 9NH, United Kingdom.

5- Cairo University, Faculty of Science, Department of Chemistry, Giza, 12613 Egypt

Azhar Abbas: azharabbas73@yahoo.com
Hatem M. A. Amin: hatem@pc.uni-bonn.de
Muhammad Akhtar: muhammad.akhtar@iub.edu.pk
Muhammad A. Hussain: majaz172@yahoo.com
Christopher Batchelor-McAuley: christopher.batchelor-mcauley@chem.ox.ac.uk
Richard G. Compton: richard.compton@chem.ox.ac.uk

[*]Azhar Abbas: azhar.abbas@chem.ox.ac.uk; azharabbas73@yahoo.com

Phone: +44 (0) 7448775793

ABSTRACT

A facile green method is used to synthesize silver nanoparticles (Ag Nps) in one minute. The colloidal stability of two types of Ag Nps (namely, hydroxypropylcellulose-succinate (HPC-Suc) capped silver nanoparticles (Ag Nps@suc) and citrate-capped silver nanoparticles (Ag Nps@cit)) is investigated using UV-Vis spectrometry and electrochemical particle impacts "nano-impacts" measurements. Ag Nps@suc were newly synthesized by simply mixing aqueous solutions of HPC-Suc and silver nitrate and exposure to sunlight. The growth of Ag Nps was controlled by adjusting the exposure time to sun light. Local surface plasmon resonance (LSPR) study was conducted using UV-Vis spectrophotometer. The surface morphology, size, elemental analysis and composition of Ag NPs@suc was determined by SEM-EDX, while ATR-FTIR was used to assess any type of chemical reactions between the precursors. For stability and size distribution measurements zeta-potential (ZP), dynamic light scattering (DSL) and anodic particle coulometry (APC) were performed. The as-prepared Ag Nps@suc exhibited a narrow size distribution with an average diameter of 20 nm. Nps sizing using particles electrochemical impacts method is consistent with SEM and DLS techniques. The results show that Ag Nps@cit are prone to relatively rapid clustering upon addition of electrolyte (100 mM K_2SO_4). On the other hand, Ag Nps@suc exhibit excellent stability with only ~ 9% decay in absorbance over 24 h even at high electrolyte concentration. Using KCl, KBr and NaCl electrolytes, the stability of the synthesized Ag Nps@suc also compares favorably to Ag Nps@cit.

Keywords: Silver nanoparticles, Succinate capping agent, Nanoparticle stability, UV-Vis spectrometry, Nanoparticle-electrode impact

Introduction

There are numerous nano-enabled products of silver in the market, *e.g.*, sportswear, medical implants, bioimaging, biosensors *etc.*, which make use of increased catalytic activity (Amin et al., 2015; Amin et al., 2017), electrical conductivity (Hayward et al., 2000; Shipway et al., 2000; Shamaila et al., 2016), anticancer (Mfouo-Tynga et al., 2014; Zhao et al., 2014) and antibacterial characteristics of Ag Nps (Khan et al., 2014) as compared with bulk silver.

Ag Nps undergo several changes such as aggregation, agglomeration, dissolution or surface adsorption. The occurrence of the reaction depends on nanoparticles properties and their local environment (Baalousha, 2017; Peijnenburg et al., 2015). These changes in structure and chemical properties will influence the particle transport, diffusion, reactivity and toxicity (Afshinnia et al., 2017). Clustering (agglomeration and/or aggregation) of Nps reduces their opportunity of uptake into biological systems (Jang et al., 2014). Conversely, increased stability of aqueous dispersions of the Ag Nps may increase environmental persistence (Stuart et al., 2013). For instance, the stability of Ag Nps has been shown to be a crucial factor for their long-term antimicrobial durability (Korshed et al., 2018). Laser generated Ag Nps show 10 days longer activity as compared to chemically modified Ag Nps when tested for an air exposure of 45-days (Korshed et al., 2018).

Different capping agents including natural compounds are used to stabilize Ag Nps (Banach and Pulit-Prociak, 2017). The nature of capping agent affects the size and appearance of the NPs and their interaction with solvent (Raveendran et al., 2003). Therefore, capping agent plays a vital role in the nanoparticle synthesis process.

Carboxylic acid based capping agents are widely used for the capping of Nps because carboxyl groups are recognized as active functional groups for reducing Ag^+ (Bastús et al., 2014). Moreover, carboxylic acids are known to coordinate effectively to Ag Nps (Xie et al., 2007). Among all carboxylic acid capping agents, citrate reduction of silver ions remains the overwhelmingly most popular method to quickly form citrate capped silver nanoparticles (Ag Nps@cit) (Bastús et al., 2014). However, a significant drawback of the Ag Nps@cit is their low stability in electrolyte solutions (Huynh and Chen, 2011).

Nanoparticles stabilized by polymers carrying functional groups are relatively stable (Richard et al., 1991). Coordination of the hydroxyl group of polyethylene glycol (PEG) and polyvinyl alcohol (PVA) to Ag Nps is relatively less effective as compared to carboxylic acids and this limits their use as stabilizing and capping agent (Luo et al., 2005). Polymers carrying carboxylic acid functional groups may be employed to synthesize stable Ag Nps with enhanced stability. The carboxylic acid functional group has

been widely exploited for surface modification of cellulose based polymers (Abbas et al., 2015). Recently, AgNps were developed from a soy protein that contains a large number of hydroxyl groups and has been used as capping and reducing agent, employing one-pot solid state method (Abdelgawad et al., 2017). The hydroxyl groups can help the co-ordination of Ag^+ to the molecular matrix. COOH groups can easily be built on to polysaccharides such as hydroxypropyl cellulose (HPC) by esterification using cyclic anhydrides (*e.g.*, succinic anhydride) (Abbas et al., 2015). These carboxylated polymers are expected to have high attachment of succinate groups which might be exploited for the reduction of Ag^+ to form stable metal Nps. Moreover, if COOH carrying polysaccharides are used to prepare and to cap nanoparticles, their resulting surfaces will also be capped with polysaccharide chains *via* succinate linkers which may further stabilize the formed nanoparticles *via* surface adsorption.

In this study, we evaluate the stability of novelly-synthesized hydroxypropyl cellulose succinate (HPC-Suc) capped Ag Nps using UV-Vis and nano-impacts against agglomeration/aggregation. Herein, nano-impacts is based on anodic particle coulometry (APC) approach which is used to size metal nanoparticles by oxidizing them upon collision with a micro electrode. The as-synthesized Ag Nps@suc were characterized using different spectroscopic and electrochemical techniques. UV-Vis and nano-impacts results revealed significant and useful enhancement in stability of Ag Nps@suc compared to that of Ag Nps@cit. Based on the natural origin of the used cellulose-containing reducing and capping agent, our method can be described as eco-friendly and could have further emerging applications.

Experimental

Materials

Hydroxypropyl cellulose (HPC) (3.46 moles of hydroxypropyl per mole of glucose unit) was provided by a Chinese company, Nanjing Yeshun Industry and International Trading Co. Ltd. Before use it was vacuum dried at 110°C for 5 h. Succinic anhydride was acquired from Fluka. All solvents used were of analytical grade. Silver nitrate, potassium chloride, sodium chloride, potassium sulphate and potassium bromide having maximum reported purity were purchased from Sigma Aldrich. All solutions were prepared with deionized water (18.2 MΩ cm resistivity at 25°C). Spherical citrate capped Ag Nps (Ag Nps@cit) of about 20 nm diameter were synthesized and characterized as previously reported (Lees et al., 2013).

Synthesis of hydroxypropyl cellulose-succinate-capped silver nanoparticles (Ag Nps@suc)

Hydroxypropyl cellulose succinate (HPC-Suc) was synthesized as reported (Abbas et al., 2015). HPC-Suc (100 mg) was dissolved in 10 mL of deionized water (10 mL) and added to 50 mM $AgNO_3$ aqueous solution (10 mL) in the dark. The resultant mixture was then kept in sunlight and progress of the reaction was checked periodically using UV-Vis spectrophotometer. Over a period of 25 min of exposure to sunlight the color of the solution was turned from colorless to light yellow and then to dark brown (Figure 1). This color change is attributed to the formation of Ag Nps@suc of different sizes. The solution was centrifuged for 30 min at 4400 rpm after exposure to sunlight for 60 s and the supernatant containing some unreacted material was removed, leaving solid Ag Nps@suc at the bottom of a falcon tube. Deionized water was added to the tube and centrifuged further for 30 min at 4400 rpm in order to remove any unreacted material. This washing was carried out twice. After washing, solid sample of Ag Nps@suc was isolated and 15 mL of deionized water was added to solid Ag Nps@suc and sonicated for 15 min. This gave a suspension of Ag Nps@suc which was used as a stock for additional studies. This suspension was analysed for quantitation using UV-Vis spectrophotometer (Ngamchuea et al., 2017). The synthesized Ag Nps@suc were also characterized using ATR-FTIR, SEM-EDX, DLS, ZP measurements and impact electrochemistry.

Characterization of Ag Nps@suc

UV-Vis spectrophotometry

UV-Vis experiments were carried out with a Shimadzu UV-1800 spectrophotometer in high precision quartz cells (Hellma Analytics, Germany) having an optical path length of 10 mm. A baseline correction was made with empty cells inside the instrument prior to each experiment. The absorbance was recorded from 300-800 nm. 12 pM solution of Ag Nps@suc and Ag Nps@cit were used to record the UV-Vis spectra.

Stabilities of the Ag Nps@suc and Ag Nps@cit in different electrolytes solutions

UV-Vis experiments (300-800 nm) were also carried out to study the stabilities of 4 pM and 12 pM of Ag Nps@suc and Ag Nps@cit, respectively each in 2 mM, 20 mM and 100 mM of KCl, KBr, NaCl or K_2SO_4 electrolyte solutions over a period of 24 h.

SEM-EDX characterization

High-resolution SEM equipped with EDX (Zeiss Merlin Field Emission Gun (FEG)-SEM) was used to probe the morphology, size, elemental analysis and composition of Ag Nps@suc. The SEM-EDX images were recorded at 5 kV acceleration voltage. As a substrate for the SEM sample, a glassy carbon (GC) plate was used. Previously, the GC plate was immersed in aqua-regia and then was rinsed with nanopure water followed by mechanical polishing with successively smaller diameter alumina powder (1.0 µm, 0.3 µm and 0.05 µm; Buehler, USA) slurries with nanopure water on lapping pads (Buehler, USA). Area calculations and particle size analysis were carried out by ImageJ software.

ATR-FTIR characterization

FTIR spectra of HPC, HPC-Suc and Ag Nps@suc were recorded using a FTIR spectrometer (IRAffinity-1S, SHIMADZU, Japan) equipped with a diamond ATR device (SHIMADZU). FTIR measurements were performed in the range of 400–4000 cm^{-1}. Each spectrum represents an average of 20 scans with 2 cm^{-1} resolution to increase the signal to noise ratio.

DLS and ZP measurements

In order to determine the hydrodynamic diameter, ZP and the stability of the nanoparticles (Ag Nps@suc and Ag Nps@cit), a Malvern Zetasizer Nano ZS was used. The measurements were done using a 633 nm He-Ne laser. To remove any solid contaminants the sample suspension was filtered using Whatman 0.2 µm filter. The filtered sample was hold in a solvent-resistant micro cuvette with a path length of 10 mm. Every sample was equilibrated at 25°C for 2 min in instrument before analysis. Three sets of 12 light scattering measurements were recorded and results were presented as mean ± SD. To measure ZP, AgNPs suspension was placed in disposable folded capillary cells. The Zetasizer software from Malvern was used to analyze the data.

Nano-impacts

A three-electrode arrangement was used in all electrochemical experiments. The cell and the electrodes were placed in a thermally controlled Faraday cage at 25°C. A home-built low noise potentiostat was used to carry out nano-impact experiments. The analog signal was filtered and digitized at a rate of 50 kHz by applying two cascaded RC filters of 100 Hz. This was followed by digital filtering using a four pole Bessel filter (100 Hz). The equipment was validated for the total charge transferred in an impact event (Batchelor-McAuley et al., 2015; Kätelhön et al., 2016). These experiments were performed using a carbon microdisc of 33 µm diameter (IJ Cambria Scientific Ltd, UK) serving as the working

electrode and a leakless Ag/AgCl (in 3.4 M KCl, eDAQ) as a reference electrode while a platinum wire was used as a counter electrode. For sizing the Ag Nps@suc, current-time measurements were performed using a 12 pM solution of Ag Nps@suc in 20 mM KCl by holding the working electrode at 0.8 V against leakless Ag/AgCl for 50 s per scan. In addition to the chronoamperometry experiments, cyclic voltammetry was also carried out to calculate diameter of Ag Nps@suc using the same concentration of Ag Nps@suc (12 pM solution of Ag Nps@suc in 20 mM KCl) at a scanning rate of 50 mV per second. Nano-impact spikes collected from both chronoamperometric and cyclic voltammetric experiments were identified and analyzed to calculate the charge using SignalCounter software developed by Dario Omanovic (Croatia). In order to have an insight into agglomeration state of AgNps, nano-impact experiments were carried out with 12 pM solution of Ag Nps@suc or Ag Nps@cit each in 100 mM K_2SO_4 by holding the working electrode at 0.8 V against leakless Ag/AgCl for 50 s per scan over a time of solution for 3 h.

Results and Discussion

This section reports the synthesis and characterization of Ag Nps@suc. The synthesized Ag Nps@suc were evaluated using the techniques including UV-Vis, SEM-EDX, DLS and ZP, ATR-FTIR and nano-impacts. The clustering of Ag Nps@suc and Ag Nps@cit was investigated using UV-Vis spectrophotometry and nano-impacts in K_2SO_4. This section also reports the stabilities of both types of Nps studied in different concentrations of the electrolytes KCl, KBr and NaCl.

Synthesis of Ag Nps@suc

The aqueous solution of HPC-Suc was mixed with $AgNO_3$ aqueous solution and exposed to sunlight. The color of solution started changing immediately after exposure to sunlight indicating formation of Ag Nps@suc. The synthesized Ag Nps@suc suspensions exhibited different colors at different sunlight exposure times. A photograph showing the color change upon exposure of the mixture to sunlight is presented in Figure 1.

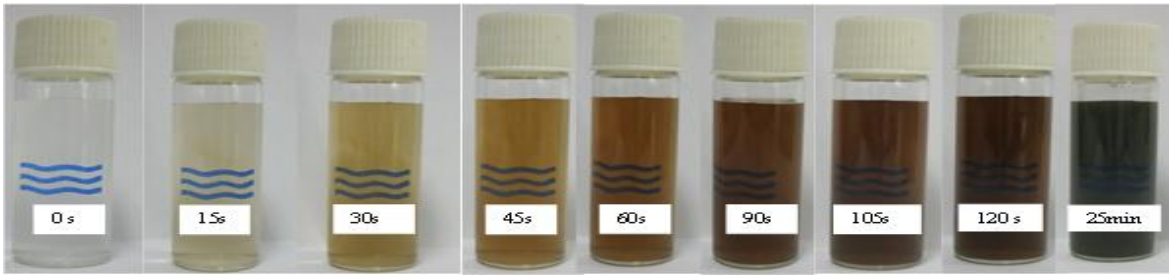

Figure 1. Photographs of mixture of HPC-Suc and Ag^+ solutions showing a change in color due to reduction of Ag^+ upon different time of exposure to sunlight

The change in color of these Ag Nps@suc suspensions upon exposure to sunlight is likely due to reduction of Ag^+ to Ag^0 forming hydroxypropyl cellulose succinate capped silver nanoparticles (Ag NPs@suc). Figure 2B shows the proposed scheme of synthesis of Ag Nps@suc by light induced reduction of Ag^+. The carboxylate groups of HPC-Suc are thought to reduce Ag^+ to Ag^0 (upon exposure to light) to form Ag Nps accompanied by decarboxylation of the reducing agent (Stankus et al., 2010). These succinate groups of HPC-Suc are thought to act as capping agents in addition to their role as a reducing agent.

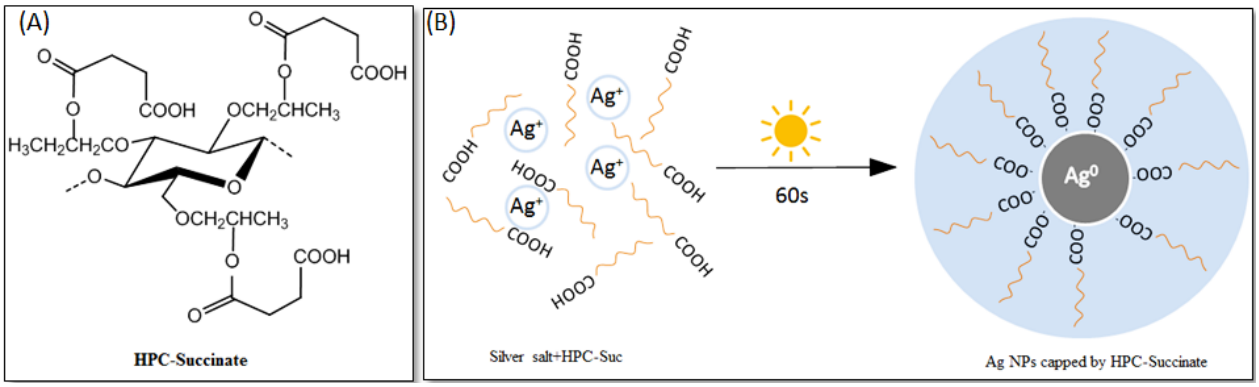

Figure 2. (A) Structure of HPC-Suc and (B) likely structure of Ag Nps-capped with HPC-Suc

Characterization of Ag Nps@suc

The UV-Vis, SEM-EDX, DLS and ZP, ATR-FTIR and nano-impacts were used for characterization of synthesized Ag Nps@suc. UV-Vis spectrometry showed that the collective oscillation of conduction electrons in Ag NPs@suc results in LSPR with a single and broad LSPR peak was observed in the range 411-452 nm confirming the synthesis of Ag Nps (Section S1, Figure S1) (Mulvaney, 1996). The size and morphological characterizations of Ag Nps@suc were determined by

SEM-EDX (Table 1). SEM images are provided in Section S2 in the Supplementary Information. Figure 3C shows the histogram for the distribution of AgNps@suc sizes determined by SEM. The Ag Nps were mostly spheroid shaped and a mean diameter value of 19.6 ± 6.8 nm was calculated (Figure S2A-D). Elemental EDX mapping (Figure S2 E-G) of Ag Nps@suc shows that Ag Nps are randomly dispersed throughout the Ag Nps@suc sample. The EDX elemental analysis also showed the presence of the elements (Ag, C and O) expected to be present in the Ag Nps@suc (Figure S3). To find out various functional groups present in HPC-Suc and Ag Nps@suc ATR-FTIR spectra of HPC, HPC-Suc and Ag Nps@suc were recorded as shown in Section S3 (Figure S4). The ATR-FTIR spectrum of HPC shows absorption bands at 3433, 2902 and 1160-1057 cm^{-1} indicating the presence of –OH, -CH_2- and C-O-H and C-O-C bonds, respectively. The appearance of absorption peaks in the FTIR spectrum of HPC-Suc at 1726, 1618, 1399, 1260 and 1140-1007 cm^{-1} due to C=O, COOH, C-O, C-O-H and C-O-C bonds, respectively is attributed to the successful esterification of of HPC to form HPC-Suc. The FTIR spectrum of Ag Nps@suc showed bands closely similar to those in FTIR spectrum of HPC-Suc. Retention of all these signals with the expected slight shift of frequency, in the ATR-FTIR spectrum of Ag Nps@suc is a strong evidence that HPC-Suc is present as capping agent of Ag in this study.The shifting of the C=O signal to 1724 cm^{-1}, -COOH signal to 1602 cm^{-1}, C-O signal to 1293 cm^{-1}, C-O-H, C-O-C signal to 1020-1057 cm^{-1} and the appearance of a 527-569 cm^{-1} signal due to Ag---O weak interactions in FTIR spectrum of Ag Nps@suc shows a success of reduction and capping of Ag^+ to form Ag Nps by HPC-Suc (Gupta et al., 2010; Shameli et al., 2012).

The ZP value measured for Ag Nps@suc (in water) was -31.8 ± 2.4 mV (Figure S5A). The higher and longer stability of nanoparticles is due to relatively high values of negative ZP. The size of Ag Nps@suc was also measured by DLS and the z-average was found to be 19.7 ± 1.7 nm (Section S4, Table 1, Figure S5 B).

In addition to SEM and the DLS measurements, the size of Ag Nps@suc was also investigated using nano-impacts experiments. Nanoparticle-electrode impacts embraces APC and record single events through the generation of electrochemical signal by a redox reaction taking place on a nanoparticle. The oxidation of silver nanoparticles is a model of the well characterized system and the electrode reaction in this case can be described as (Allerston and Rees 2018; Sokolov et al., 2017; Stevenson and Tschulik, 2017):

$$Ag_N \rightarrow N\,Ag^+ + Ne^- \qquad (1)$$

In the present study, a 12 pM solution of Ag Nps@suc in 20 mM KCl was subjected to APC measurement. Ag Nps@suc diffuse through the solution under Brownian movement and collide with the carbon microelectrode of 33 µm diameter held at a suitable oxidising potential (in this case +0.8V). Oxidation of Ag Np takes place from Ag^0 to Ag^+ (likely resulting in the formation of AgCl) (Ngamchuea

et al., 2017b) generating a current 'spike'. These spikes can be recorded as current-time transients or through a cyclic voltammogram. The later type of measurement is helpful for knowing the potential at which the potential oxidation onset. The area under a single nano-impact spike corresponds to the total charge required for the oxidation of the colliding Ag Nps. The size of the later can be estimated by Eq. 2 which assumes that silver nanoparticle is spherical and is fully oxidized (Little et al., 2018):

$$r = \sqrt[3]{\frac{3MQ}{4\pi Fz\rho}} \quad (2)$$

where r is the radius of Ag Nps@suc, M is the atomic mass of silver (107.9 g mol^{-1}), Q is the charge calculated from area under each 'spike', z is the number of electrons transferred per oxidised silver atom, F is the Faraday constant (96485 C mol^{-1}), and ρ is the density of bulk silver (10.5×10^{6} g m^{-3}). Figure 3A displays a typical current-time transient.

In addition to nano-impact studies carried out using chronoamperometry at a fixed potential, cyclic voltametry is also be employed to calculate the diameter of Ag Nps@suc. In the present case, 12 pM solution of Ag Nps@suc in 20 mM KCl was used and voltammograms were recorded as soon as the solution was prepared using a three electrode system containing carbon micro-electrode of 33 µm diameter at a scan rate of 50 mV s^{-1}. These voltammograms were analysed and the area under each spike was calculated again. Figure 3B shows a typical voltammogram. The area under each spike is related to charge transferred during a single nanoparticle oxidation event. This area is divided by scan rate to get charge, Q. The charge calculated from chronoamperometric and cyclic voltametric spikes is combined. Eq. 2 is used to get the radius and hence diameter or size of the Ag Np. In the present study total of 1036 spikes from 8 scans were analysed and a mean diameter of Ag Nps@suc was calculated to be 16.7 ± 3.3 nm. This value is in a good agreement with results obtained from SEM and DLS as shown in Table 1. Figure 3C shows the distribution of AgNps@suc sizes obtained independently from nano-impacts and SEM; good agreement is apparent. SEM and impacts assume particles as spheres. Table 1 shows the characteristics parameters for the as synthesized silver nanoparticles.

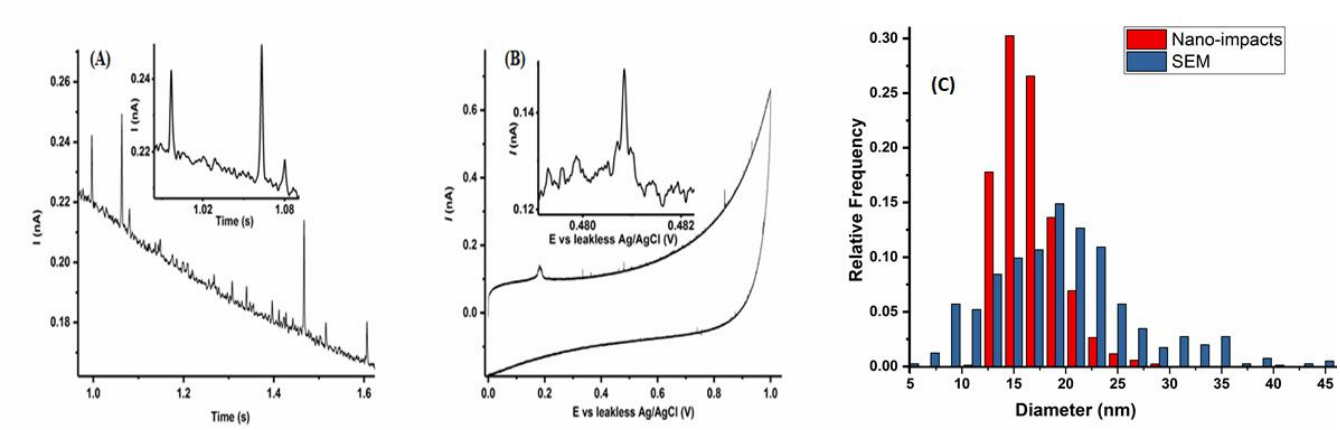

Figure 3. (A) Chronoamperogram at E= +0.8 V *vs* leakless Ag/AgCl (inset depicts the enlarged chronoamperogram) (B) Cyclic voltammogram at scan rate 50 mVs^{-1} (inset depicts the enlarged voltammogram) showing nano-impact spikes of 12 pM Ag Nps@suc in 20 mM KCl using 33µm carbon microdisc electrode, leakless Ag/AgCl reference electrode and platinum counter electrode and (C) The histograms show the distribution of AgNps@suc sizes calculated from the charge of nano-impact spikes of 12 pM Ag Nps@suc oxidation events in 20 mM KCl electrolyte solutions compared with sizes determined by SEM

Table 1. Sizing results of the as-synthesized Ag Nps@suc

Method	Diameter (nm)
Nano-impacts	16.7±3.3
SEM	19.8±6.8
DLS (z-ave)	19.7±1.7

Determination of the concentration of Ag Nps@suc in a suspension

On the basis of the diameter (ca. 20 nm) of Ag Nps@suc determined by SEM, the concentration of a Ag Nps suspension was estimated by UV-Vis and was found to be 189 ± 6.5 pM using the procedure of Ngamchuea and co-workers (Ngamchuea et al., 2017). Details are available in Section S5 of the Supplementary Information.

Stability study of Ag Nps in K_2SO_4 (citrate *vs* succinate capping)

The stability of the Ag Nps@suc was studied in K_2SO_4 electrolyte using UV-Vis and nano-impacts measurements and compared with the stability of Ag Nps@cit. Two different concentrations of the synthesized Ag Nps@suc (4 pM and 12 pM) were examined in three different concentrations (2 mM,

20 mM and 100 mM) of K_2SO_4 using UV-Vis and the results were compared with those from Ag Nps@cit in order to provide insights into the relative clustering rates of the Ag Nps@suc and Ag Nps@cit at different concentrations of K_2SO_4. Besides UV-Vis, the clustering state of the Ag Nps was also investigated using the nano-impact technique in 100 mm K_2SO_4 where the term 'clustering' covers both agglomeration and aggregation.

Stability study of Ag Nps using UV-Vis

A comparison of the stability of succinate and citrate capped silver nanoparticles in different concentrations of K_2SO_4 was made to show that colloidal suspensions of Ag Nps@suc are significantly more stable than those of Ag Nps@cit. Figure 4 shows representative UV-Vis spectra of 12 pM silver nanoparticles (Ag Nps@suc and Ag Nps@cit) in 100 mM K_2SO_4 recorded at different time intervals after making solutions. There is a negligible decrease in absorbance (Figure 4A) with a slight shift in λ_{max} from 428.5 nm to 419.5 nm for Ag Nps@suc after 24 h. No change in peak shape is observed even after 24 h for Ag Nps@suc. On the other hand, for the Ag Nps@cit, a relatively broader peak appeared with a decrease in λ_{max} from 397.5 nm to 390 nm immediately after adding the salt (100 mM K_2SO_4) and importantly a shoulder at around 570 nm was observed in the peak. For the Ag Nps@cit, there was a significant change in the LSPR peak shape and peak height between 1 h and 24 h. The reason behind these losses might be a rapid clustering of Ag Nps@cit. Figure 5A shows a plot of absorbance against time of Ag Nps@suc and Ag Nps@cit (12 pM) in 100 mM K_2SO_4. It is clear from Figure 4B that the absorbance for Ag Nps@cit in 100 mM K_2SO_4 decreased markedly after 24 h, suggesting complete clustering of the Nps. About half of the peak decay was observed within seconds immediately after adding the electrolyte. On the contrary, Ag Nps@suc showed a little clustering as can be evidenced from only a slight decrease in absorbance over 24 h. Similar results were obtained at lower concentration of Ag Nps (4 pM of Ag Nps@suc and Ag Nps@cit in 100 mM K_2SO_4) where Ag Nps@cit lost almost one-third of the peak absorbance only within 1 h while there was only a small absorbance loss in case of Ag Nps@suc after 24 h (Figure S6 B, Table S1). This negligible decrease in absorbance in case of succinate capped silver nano-particles at high ionic strength shows that Ag Nps@suc are usefully more stable than Ag Nps@cit. The decrease in absorbance of the Ag Nps in the electrolyte is attributed to clustering of the nanoparticles.

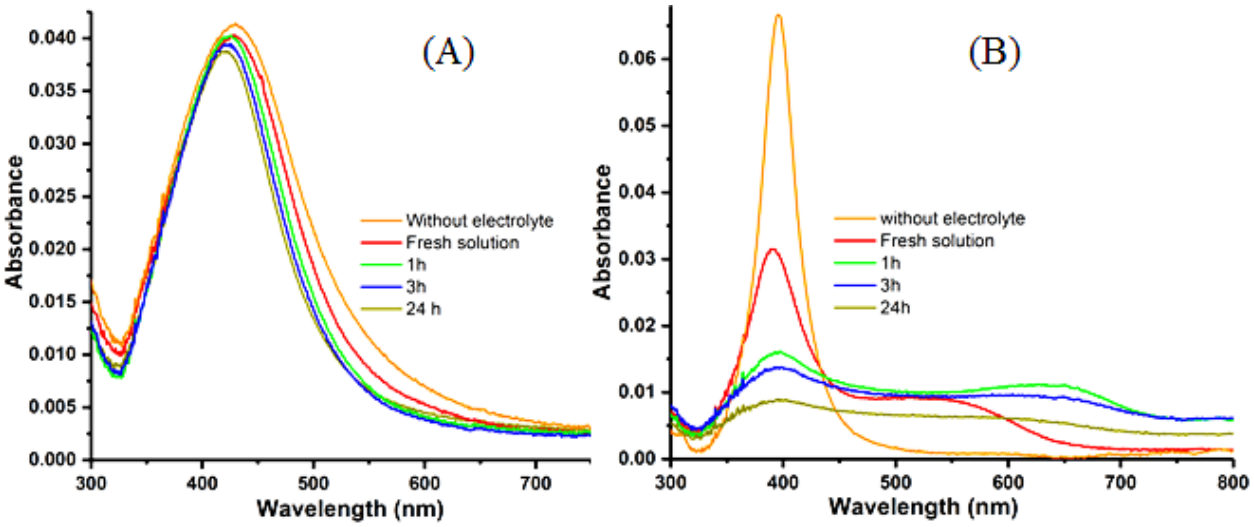

Figure 4. Representative UV-Vis spectra of (A) 12 pM Ag Nps@suc (B) 12 pM Ag Nps@cit in 100 mM K_2SO_4 over a period of 24 h. Orange lines in both spectra represent 12 pM Ag Nps without the electrolyte

At lower ionic strengths of the electrolyte (20 mM K_2SO_4) there was only a negligible loss of peak absorbance for 12 pM Ag Nps@suc. On the other hand, for 12 pM Ag Nps@cit, about half of the Ag Nps were clustered which can be seen from half of the decay in absorbance to half (Figure S6 B). For 4 pM concentration of Ag Nps in 20 mM K_2SO_4,there was almost a complete loss in absorbance for Ag Nps@cit after 24 h while for Ag Nps@suc, there was a slight decay in absorbance after the same time (Figure S6 A). All these results show that Ag Nps@suc are more stable than Ag Nps@cit. Ag Nps@suc showed a mean λ_{max} value of 425.5 ± 6.0 nm for all the concentration of Ag Nps@suc in all the studied concentrations of electrolytes. The wavelength of maximum absorbance (λ_{max}) in case of Ag Nps@cit in all concentrations of K_2SO_4 was 395.5 ± 2.0 nm.

The analyses of the absorbance data in the other concentrations of electrolyte K_2SO_4 are presented in Figure S6 and Table S1.

Stability study of Ag Nps using electrochemical Nano-impacts

The clustering of Nps in a specific liquid environment can also be investigated using the nano-impact method (Ellison et al., 2013; Jiao et al., 2017; Kätelhön et al., 2017; Rees et al., 2011; Shimizu et al., 2017). The clustering of silver nanoparticles (12 pM) in a solution containing 100 mM K_2SO_4 was studied *via* impact-based APC over a period of 3 h. Figure S7 displays representative chronoamperograms showing nano-impact spikes of 12 pM Ag Nps@suc and Ag Nps@cit in 100 mM K_2SO_4 for a fresh solution of silver nanoparticles and a solution aged for 1 h and 3 h. The charge needed for quantitative

oxidation of Ag Nps@suc and Ag Nps@cit is measured by integrating the area of nano-impact spike which is obtained when a nanoparticle collides with a micro-electrode (Suherman et al., 2018; Zampardi et al., 2018; Zhou et al., 2012). This charge is then related to the number of atoms present in the nanoparticle or nanoparticle clusters. This number of atoms is related to the number of nanoparticle monomers which in turn gives the size of each impacting clusters. Figure 5 B shows the mean size of 12 pM each of Ag Nps@suc and Ag Nps@cit in 100 mM K_2SO_4 plotted against time. It is clear from the plot that the mean size in case of Ag Nps@cit increases from 26.7 ± 8.9 nm to 35.8 ± 7.5 nm over a period of 3 h while in case of Ag Nps@suc, the size almost remains constant (17.4 ± 3.2 nm to 18.3 ± 5.1 nm). Although, both types of the Ag Nps have almost the same size (~20 nm) in stock solution, Ag Nps@cit shows a larger size (26.7 ± 8.9 nm) after the very few seconds of making the solution due to the rapid clustering of Ag Nps@cit immediately after adding the K_2SO_4 salt. This confirms the higher stability of Ag Nps@suc over Ag Nps@cit. This sudden clustering in case of Ag Nps@cit is also supported by the sudden decrease in peak absorbance in UV-Vis immediately after adding electrolyte (Figure 4 B). These clusters on colliding with the micro-electrode cause a greater oxidative charge, as they are larger. This can also be evidenced by a significant increase in duration of spike in the case of Ag Nps@cit (Figure S7 A). While in case of Ag Nps@suc no appreciable increase in size is observed showing negligible clustering in these nanoparticles.

Figure S8 B shows the frequency of spikes of 12 pM Ag Nps@suc and Ag Nps@cit in 100 mM K_2SO_4 as a function of time. The clustering in case of Ag Nps@cit can also be evidenced by a prominent reduction in frequency of spikes with time over a period of 3 h (Figure S8 B). According to the Stokes-Einstein equation (Einstein, 1905), the clustered nanoparticles will have a decreased diffusion coefficient which results in a decreased number of observable impacts at microelectrode and hence less frequency. The decrease in frequency of spikes in case of Ag Nps@cit can also be attributed to the fact that number of observed impacts decrease due to the decrease in number of the diffusing species due to clustering of Nps.

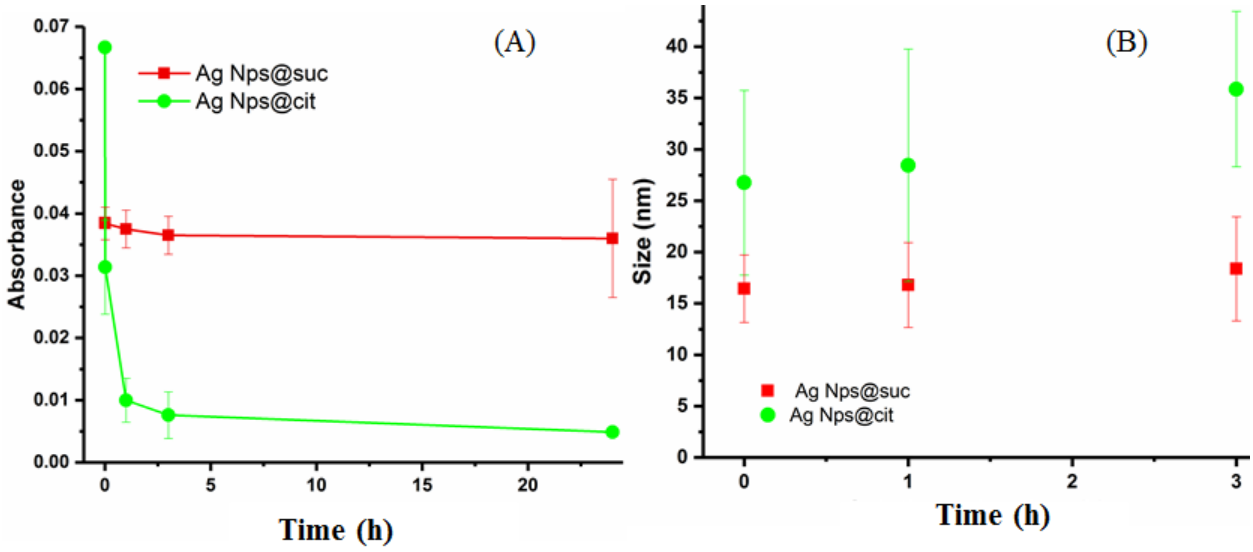

Figure 5. Absorbance (A) and mean size by nano-impact (B) as a function of time of Ag Nps@suc and Ag Nps@cit (12 pM) in 100 mM K_2SO_4

Effect of different electrolytes on clustering

The stability of the Ag Nps@suc was also studied in three other different electrolytes (KCl, KBr and NaCl) using UV-Vis and results are compared with those from Ag Nps@cit. Two different concentrations of Ag Nps solutions (4 pM and 12 pM) are studied in three different concentrations (2 mM, 20 mM and 100 mM) of all the three electrolytes.

UV-Vis spectra in different electrolytes

In order to have an insight into the stabilities of Ag Nps@suc and Ag Nps@cit, clustering of Ag Nps was also investigated in three more electrolytes (KCl, KBr and NaCl). UV-Vis spectra of different concentrations of both types of Ag Nps in different concentrations of electrolytes were recorded over a period of 24 h. Figure 6 shows representative UV-Vis spectra of fresh solutions of 12 pM silver nanoparticles (Ag Nps@suc and Ag Nps@cit) in 20 mM KCl at different time. The λ_{max} is shifted from 408.5 nm to 398.5 nm for Ag Nps@suc and from 395 nm to 391 nm for the Ag Nps@cit after 24 h (Figure 5). The λ_{max} for Ag Nps@cit in all electrolytes was 394.5 ± 4 nm. For Ag Nps@suc, the value of λ_{max} in KCl, KBr and NaCl was found to be 406 ± 6 nm. It is clear from the spectra (Figure 6), that the absorbance for Ag Nps@cit in KCl significantly decreases over time. The reason of the decrease in absorbance in Ag Nps@cit may be attributed to clustering of particles in the presence of electrolyte. Clustering of Nps is normally evidenced by a decrease in absorbance in UV spectra. On the contrary, Ag Nps@suc shows a small increase in absorbance over 24 h. Increase in absorbance of the Ag Nps in the

presence of electrolyte might be due to two reasons (i) formation of more Ag Nps due to reduction of any interested silver ions in suspension (ii) a relatively big agglomerate of silver nanoparticles disintegrate to yield more isolated particles. The first possibility can be excluded because we do not expect any silver ions after centrifugation and washing. So, the second reason could be the most probable. This hypothesis is also supported by the fact that a decrease in λ_{max} (~10 nm in all electrolytes) is observed for Ag Nps@suc solution in KCl after 24 h.

Results of analysis of the absorbance data for different concentrations of Ag Nps in different concentrations of different electrolytes are displayed in Table S2 and Figure S9. In case of 12 pM and 4 pM concentrations of Ag Nps in 20 mM and 2 mM concentrations of all the three electrolytes, the absorbance in case of Ag Nps@suc does not show any significant decrease over the period of 24 h (except in 20 mm KBr where a greater decrease in absorbance was observed as can be seen from Figure S9 D). For instance, in 20 mM NaCl, the Ag Nps@suc showed no decrease in peak absorbance after 24 h which suggested negligible clustering in these Nps and thus excellent stability. However, for the Ag Nps@cit, a greater decrease in peak absorbance in 20 mM of NaCl was found after 24 h showing higher clustering of these Nps. A complete decay in peak absorbance for Ag Nps@cit was observed in 20 mM KBr after 24 h (Figure S9 C), which could be due to significant clustering in suspension. A higher decrease in absorbance for Ag Nps@suc was observed in KBr electrolyte after 24 h but it was still less than in the case of Ag Nps@cit showing their higher stability. In case of higher ionic strength of electrolytes (100 mM), both types of Ag Nps (Ag Nps@suc and Ag Nps@cit) were almost completely clustered after 24 h but the clustering rate in both types of Ag Nps was found to be different. For instance, a very rapid loss in peak absorbance was observed for Ag Nps@cit after 1 h while in case of Ag Np@suc, there was only one-third loss in peak absorbance within the same time (Figure S9 A). This rapid decrease in absorbance after 1 h in case of Ag Nps@cit may be due to the fact that these Nps are charge stabilized while steric stabilization of Ag Nps@suc might be a reason for comparatively slow rates of clustering in these Nps. The observed significant differences in the decrease in absorbance at different ionic strengths of different electrolytes are due to preferential absorption of a specific ion which causes clustering and alters surface chemistry.

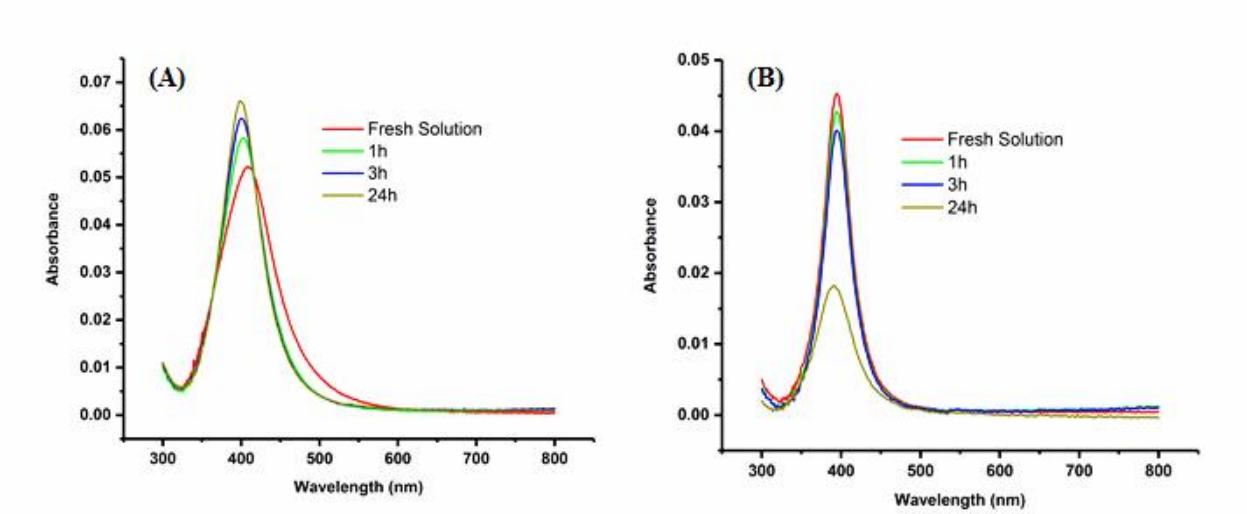

Figure 6. Representative UV-Vis spectra of (A) 12 pM Ag Nps@suc (B) 12 pM Ag Nps@cit of diameter 20 nm in 20 mM KCl over a period of 24 h

From the above results we conclude that Ag Nps@suc are more stable than Ag Nps@cit. This enhanced stability might be attributed to the inclusion of HPC polymer in the capping agent which acts as a substrate for linking carboxylic acid to the Ag Nps. Additionally, the polymer chain might help in forming uniformly capped Ag Nps thus improving the stability.

Conclusions

Stable Ag Nps@suc of diameter ~20 nm were successfully fabricated using a simplified and green strategy. LSPR peak of synthesized Ag Nps@suc was observed in the range 411-452 nm. SEM-EDX images showed that the Ag Nps were mostly randomly dispersed spheroid containing elements Ag, C and O. Sizing of NPs using nanoparticle collision method was consistent with SEM and DLS results. UV-Vis spectrometry and nano-impact studies in high concentration of K_2SO_4 showed excellent stability of developed Ag Nps@suc as compared with the widely employed Ag Nps@cit. The high stability of Ag Nps@suc is consistent with a high negative value of ZP (-31.8 ± 2.4 mV) for these nanoparticles. The high stability of such Ag Nps@suc, which are synthesized *via* a simple method, could encourage their use as a potential stable catalysts and as possible carriers in drug delivery.

Acknowledgments

A. Abbas thanks the Punjab Higher Education Commission (PHEC), Pakistan (Grant No. PHEC/A&R/FPDF/1-18/2017) for a post-doctoral grant. H. M. A. Amin thanks the German Research Foundation DFG for funding (Grant No. AB 702/1-1). M.A is a recipient of Foreign Post-Doctoral Fellowships Program FY 2016-2017 funded by Punjab Higher Education Commission (PHEC/A&R/FPDF/1-15/2017), Government of Punjab, Pakistan.

Conflict-of-Interest Statement

There are no conflicts of interest to declare.

References

Abbas, A., Hussain, M.A., Amin, M., Tahir, M.N., Jantan, I., Hameed, A., & Bukhari, S.N.A. (2015). Multiple cross-linked hydroxypropylcellulose–succinate–salicylate: prodrug design, characterization, stimuli responsive swelling–deswelling and sustained drug release. RSC Advances, 5, 43440-43448.

Abdelgawad, A.M., El-Naggar, M.E., Eisa, W.H., & Rojas, O.J. (2017). Clean and high-throughput production of silver nanoparticles mediated by soy protein via solid state synthesis. Journal of Cleaner Production, 144, 501-510.

Afshinnia, K., Sikder, M., Cai, B., & Baalousha, M. (2017). Effect of nanomaterial and media physicochemical properties on Ag NM aggregation kinetics. Journal of Colloid and Interface Science, 487, 192-200.

Allerston, L.K., & Rees, N.V. (2018). Nanoparticle impacts in innovative electrochemistry. Current Opinion in Electrochemistry, 10, 31-36.

Amin, H.M.A., Baltruschat, H., Wittmaier, D., & Friedrich, K.A. (2015). A highly efficient bifunctional catalyst for alkaline air-electrodes based on a Ag and Co_3O_4 hybrid: RRDE and online DEMS insights. Electrochimica Acta, 151, 332-339.

Amin, H.M.A., Bondue, C.J., Eswara, S., Kaiser, U., & Baltruschat, H. (2017). A carbon-free Ag–Co_3O_4 composite as a bifunctional catalyst for oxygen reduction and evolution: spectroscopic, microscopic and electrochemical characterization. Electrocatalysis, 8, 540-553.

Baalousha, M. (2017). Effect of nanomaterial and media physicochemical properties on nanomaterial aggregation kinetics. NanoImpact, 6, 55-68.

Banach, M., & Pulit-Prociak, J. (2017). Proecological method for the preparation of metal nanoparticles. Journal of Cleaner Production, 141, 1030-1039.

Bastús, N.G., Merkoçi, F., Piella, J., & Puntes, V. (2014). Synthesis of highly monodisperse citrate-stabilized silver nanoparticles of up to 200 nm: kinetic control and catalytic properties. Chemistry of Materials, 26, 2836-2846.

Batchelor-McAuley, C., Ellison, J., Tschulik, K., Hurst, P.L., Boldt, R., & Compton, R.G. (2015). *In situ* nanoparticle sizing with zeptomole sensitivity. Analyst, 140, 5048-5054.

Einstein, A. (1905). On the movement of small particles suspended in stationary liquids required by molecular-kinetic theory of heat. Annalen der Physik, 17, 549−560.

Ellison, J., Tschulik, K., Stuart, E.J.E., Jurkschat, K., Omanovic´, D., Uhlemann, M., Crossley, A., & Compton, R.G. (2013). Get more out of your data: a new approach to agglomeration and aggregation studies using nanoparticle impact experiments. ChemistryOpen, 2, 69-75.

Gupta, K., Jana, P.C., & Meikap, A.K. (2010). Optical and electrical transport properties of polyaniline–silver nanocomposite. Synthetic Metals, 160, 1566-1573.

Hayward, R.C., Saville, D.A., & Aksay, I.A. (2000). Electrophoretic assembly of colloidal crystals with optically tunable micropatterns. Nature, 404, 56-59.

Huynh, K.A., & Chen, K.L. (2011). Aggregation kinetics of citrate and polyvinylpyrrolidone coated silver nanoparticles in monovalent and divalent electrolyte solutions. Environmental Science and Technology, 45, 5564-5571.

Jang, M.-H., Bae, S.-J., Lee, S.-K., Lee, Y.-J., & Hwang, Y.S. (2014). Effect of material properties on stability of silver nanoparticles in water. Journal of Nanoscience and Nanotechnology, 14, 9665-9669.

Jiao, X., Sokolov, S.V., Tanner, E.E.L., Young, N.P., & Compton, R.G. (2017). Exploring nanoparticle porosity using nano-impacts: platinum nanoparticle aggregates. Physical Chemistry Chemical Physics, 19, 64-68.

Kätelhön, E., Sokolov, S.V., Bartlett, T.R., & Compton, R. G. (2017). The role of entropy in nanoparticle agglomeration. Chemphyschem, 18 51-54.

Kätelhön, E., Tanner, E. E. L., Batchelor-McAuley, C., & Compton, R.G. (2016). Destructive nano-impacts: What information can be extracted from spike shapes? Electrochimica Acta, 199, 297-304.

Khan, M., Khan, S.T., Khan, M., Adil, S.F., Musarrat, J., Al-Khedhairy, A.A., Al-Warthan, A., Siddiqui, M.R.H., & Alkhathlan, H.Z. (2014). Antibacterial properties of silver nanoparticles synthesized using *Pulicaria glutinosa* plant extract as a green bioreductant. International Journal Nanomedicine, 9, 3551-3565.

Korshed, P., Li, L., Ngo, D.-T., & Wang, T. (2018). Effect of storage conditions on the long-term stability of bactericidal effects for laser generated silver nanoparticles. Nanomaterials, 8, 1-12.

Lees, J.C., Ellison, J., Batchelor-McAuley, C., Tschulik, K., Damm, C., Omanovic, D., & Compton, R.G. (2013). Nanoparticle impacts show high-ionic-strength citrate avoids aggregation of silver nanoparticles. ChemPhysChem, 14, 3895-3897.

Little, C.A., Li, X., Batchelor-McAuley, C., Young, N.P., & Compton, R.G. (2018). Particle-electrode impacts: Evidencing partial versus complete oxidation via variable temperature studies. Journal of Electroanalytical Chemistry, 823, 492-498.

Luo, C., Zhang, Y., Zeng, X., Zeng, Y., & Wang, Y. (2005). The role of poly(ethylene glycol) in the formation of silver nanoparticles. Journal of Colloids and Interface Science, 288, 444-448.

Mfouo-Tynga, I., El-Hussein, A., Abdel-Harith, M., & Abrahamse, H. (2014). Photodynamic ability of silver nanoparticles in inducing cytotoxic effects in breast and lung cancer cell lines. International Journal of Nanomedicine, 9, 3771-3780.

Mulvaney, P. (1996). Surface plasmon spectroscopy of nanosized metal particles. Langmuir, 12, 788-800.

Ngamchuea, K., Batchelor-McAuley, C., Sokolov, S.V., & Compton, R.G. (2017). Dynamics of silver nanoparticles in aqueous solution in the presence of metal ions. Analytical Chemistry, 89, 10208-10215.

Ngamchuea, K., Clark, R.O.D., Sokolov, S.V., Young, N.P., Batchelor-McAuley, C., & Compton, R.G. (2017b). Single oxidative collision events of silver nanoparticles: understanding the rate-determining chemistry. Chemistry. A European Journal, 23, 16085-16096.

Peijnenburg, W.J.G.M., Baalousha, M., Chen, J., Chaudry, Q., Von der Kammer, F., Kuhlbusch, T.A.J., Lead, J., Nickel, C., Quik, J.T.K., Renker, M., Wang, Z., & Koelmans, A.A. (2015). A review of the properties and processes determining the fate of engineered nanomaterials in the aquatic environment. Critical Reviews in Environmental Science and Technology, 45, 2084-2134.

Raveendran, P., Fu, J., & Wallen, S.L. (2003). Completely "green" synthesis and stabilization of metal nanoparticles. Journal of the American Chemical Society, 125, 13940-13941.

Rees, N.V., Zhou, Y.-G., & Compton, R.G. (2011). The aggregation of silver nanoparticles in aqueous solution investigated via anodic particle coulometry. ChemPhysChem, 12, 1645-1647.

Richard, D., Couves, J.W., & Thomas, J.M. (1991). Structural and electronic properties of finely-divided supported Pt-group metals and bimetals. Faraday Discussions, 92, 109-119.

Shamaila, S., Sajjad, A.K.L., Ryma, N.-ul-A., Farooqi, S.A., Jabeen, N., Majeed, S., & Farooq, I. (2016). Advancements in nanoparticle fabrication by hazard free eco-friendly green routes. Applied Materials Today, 5, 150-199.

Shameli, K., Ahmad, M.B., Jazayeri, S.D., Sedaghat, S., Shabanzadeh, P., Jahangirian, H., Mahdavi, M., & Abdollahi, Y. (2012). Synthesis and characterization of polyethylene glycol mediated silver nanoparticles by the green method. International Journal of Molecular Sciences, 13, 6639-6650.

Shimizu, K., Sokolov, S.V., Young, N.P., & Compton, R.G. (2017). Particle-impact analysis of the degree of cluster formation of rutile nanoparticles in aqueous solution. Physical Chemistry Chemical Physics, 19, 3911-3921.

Shipway, A.N., Katz, E., & Willner, I. (2000). Nanoparticle arrays on surfaces for electronic, optical, and sensor applications. ChemPhysChem, 1, 18-52.

Sokolov, S.V., Eloul, S., Kätelhön, E., Batchelor-McAuley, C., & Compton, R.G. (2017). Electrode–particle impacts: a users guide. Physical Chemistry Chemical Physics, 19, 28-43.

Stankus, D.P., Lohse, S.E., Hutchison, J.E., & Nason, J.A. (2011). Interactions between natural organic matter and gold nanoparticles stabilized with different organic capping agents. Environmental Science & Technology, 45, 3238-3244.

Stevenson, K.J., & Tschulik, K. (2017). A materials driven approach for understanding single entity nano impact electrochemistry. Current Opinion in Electrochemistry, 6, 38-45.

Stuart, E.J.E., Rees, N.V., Cullen, J.T., & Compton, R.G. (2013). Direct electrochemical detection and sizing of silver nanoparticles in seawater media. Nanoscale, 5, 174-177.

Suherman, A.L., Zampardi, G., Kuss, S., Tanner, E.E.L., Amin, H.M.A., Young, N.P., & Compton, R.G. **(**2018). Understanding gold nanoparticle dissolution in cyanide-containing solution *via* impact-chemistry. Physical Chemistry Chemical Physics, 20, 28300-28307.

Xie, J., Lee, J.Y., Wang, D.I.C., & Ting, Y.P. (2007). Silver nanoplates: from biological to biomimetic synthesis. ACS Nano, 1, 429-439.

Zampardi, G., Thöming, J., Naatz, H., Amin, H.M.A., Pokhrel, S., Mädler, L., & Compton, R.G. (2018). Electrochemical behavior of single CuO nanoparticles: implications for the assessment of their environmental fate. Small, 14, 1801765.

Zhao, Q., Duan, R., Yuan, J., Quan, Y., Yang, H., & Xi, M. (2014). A reusable localized surface plasmon resonance biosensor for quantitative detection of serum squamous cell carcinoma antigen in cervical cancer patients based on silver nanoparticles array. International Journal Nanomedicine, 9, 1097-1104.

Zhou, Y.-G., Rees, N.V., Pillay, J., Tshikhudo, R., Vilakazi, S., & Compton, R.G. (2012). Gold nanoparticles show electroactivity: counting and sorting nanoparticles upon impact with electrodes. Chemical Communications, 48, 224-226.

Supplementary Information

Eco-friendly polymer succinate capping on silver nano-particles for enhanced stability: a UV-Vis and electrochemical particle impact study

Azhar Abbas [1,2,*], Hatem M. A. Amin [1,5], Muhammad Akhtar [3,4], Muhammad A. Hussain [2], Christopher Batchelor-McAuley [1], Richard G. Compton [1]

1- Oxford University, Department of Chemistry, Physical and Theoretical Chemistry Laboratory, South Parks Road, Oxford, OX1 3QZ, United Kingdom

2- University of Sargodha, Department of Chemistry, Ibne Sina Block, Sargodha 40100, Pakistan

3- Islamia University of Bahawalpur, Faculty of Pharmacy and Alternative Medicine, Department of Pharmacy, Bahawalpur 63100, Pakistan.

4- King's College London, Faculty of Life Sciences & Medicine, School of Cancer and Pharmaceutical Sciences, London, SE1 9NH, United Kingdom.

5- Cairo University, Faculty of Science, Department of Chemistry, Giza, 12613 Egypt

[*]Corresponding Author

Emails: azhar.abbas@chem.ox.ac.uk; azharabbas73@yahoo.com

Phone: +44 (0) 7448775793

S1 UV-Vis spectrophotometry

A solution of $AgNO_3$ and HPC-Suc was exposed to sunlight and the synthesis of the Ag NPs@suc in aqueous solution was monitored periodically (after an exposure time of 15 s, 30 s, 60 s, 90 s, 105 s, 120 s and 25 min) by recording the absorption spectra over a wavelength range of 300-800 nm. Upon exposure to sunlight during an initial period of 15 s to 25 min, the Ag^+ was reduced to Ag Nps@suc and color of solution changed from light yellow to reddish brown. A single and broad LSPR peak was observed in the range 411-452 nm, confirming the synthesis of Ag Nps (Figure S1) (Mulvaney, 1996). This LSPR absorption peak showed a red shift in λ_{max} and an increase in the intensity of absorption upon the increase of exposure time to sunlight, which suggests that the size of the Ag Nps@suc increases with an increase in exposure or reaction time (Abbas et al., 2015; Ding et al., 2017).

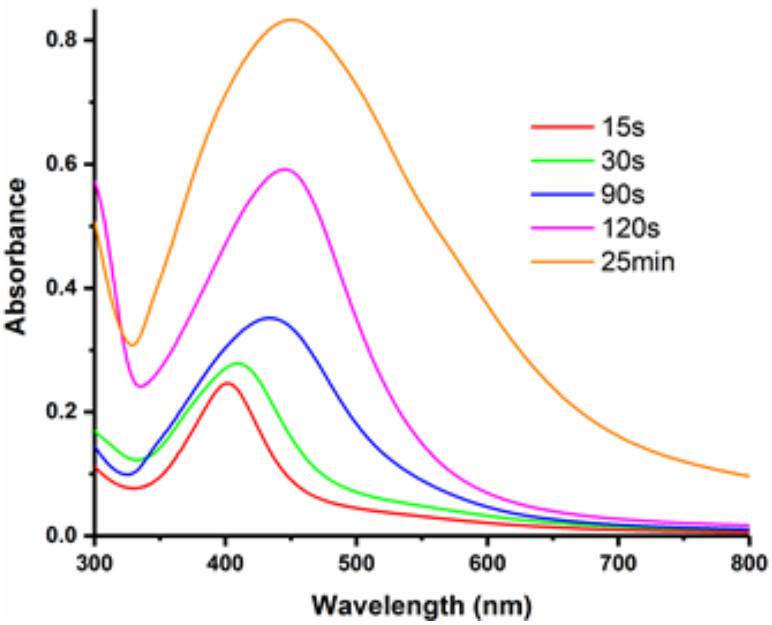

Figure S1. UV-Vis spectra of Ag Nps@suc showing a red shift and increase in absorption with exposure time to sunlight

S2 SEM-EDX measurement

The success of the synthesis of Ag Nps@suc was supported by the appearance of a signal in the silver region in the EDX spectrum (around 3 keV) (Kaviya et al., 2017) as shown by Figure S3. The EDX profile of Ag Nps@suc also shows signals for oxygen and carbon, which likely originates from the HPC-Suc capping agent or reduction product or from glassy carbon substrate. Elemental EDX mapping (Figure S2 E-G) of Ag Nps@suc shows that Ag Nps are randomly dispersed throughout the Ag Nps@suc sample. The EDX elemental analysis also showed the presence of the elements (Ag, C and O) expected to be present in the Ag Nps@suc.

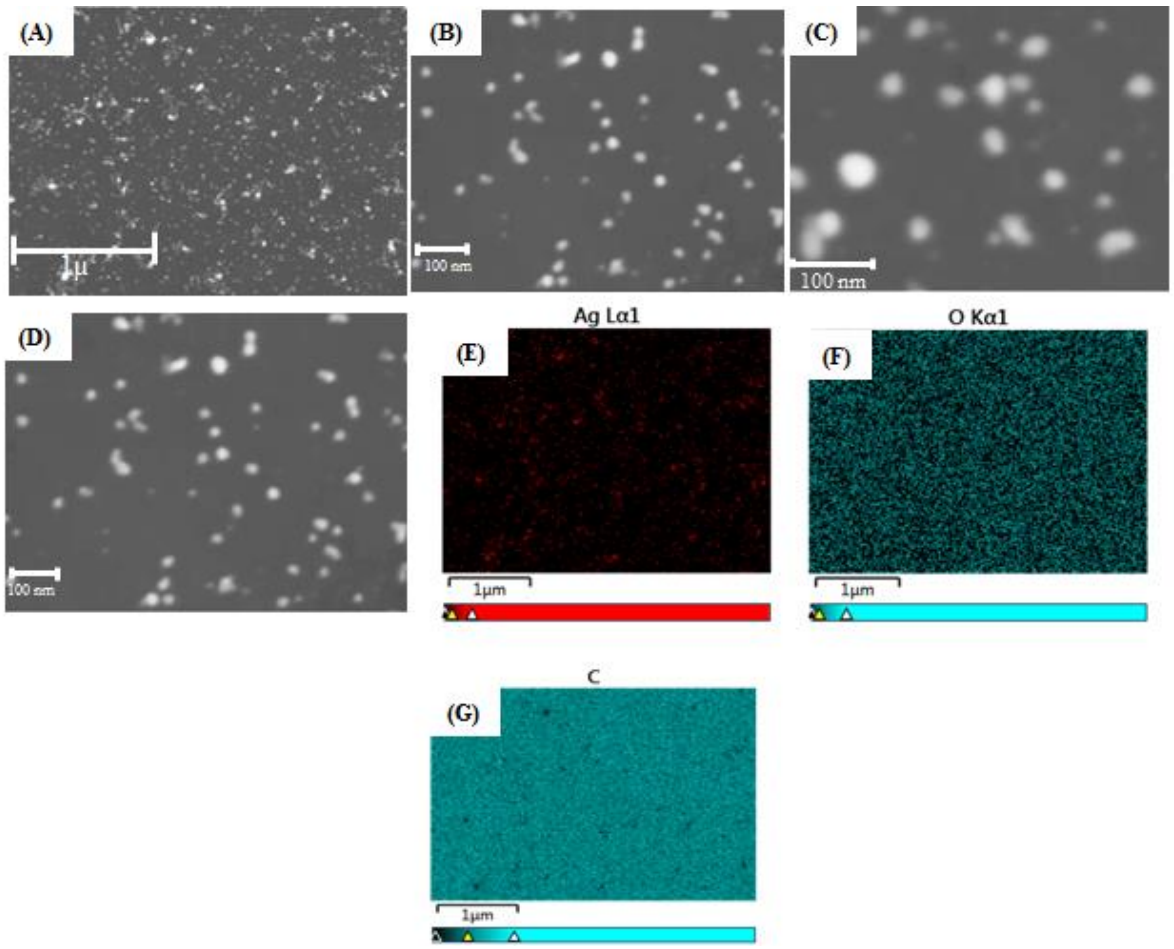

Figure S2. (A-D) SEM images of Ag Nps@suc synthesized by mixing aqueous solutions of HPC-Suc (1% w/v) and 50 mM Ag NO_3 followed by exposure to sunlight and (E-G) elemental mapping of Ag Nps@suc from EDX.

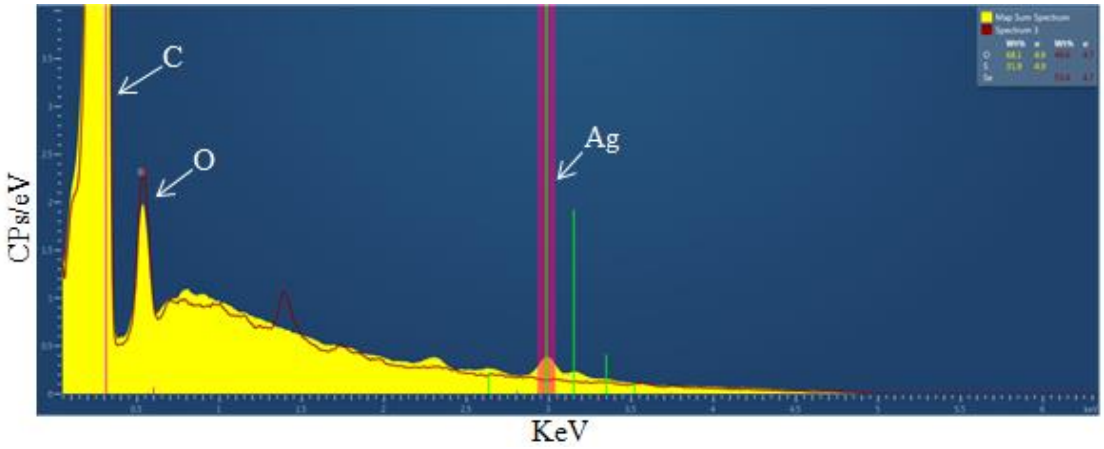

Figure S3. Representative EDX profile of corresponding area shown in Figure 3 of synthesized silver nanoparticles showing signals for C, O and Ag

S3 ATR-FTIR spectroscopic characterization

In order to identify various functional groups present in HPC-Suc and Ag Nps@suc ATR-FTIR spectra of HPC, HPC-Suc and Ag Nps@suc were recorded (Figure 4S). The ATR-FTIR spectrum of HPC shows absorption bands at 3433, 2902 and 1160-1057 cm^{-1} indicating the presence of –OH, -CH_2- and C-O-H and C-O-C bonds, respectively. The appearance of absorption peaks in the FTIR spectrum of HPC-Suc at 1726, 1618, 1399, 1260 and 1140-1007 cm^{-1} due to C=O, COOH, C-O, C-O-H and C-O-C bonds, respectively is attributed to the successful esterification of of HPC to form HPC-Suc. The FTIR spectrum of Ag Nps@suc showed bands closely similar to those in FTIR spectrum of HPC-Suc. Retention of all these signals with the expected slight shift of frequency, in the FTIR spectrum of Ag Nps@suc is a strong evidence that HPC-Suc is present as capping agent of Ag in this study.

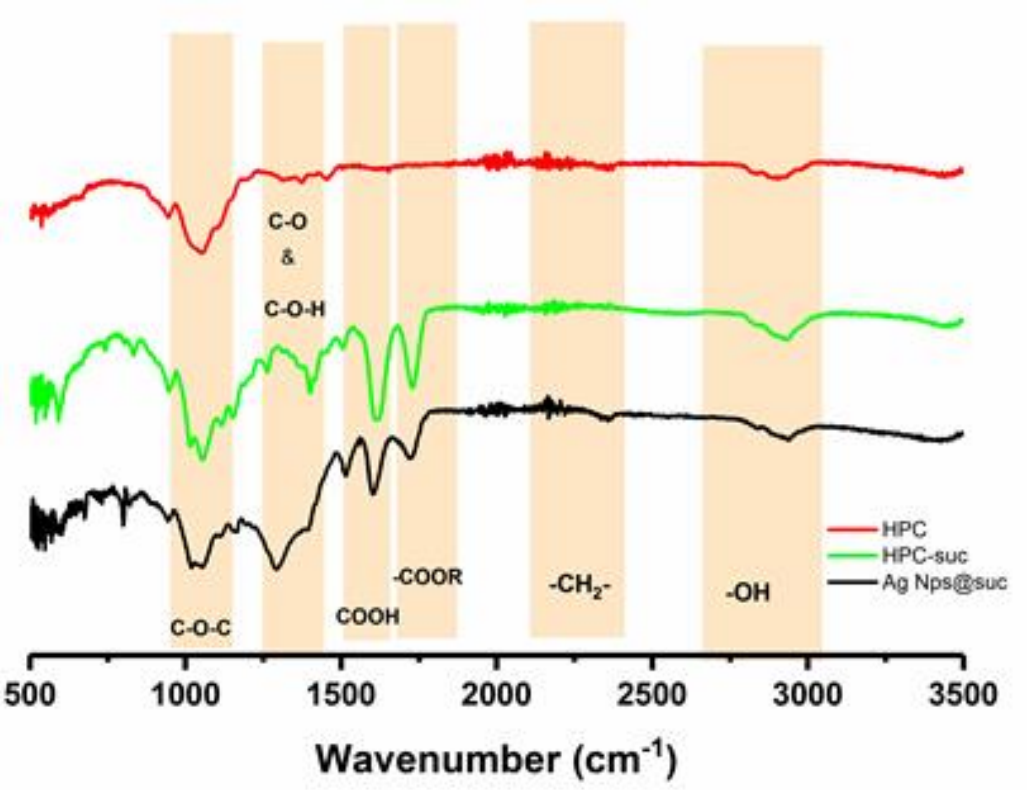

Figure S4. Overlay ATR-FTIR spectra of HPC (red), HPC-Suc (green) and Ag Nps@suc (black)

The shifting of the C=O signal to 1724 cm^{-1}, -COOH signal to 1602 cm^{-1}, C-O signal to 1293 cm^{-1}, C-O-H, C-O-C signal to 1020-1057 cm^{-1} and the appearance of a 527-569 cm^{-1} signal due to Ag---O weak interactions in FTIR spectrum of Ag Nps@suc shows successful capping of Ag Nps by HPC-Suc (Gupta et al., 2010; Shameli et al., 2012)

S4 DLS and ZP

The ZP value and the z-averag for Ag Nps@suc were also measured as shown in Figure S5 A and S5 B, respectively.

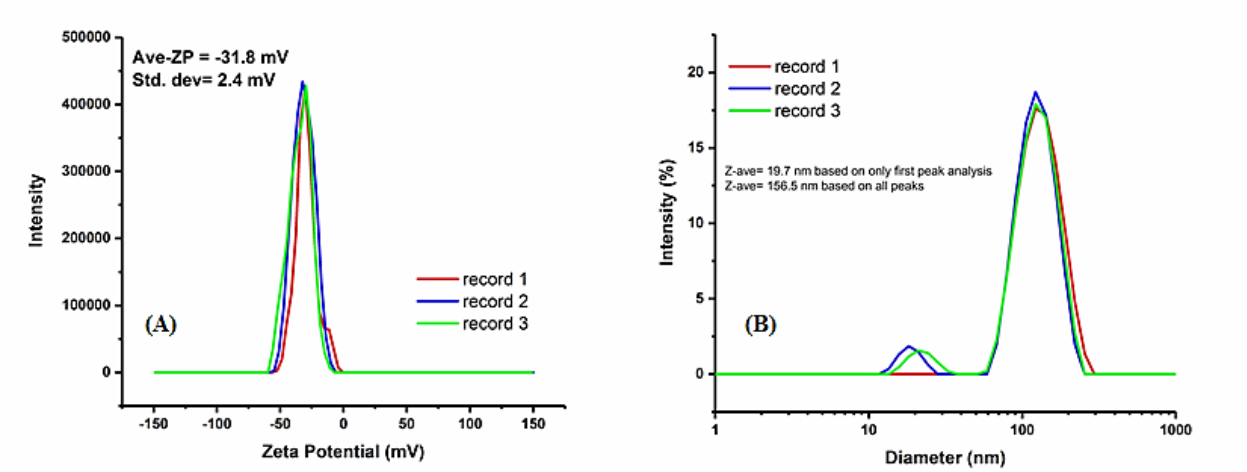

Figure S5. (A) Zeta-potential and (B) Z-averager of synthesized Ag Nps@suc

S5 Determination of the concentration of Ag Nps@suc in a suspension

The concentration of a Ag Nps suspension was estimated by UV-Vis using the procedure of Ngamchuea and co-workers (Ngamchuea et al., 2017a). Accordingly, first, the absorbance (A) of the suspension of Ag Nps@suc was determined and the molar extinction co-efficient (ϵ) for "one Ag atom" measured for citrate capped Ag Nps of size 20 nm was assumed to apply for Ag Nps@suc (15500 ± 200 M^{-1} cm^{-1}). The concentration of suspension in terms of silver atoms was determined by C=A/εl, where *l* is the optical path length of the quartz cell used for UV-Vis measurement (10 mm). This concentration is divided by the number of silver atoms in one nanoparticle to convert it into concentration in terms of Ag Nps. The number of silver atoms in one silver nanoparticle can be determined by:

Number of silver atoms in one nanoparticle = $(V_{Np}\times N_A\times\rho)/M$ (1)

where V_{Np} is the volume of one nanoparticle, N_A is the Avogadro constant, ρ is the density of silver, M is the atomic mass of silver. The number of silver atoms in one average nanoparticle of Ag Nps@suc was calculated to be $(2.45 \pm 2.5)\times10^5$. The concentration of Ag Nps was found to be 189 ± 6.5 pM.

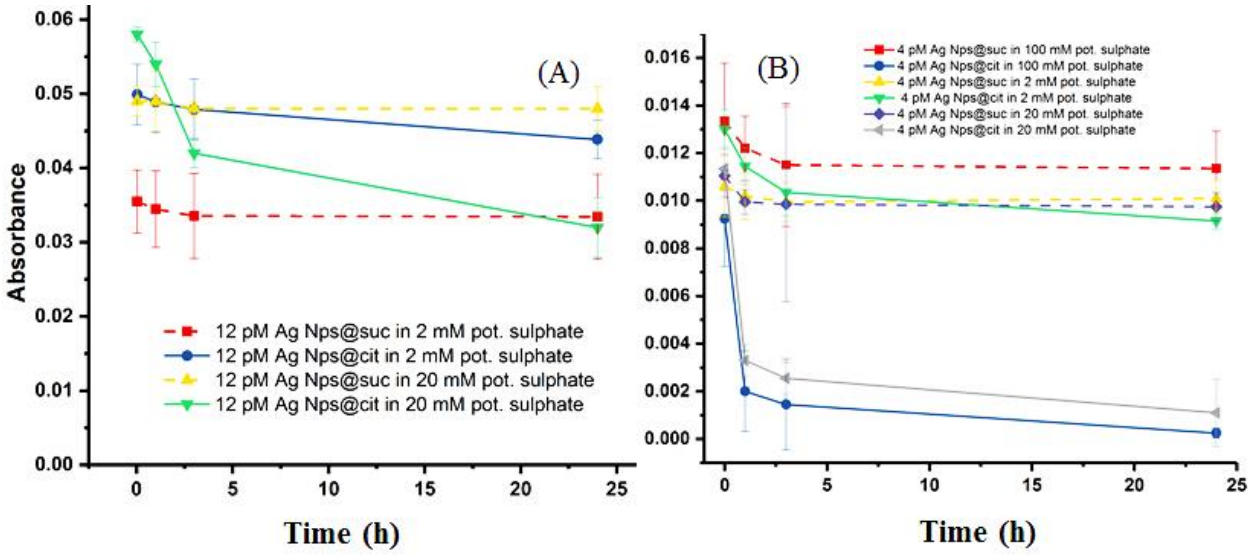

Figure S6. Absorbance as a function of time of Ag Nps@suc and Ag Nps@cit (A) 12 pM Ag Nps in 2 and 20 mM K_2SO_4 and (B) 4 pM Ag Nps in 2, 20 and 100 mM K_2SO_4

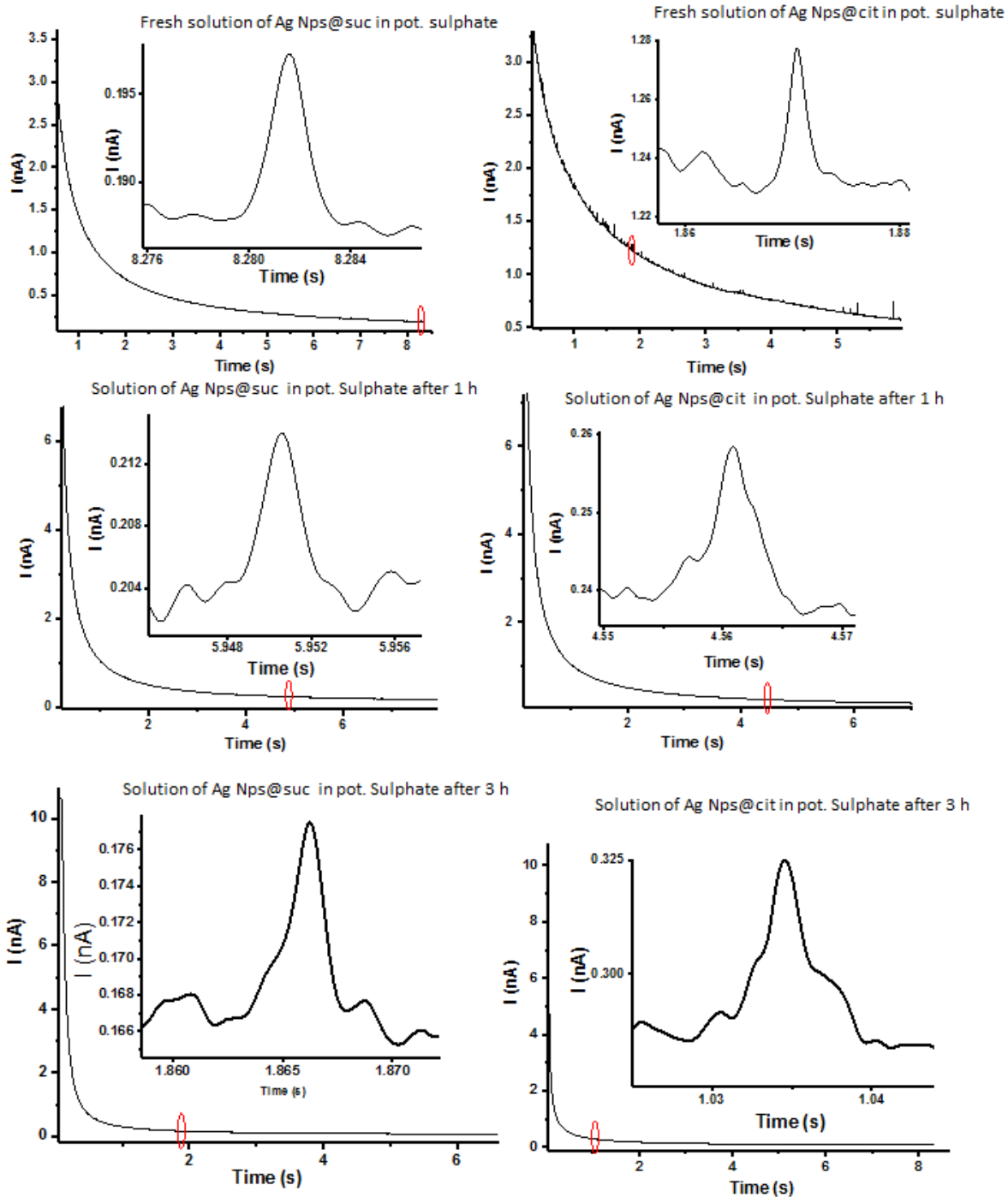

Figure S7. Chronoamperogram showing representative nano-impact spikes of 12 pM Ag Nps@suc and Ag Nps@cit in 100 mM K_2SO_4 using 33 µm carbon microdisc electrode, leakless Ag/AgCl reference electrode and platinum counter electrode in a fresh solution of silver nanoparticles and a solution kept in electrolyte for 1 h and 3 h (the inset depicts the enlarged chronoamperogram)

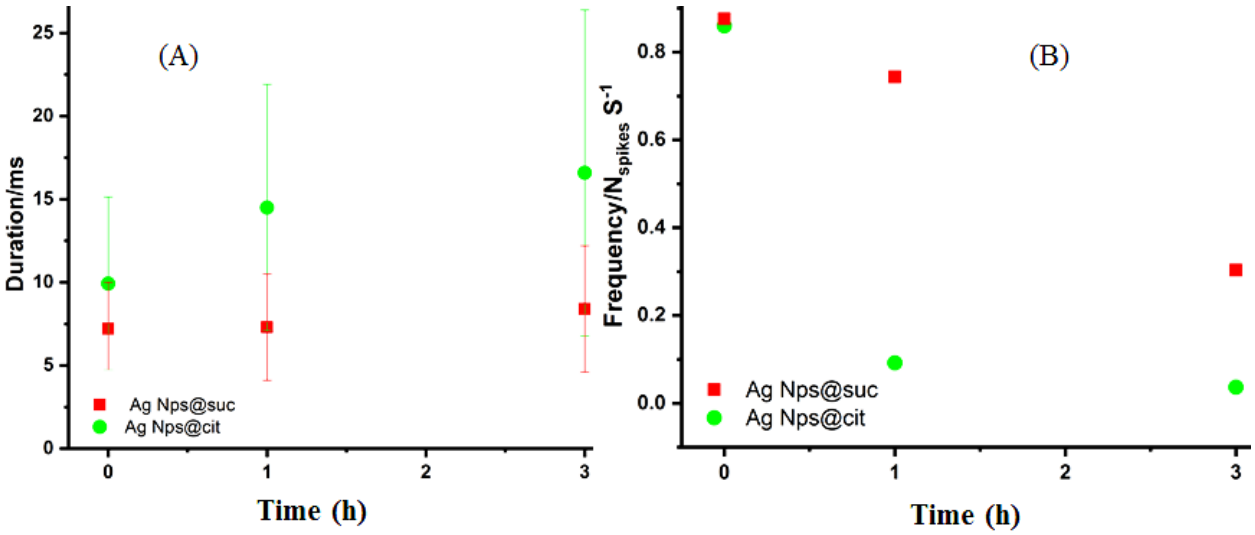

Figure S8. Duration (A) and frequency (B) of spikes of 12 pM Ag Nps@suc and Ag Nps@cit in 100 mM K_2SO_4 as a function of time

Table S1. Change in the relative absorbance for fresh solution 4 pM and 12 pM of Ag Nps in 2 mM, 20 mM and 100 mM of electrolyte K_2SO_4 with time as calculated from UV-Vis

Conc. of Ag Nps	Time (h)	AgNps@cit (relative absorbance %)			AgNps@suc (relative absorbance %)		
		100 mM K_2SO_4	20 mM K_2SO_4	2 mM K_2SO_4	100 mM K_2SO_4	20 mM K_2SO_4	2 mM K_2SO_4
12 pM	0	100	100	100	100	100	100
	0.02	47.3	87.8	87	99.8	99.8	98.8
	1	14.8	95.9	81	97.5	96.7	98.7
	3	11.4	94	63	94.5	94.2	97
	24	0.20	86	48	90.5	94.1	97
4 pM	0	100	100	100	100	100	100
	0.02	47.2	92.9	93.3	96.5	96.4	95.7
	1	10.3	82.2	17.8	87.8	92.3	86.2
	3	6.0	74	15	82.8	91.5	85
	24	0.1	66.1	10	82.8	91.4	84.5

Table S2. Change in relative absorbance for fresh solution of 4 pM and 12 pM Ag Nps in 2 mM, 20 mM and 100 mM of electrolyte (KCl, KBr and NaCl) with time as calculated from UV-Vis

Conc. of Ag Nps / Conc. of electrolyte	Time (h)	AgNps@cit (relative absorbance %)			AgNps@suc (relative absorbance %)		
		KCl	KBr	NaCl	KCl	KBr	NaCl
12 pM/100 mM	0	100	100	100	100	100	100
	1	21.2	9.9	15.9	64.6	87.8	50
	3	9.9	3.2	5	40.1	71.4	41
	24	0.9	0.01	0.001	10.1	16	5
4 pM/100 mM	0	100	100	100	100	100	100
	1	28.9	23.4	8	93.3	52.9	60.9
	3	15	0.001	0.001	42.9	14.8	29
	24	0.001	0.001	0.001	11.7	7.0	2.4
12 pM/20 mM	0	100	100	100	100	100	100
	1	94.3	91	81.1	111.5	99.9	114.4
	3	88.5	88.2	75	120	99.79	127
	24	38	5.8	58.5	127	34.3	108.3
4 pM/20 mM	0	100	100	100	100	100	100
	1	84.7	74.7	82.9	105.8	75	103.8
	3	74.4	54.9	64.3	101.9	64.1	91.3
	24	37.8	11.9	14.5	81.7	45.3	58.6
12 pM/2 mM	0	100	100	100	100	100	100
	1	98.4	95	99.1	106	111	105
	3	97.8	88.1	96.9	108	115	107
	24	96.7	42	81.6	107	40	99.6
4 pM/2 mM	0	100	100	100	100	100	100
	1	96.9	95.1	96.4	107.8	77.7	103.7
	3	95.1	95	92.6	115.4	76	109
	24	81.8	64	73	112.7	45.7	95.0

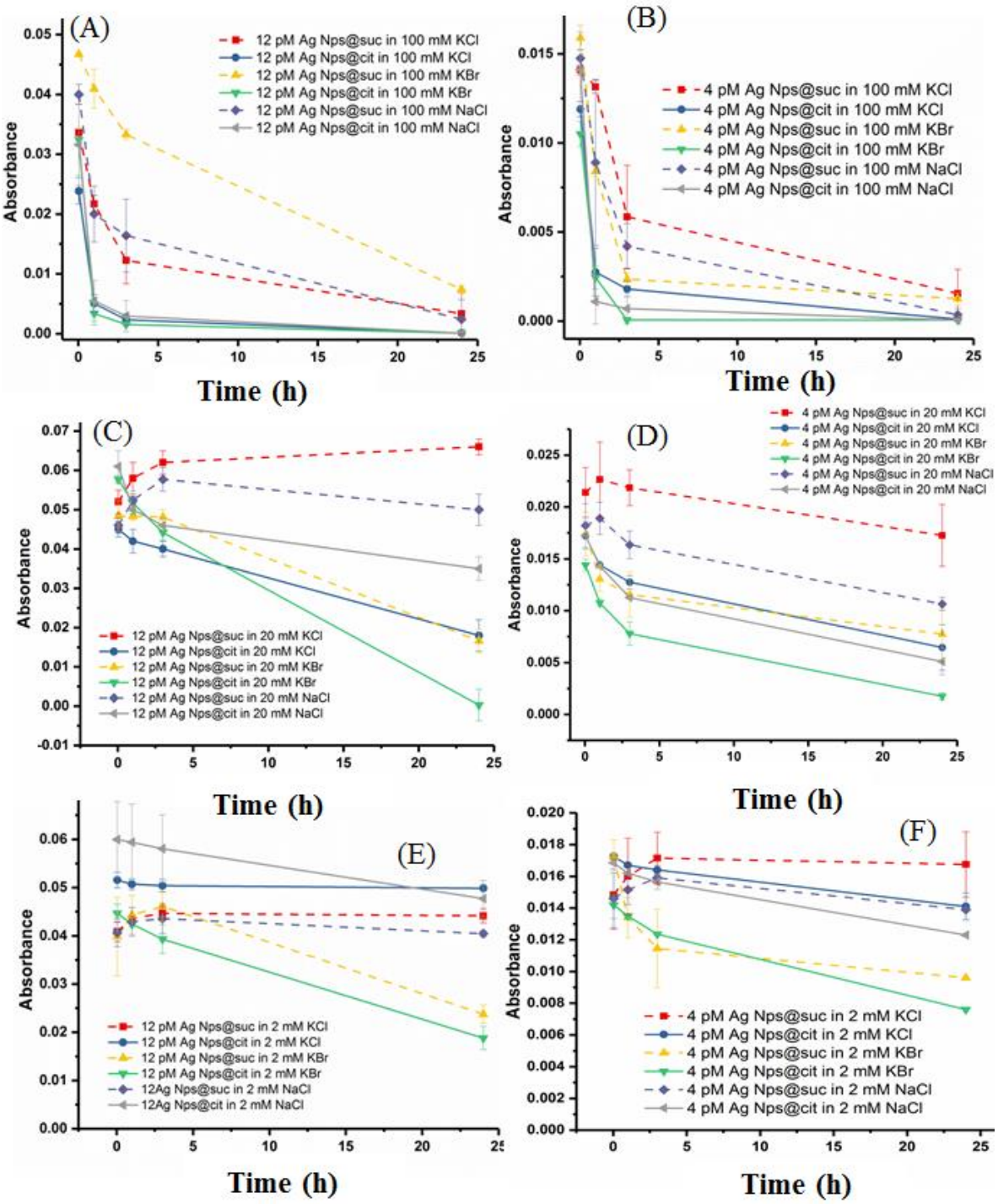

Figure S9. Absorbance as a function of time of Ag Nps@suc and Ag Nps@cit (A) 12 pM Ag Nps in 20 mM electrolyte, (B) 4 pM Ag Nps in 20 mM electrolyte, (C) 12 pM Ag Nps in 100 mM electrolyte, (D) 4 pM Ag Nps in 100 mM electrolyte, (E) 12 pM Ag Nps in 2 mM electrolyte and (F) 4 pM Ag Nps in 20 mM electrolyte

References

Abbas, A., Hussain, M.A., Amin, M., Tahir, M.N., Jantan, I., Hameed, A., & Bukhari, S.N.A. (2015). Multiple cross-linked hydroxypropylcellulose–succinate–salicylate: prodrug design, characterization, stimuli responsive swelling–deswelling and sustained drug release. RSC Advances, 5, 43440-43448.

Ding, Q., Li, R., Chen, M., & Sun, M. (2017). Ag nanoparticles-TiO_2 film hybrid for plasmon-exciton co-driven surface catalytic reactions. Applied Materials Today, 9, 251-258.

Gupta, K., Jana, P.C., & Meikap, A.K. (2010). Optical and electrical transport properties of polyaniline–silver nanocomposite. Synthetic Metals, 160, 1566-1573.

Kaviya, S., Santhanalakshmi, J., Viswanathan, B., Muthumary, J., & Srinivasan, K. **(**2011). Biosynthesis of silver nanoparticles using citrus sinensis peel extract and its antibacterial activity. Spectrochimica Acta Part A: Molecular and Biomolecular Spectroscopy, 79, 594-598.

Mulvaney, P. (1996). Surface plasmon spectroscopy of nanosized metal particles. Langmiur, 12, 788-800.

Ngamchuea, K., Batchelor-McAuley, C., Sokolov, S.V., & Compton, R.G. (2017). Dynamics of silver nanoparticles in aqueous solution in the presence of metal ions. Analytical Chemistry, 89, 10208-10215.

Shameli, K., Ahmad, M.B., Jazayeri, S.D., Sedaghat, S., Shabanzadeh, P., Jahangirian, H., Mahdavi, M., & Abdollahi, Y. (2012). Synthesis and characterization of polyethylene glycol mediated silver nanoparticles by the green method. International Journal of Molecular Sciences, 13, 6639-6650.

Chemia Naissensis, Vol 3, Issue 1, RESEARCH ARTICLE, 84-85

Ekološki prihvatljiv sukcinatni polimer koji obavija nanočestice srebra za poboljšanu stabilnost: UV-Vis i elektrohemijsko proucavanje udara cestica

Azhar Abbas [1,2], Hatem M. A. Amin [1,5], Muhammad Akhtar [3,4], Muhammad A. Hussain[2], Christopher Batchelor-McAuley[1], Richard G. Compton [1]

1- Univerzitet u Oksfordu, Departman za hemiju, Laboratorija za fizičku i teorijsku hemiju, South Parks Road, Oxford, OX1 3QZ, Ujedinjeno Kraljevstvo

2- Univerzitet u Sargodha-i, Ibne Sina Block, Departman za hemiju, Sargodha 40100, Pakistan

3- Islamia Univerzitet u Bahavalpuru, Fakultet farmacije i alternativne medicine, Departman za farmaciju, Bahavalpur 63100, Pakistan

4- Kraljevski koledž London, Fakultet nauoka o životu i medicine, Škola za izučavanje kancera i farmaceutskih nauka, London SE1 9NH, Ujedinjeno Kraljevstvo

5- Kairo univerzitet, Fakultet prirodnih nauka, Departman za hemiju, Giza, 12613 Egipat

Sažetak

Jednostavna zelena metoda koristi se za sintezu srebrnih nanočestica (Ag Nps) u jednom minutu. Koloidna stabilnost dva tipa Ag Nps (naime, hidroksipropilceluloz-sukcinatno (HPC-Suc) obavijene srebrne nanočestice (Ag Nps@suc) i citratno obavijene srebrne nanočestice (Ag Nps@cit)) ispitivana je korišćenjem UV-Vis spektrometrije i "nano-impakt" merenjima uticaja elektrohemijskih čestica. Ag Nps@suc su polako sintetisane jednostavnim mešanjem vodenih rastvora HPC-Suc i srebro-nitrata i izlaganjem sunčevoj svetlosti. Rast Ag Nps kontrolisan je podešavanjem vremena izlaganja sunčevoj svetlosti. Proučavanje plazmonskom rezonancom lokalne površine (engl. LSPR) izvršeno je korišćenjem UV-Vis spektrofotometra. Morfologija površine, veličina, elementna analiza i sastav Ag NPs@suc određena je korišćenjem SEM-EDX, dok je ATR-FTIR korišćen da bi se ispitala bilo koja vrsta hemijskih reakcija između prekursora. Za određivanje stabilnosti i distribuciju veličine, izvršena su merenja zeta potencijala (engl. ZP), rasipanje dinamičke svetlosti (engl. DSL) i kulometrija anodne čestice (engl. APC). Pripremljene Ag Nps@suc pokazuju usku raspodelu sa prosečnim prečnikom od 20 nm. Određivanje

veličine nanočestica korišćenjem metode elektrohemijskog uticaja čestica je u skladu sa SEM i DLS tehnikama. Rezultati pokazuju da su Ag Nps@cit podložne relativno brzom klasterovanju po dodatku elektrolita (100 mM K_2SO_4). Na drugoj strani, Ag Nps@suc pokazuju odličnu stabilnost sa samo ~ 9% opadanja absorbance u toku 24 h čak i pri visokim koncentracijama elektrolita. Korišćenjem elektrolita KCl, KBr i NaCl stabilnost sintetisanih Ag Nps@suc takođe se može uporediti pozitivno sa Ag Nps@cit.

Ključne reči: srebrne nanočestice, sukcinatni keping agens, stabilnost nanočestica, UV-Vis spektrometrija, udar nanočestica-elektroda

Capsule de succinate de polymère écologique sur nanoparticules d'argent pour une stabilité accrue : étude d'impact UV-Vis et électrochimique des particules

Azhar Abbas[1,2], Hatem M. A. Amin[1,5], Muhammad Akhtar[3,4], Muhammad A. Hussain[2], Christopher Batchelor-McAuley[1], Richard G. Compton[1]

1- Université d'Oxford, Département de chimie (Laboratoire de physique et de chimie théorique), South Parks Road, Oxford, OX1 3QZ, Royaume-Uni
2- Université de Sargodha, Département de chimie, Ibne Sina Block, Sargodha 40100, Pakistan
3- Islamia Université de Bahawalpur, Faculté de pharmacie et de médecine alternative, Département de pharmacie, Bahawalpur, 63100, Pakistan
4- King's College London, Faculté des sciences de la vie et de médecine, École du cancer et des sciences pharmaceutiques, Londres SE1 9NH, Royaume-Uni
5- Université du Caire, Faculté des sciences, Département de chimie, Gizeh, 12613 Égypte

Résumé

Une méthode simple verte s'emploie pour synthétiser des nanoparticules d'argent (Ag Nps) en une minute. La stabilité colloïdale de deux types d'Ag Nps (en effet, les nanoparticules d'argent coiffées d'hydroxypropylcellulose succinate (HPC-Suc) (Ag Nps@suc) et les nanoparticules d'argent coiffées de citrate (Ag Nps@cit)) est examinée à l'aide de la spectrométrie UV-Vis et des mesures d'impacts de particules électrochimiques « nano-impacts ». Les Ag Nps@suc ont été doucement synthétisées par un simple mélange des solutions aqueuses de HPC-Suc et du nitrate d'argent et par l'exposition à la lumière du soleil. La croissance de l'Ag Nps a été contrôlée en ajustant le temps d'exposition à la lumière du soleil. L'étude de la surface locale (angl. LSPR) par la résonance plasmonique a été effectuée à l'aide d'un spectrophotomètre UV-Vis. La morphologie de la surface, la taille, l'analyse d'éléments et la composition de l'Ag Nps@suc ont été déterminées moyennant le SEM-EDX, tandis que l'ATR-FTIR a été utilisé pour examiner le type de réactions chimiques entre les précurseurs. Pour la détermination de la stabilité et la distribution de la taille, ont été réalisés les mesures du potentiel zêta (angl. ZP), la diffusion dynamique de la lumière (angl. DSL) et la coulométrie des particules anodiques (angl. APC). Les Ag Nps@suc faites démontrent une distribution étroite d'un diamètre moyen de 20 nm. Le dimensionnement du Nps à l'aide de la méthode des impacts électrochimiques des particules est cohérent avec les techniques SEM et DLS.

D'une part, les résultats montrent que les Ag Nps@cit sont sujets à un regroupement relativement rapide après l'ajout des électrolytes (100 mM K_2SO_4). D'autre part, les Ag Nps@suc démontrent une excellente stabilité n'ayant qu'une décroissance de ~ 9% de l'absorbance sur 24 h, et ceci même lors des hautes concentrations d'électrolytes. Au moyen des électrolytes KCl, KBr et NaCl, la stabilité des Ag Nps@suc synthétisés peut être également comparée favorablement avec les Ag Nps@cit.

Mots-clés: nanoparticules d'argent, agent de coiffage succinate, stabilité des nanoparticules, spectrométrie UV-Vis, impact nanoparticule-électrode

Экологически чистое полимерное покрытие сукцината на наночастицах серебра для повышения стабильности: исследование воздействия ультрафиолетовых и видимых частиц и электрохимического воздействия на частицы

Азхар Аббас [1,2], Хатем М.А. Амин [1,5], Мухаммад Ахтар [3,4], Мухаммад А. Хуссейн[2], Кристофер Бэтчелор-Маколи[1], Ричард Г. Комптон[1]

1 – Оксфордский университет, Кафедра химии, Лаборатория физической и теоретической химии, South Parks Road, Oxford, OX1 3QZ, United Kingdom

2 – Университет Саргодха, Факультет химии, Блок Ибн Сина, Саргодха 40100, Пакистан

3 – Исламский университет Бахавалпура, Факультет фармации и альтернативной медицины, Кафедра фармации, Бахавалпур 63100, Пакистан

4 – Королевский колледж Лондона, Факультет наук о жизни и медицины, Школа рака и фармацевтических наук, Лондон SE1 9NH, Великобритания

5- Каирский университет, Факультет естественных наук, Кафедра химии, Гиза, 12613 Египет

Аннотация

Простой зеленый метод используется для синтеза наночастиц серебра (Ag Nps) за одну минуту. Коллоидная стабильность двух типов Ag Nps (а именно, наночастиц серебра с блокировкой гидроксипропилцеллюлозы (HPC-Suc) (Ag Nps @ suc) и наночастиц серебра с блокировкой цитратом (Ag Nps @ cit)) исследуется с использованием спектрометрии в УФ-видимой области и электрохимические столкновения с частицами измерения «наноударов». Ag Nps @ suc были синтезированы простым смешиванием водных растворов HPC-Suc и нитрата серебра и воздействием солнечного света. Рост Ag Nps контролировали, регулируя время воздействия солнечного света. Исследование локального поверхностного плазмонного резонанса (LSPR) проводили с использованием спектрофотометра UV-Vis. Морфология поверхности, размер, элементный анализ и состав Ag NPs @ Succ определяли с помощью SEM-EDX, в то время как ATR-FTIR использовали для оценки любого типа химических реакций между предшественниками. Для

измерений стабильности и распределения по размерам были выполнены дзета-потенциал (ZP), динамическое рассеяние света (DSL) и кулонометрия анодных частиц (APC). Свежеприготовленный Ag Nps @ Succ показал узкое распределение по размерам со средним диаметром 20 нм. Калибровка NPS с использованием метода электрохимических ударов частиц соответствует методикам SEM и DLS. Результаты показывают, что Ag Nps @ cit склонны к относительно быстрой кластеризации при добавлении электролита (100 мМ K_2SO_4). С другой стороны, Ag Nps @ Succ демонстрирует превосходную стабильность со снижением оптической плотности только ~ 9% в течение 24 часов даже при высокой концентрации электролита. При использовании электролитов KCl, KBr и NaCl стабильность синтезированного Ag Nps @ su также выгодно отличается от Ag Nps @ cit.

Ключевые слова: наночастицы серебра, сукцинатный укупоривающий агент, стабильность наночастиц, УФ-видимая спектрометрия, удар наночастиц и электрода

Umweltfreundliche Polymer-Succinat-Verkappung auf Silbernanopartikeln für verbesserte Stabilität: eine Studie zu UV-VIS und zum Einfluss elektrochemischer Partikel

Azhar Abbas[1,2], Hatem M.A. Amin[1,5], Muhammad Akhtar[3,4], Muhammad A. Hussain[2], Christopher Batchelor-McAuley[1], Richard G. Compton[1]

1- Universität Oxford, Department für Chemie, Labor für Physikalische und Theoretische Chemie, South Parks Road, Oxford, OX1 3QZ, Vereinigtes Königreich

2- Universität Sargodha, Department für Chemie, Ibne Sina Block, Sargodha 40100, Pakistan

3- Islamia Universität von Bahawalpur, Fakultät für Pharmazie und alternative Medizin, Department für Pharmazie, Bahawalpur 63100, Pakistan

4- King's College London, Fakultät für Biowissenschaften und Medizin, Schule für Krebs und Pharmazeutische Wissenschaften, London SE1 9NH, Vereinigtes Königreich

5- Universität Kairo, Fakultät für Naturwissenschaften, Department für Chemie, Gizeh, 12613 Ägypten

ABSTRAKT

Mit einer einfachen grünen Methode werden Silbernanopartikel (Ag Nps) in einer Minute synthetisiert. Die kolloidale Stabilität von zwei Arten von Ag-Nps (nämlich Hydroxypropylcellulose-Succinat (HPC-Suc) - verkappte Silbernanopartikel (Ag Nps @ suc) und Citrat-verkappte Silbernanopartikel (Ag Nps @ cit)) wird unter Verwendung der UV-Vis-Spektrometrie und „Nano-Impact“ –Messungen des Einflusses elektrochemischer Partikel untersucht. Ag Nps@suc wurden neu synthetisiert, indem einfach wässrige Lösungen von HPC-Suc und Silbernitrat gemischt und der Sonnenlicht ausgesetzt wurden. Das Wachstum von Ag Nps wurde durch das Einstellen der Expositionszeit gegenüber dem Sonnenlicht gesteuert. Eine lokale Oberflächen-Plasmon-Resonanz (LSPR) - Untersuchung wurde unter Verwendung eines UV-Vis-Spektrophotometers durchgeführt. Die Oberflächenmorphologie, Größe, Elementaranalyse und Zusammensetzung von Ag-NPs@suc wurde durch SEM-EDX bestimmt, während ATR-FTIR dazu verwendet wurde, um jede Art von chemischen Reaktionen zwischen Präkursoren zu untersuchen. Zur Bestimmung der Stabilitäts- und Größenverteilung wurden die Messungen des Zeta-Potential (ZP), der dynamischen Lichtstreuung (DSL) und der Anoden-Partikel-Coulometrie (APC) durchgeführt. Das so

hergestellte Ag Nps@suc zeigte eine enge Größenverteilung mit einem durchschnittlichen Durchmesser von 20 nm. Die Bestimmung der Nanopartikelgröße unter Verwendung der Methode des elektrochemischen Einflusses von Partikeln erfolgt gemäß SEM- und DLS-Techniken. Die Ergebnisse zeigen, dass Ag Nps@cit bei Zugabe von Elektrolyt (100 mM K_2SO_4) zu einer relativ schnellen Clusterbildung neigt. Andererseits zeigt Ag Nps@suc sogar bei hoher Elektrolytkonzentration eine ausgezeichnete Stabilität mit nur ~ 9% Absorptionsabfall während 24 Stunden. Unter Verwendung von KCl-, KBr- und NaCl-Elektrolyten kann die Stabilität des synthetisierten Ag Nps@suc auch positiv mit Ag Nps@cit verglichen werden.

Schlüsselwörter: *Silbernanopartikel, Succinat-Verkappungsmittel, Nanopartikelstabilität, UV-Vis-Spektrometrie, Einfluss von Nanopartikel-Elektroden*

In vitro antimicrobial activity of *Carum carvi* L. seed essential oil against pink potato spoilage flora

Ahmed Snoussi[1,2*], Hayet Ben Haj Koubaier [1,2], Saoussen Bouacida[1,2], Ismahen Essaidi[3], Faten Kachouri[1] and Nabiha Bouzouita [1,2]

1- Higher School of Food Industries of Tunisia, University of Carthage, 58 Alain Savary Avenue, 1003, Tunisia

2- Tunis El Manar University, Sciences Faculty of Tunis, Laboraotry for Structural Organic Chemistry : Chemical Synthesis and Physico-chemical Analysis , 2092, Tunisia

3- Higher Agronomic Institute of Chott Meriem, University of Sousse, 4042, Sousse Tunisia

Ahmed Snoussi: ahmedsnoussi.esiat@yahoo.fr
Hayet Ben Haj Koubaier: h.kbaier@gmail.com
Saoussen Bouacida: bouacidasaoussen1405@gmail.com
Ismahen Essaidi: saidi.ismahen@gmail.com
Faten Kachouri: kachouri.esiat@gmail.com
Nabiha Bouzouita: bouzouita.nabiha@gmail.com

ABSTRACT

The objective of this research is to assess the ability of using *Carum carvi* L. seeds essential oil as a biological substance for controlling spoilage germs growth in potatoes during storage. The chemical composition of caraway seeds essential oil, analyzed by GC-MS and by gas chromatography with flame ionization detector (GC-FID), led to the identification of twelve compounds, where carvone was the main one with a percentage of 75.64 % of the total oil. The comparison of the microbial profiles of different potatoes samples showed the presence of the genus Citrobacter and three distinct fungi genera: *Aspergillus*, *Phytophthora* and *Fusarium* only for contaminated potato tubers with internal pink pigmentation. Thus, the antimicrobial activity of caraway seeds essential oil was studied against these strains. The antimicrobial activity of the oil against the isolated strains was evaluated through the agar diffusion method using different volumes (10, 20, 50 and 100 µl). All tested strains were inhibited by caraway seeds essential oil in a dose-

* Ahmed Snoussi
e-mail address: ahmedsnoussi.esiat@yahoo.fr

dependent manner. The obtained results suggest the use of *Carum carvi* L. as a promising natural substance for the preservation of potatoes by contact vapor method.

Keywords: potato, Essential oil, Carum carvi L. seeds, antimicrobial activity, Enterobacteria, fungi

Introduction

Solanum tuberosum, commonly known as potato, is a tuberous herbaceous plant native to Latin America, belongs to the family of *Solanaceae* (Sharma et al., 2014). The potato is a globally important crop, with an estimated 377 million tons harvested in 2016, only falling short of the other starch staples, maize, wheat, and rice (FAO, 2016).

In addition to this high starch content, potatoes are an important source of micronutrients, such as vitamin C, vitamin B6, potassium, folate, and iron and contribute a significant amount of fiber to the diet (Robertson et al., 2018).

However, the cultivation of harvested potatoes and tubers is subject to numerous bacterial, fungal, or viral attacks causing several diseases which are responsible for significant economic losses (Abd El-Azeim, 2020). Resorting to conservation is therefore essential to preserve the organoleptic and nutritional qualities of potatoes while strongly inhibiting the development of spoilage flora. The pesticides used in the past to improve the quality and productivity of agricultural products often remain as residues in agricultural soils, a portion of which may be taken up by plant crops. This may pose a major concern with respect to the safety of these products for animal and human consumption (Hwang et al., 2018).

Currently, consumers are increasingly concerned about the harmful effects of pesticides and are more demanding on the treatment used on fruits and vegetables. Hence the use of biotechnology, based on biological substances and biocontrol formulation is gaining more attention among the scientific community in order to avoid most of the negative impact of chemical compounds on food systems and therefore on human health (Larkin, 2016).

Some essential oils extracted from aromatic and medicinal plants are candidates for exploiting their full preservation potential. In fact, studies have shown that these essential oils are effective in controlling the growth of a wide variety of microorganisms, including filamentous fungi, yeasts, and bacteria (Essaidi et al., 2014; Lasrem et al., 2019). Such antimicrobial activities make the use of these oils recommended in food industries (Karameşe and Özgür, 2020).

Caraway (*Carum carvi* L.) is a condiment species belonging to the *Apiaceae* family and it is mainly cultivated for its aromatic seeds. It is one of the common well-known herbs, naturally found in Northern and Central Europe, Siberia, Turkey, Iran, India and North Africa (Saghir et al., 2012; Kazemipoor et al., 2016). In Tunisia, it is the most cultivated condiment species after coriander. It is widely used as a culinary, aromatic, and medicinal plant (Agrahari and Singh, 2014). Additionally, *C. carvi* seeds have antispasmodic, antiflatulence, antibacterial, anticancer, lactiferous, expectorant, and energizing effects; also, they can improve menstruation and appetite (Agrahari and Singh, 2014; Al-Snafi, 2015).

The aim of this research was to extract and determine the chemical composition of caraway seed essential oil in addition to examine the antibacterial and antifungal activity towards isolated strains of contaminated potato tubers with internal pink pigmentation.

Experimental

Biological Material

The potato tubers and caraway seeds used in this research were purchased from a local market in Tunis. Two types of potato samples were used: unpigmented potatoes (sound) and potatoes with internal pink pigmentation (infected) for the microbiological characterization.

Essential oil extraction and chemical composition analysis

The caraway essential oil (EO) was obtained by hydrodistillation using a Dean-Stark apparatus. The extraction was carried on until there was no significant increase in the volume of oil collection. The obtained essential oil was dried over anhydrous sodium sulfate and preserved in a sealed vial at 4°C until further analysis.

The chemical composition was analyzed by gas chromatography coupled with mass spectrometry using a GC system apparatus type HP 6890N, connected to a mass spectrometer (MS) with a selective detector HP 59758 N and equipped with a flame-ionization detector (FID). A capillary column type HP5-MS (30m x 0.25mm x 0.25µm) was used for the purpose of separation. The temperature of the column was set from 40 to 280 °C at a rate of 2 °C.min^{-1}. Helium was used as carrier gas at a flow rate of 0.9 mL/min and the sample was injected in the split mode (1:10).

The compounds identification was performed according to their GC retention indices, by comparison of their MS spectra by computer matching with the Wiley 238.L mass spectra library, and when possible, co-injection with standard available in our laboratory.

Microbial analysis of potato samples

Enumeration of the microflora of the studied potatoes was carried out on grounded samples which were diluted (10^{-3} to 10^{-7}) and then cultured in selective agar culture media: PCA (total plate count of bacteria), VRBG (total enterobacteria and coliforms), Sabouraud agar (yeasts and molds). The isolated strains were identified by morphological, physiological, and biochemical tests (Gram stain, glucose fermentation test, lactose, gas production and H_2S, oxidative/fermentation test, and IMViC test). The metabolic study of the microorganisms was achieved via API E 20 system (bioMérieux, France) for enterobacteria and API 20C AUX (bioMérieux, France) for yeasts. These tests were read after 24 and 72 hours for enterobacteria and for yeasts, respectively. The analysis results were obtained using Apilab®

identification software. The identification of isolated molds was carried out in the Nabeul health hygiene laboratory (Cape Bon region, Tunisia) through microscopic readings.

Antimicrobial activity

Caraway essential oil was screened for its antimicrobial activity against five strains isolated from the infected potato by agar disk diffusion method defined by Cushine and Lamb (2005). A soft agar, previously sterilized, was inoculated with 50 µl of a fresh culture sample of the isolated microorganisms (10^6 CFU / ml) and poured into petri dishes. After the medium has solidified, sterile disks (6 mm) soaked in essential oil (10, 20, 50 and 100 µl) were placed on the surfaces of the plates. The effectiveness of essential oil was determined after 24-48 hours at 37°C of incubation by the measurement of the inhibition zone diameters (IZDs) around the disk, including the diameter of the disk (in millimeters).

Results and Discussion

Chemical composition of the essential oil of *Carum carvi* L. seed

The analysis of the essential oil of *Carum carvi* L. seeds using the GC-MS and GC-FID approach led to the identification of 12 terpene compounds (Figure 1) which constitute 99.74% of the total oil including 78.44% oxygenated monoterpene derivatives, 21.01% monoterpene hydrocarbons, and 0.29% sesquiterpenes.

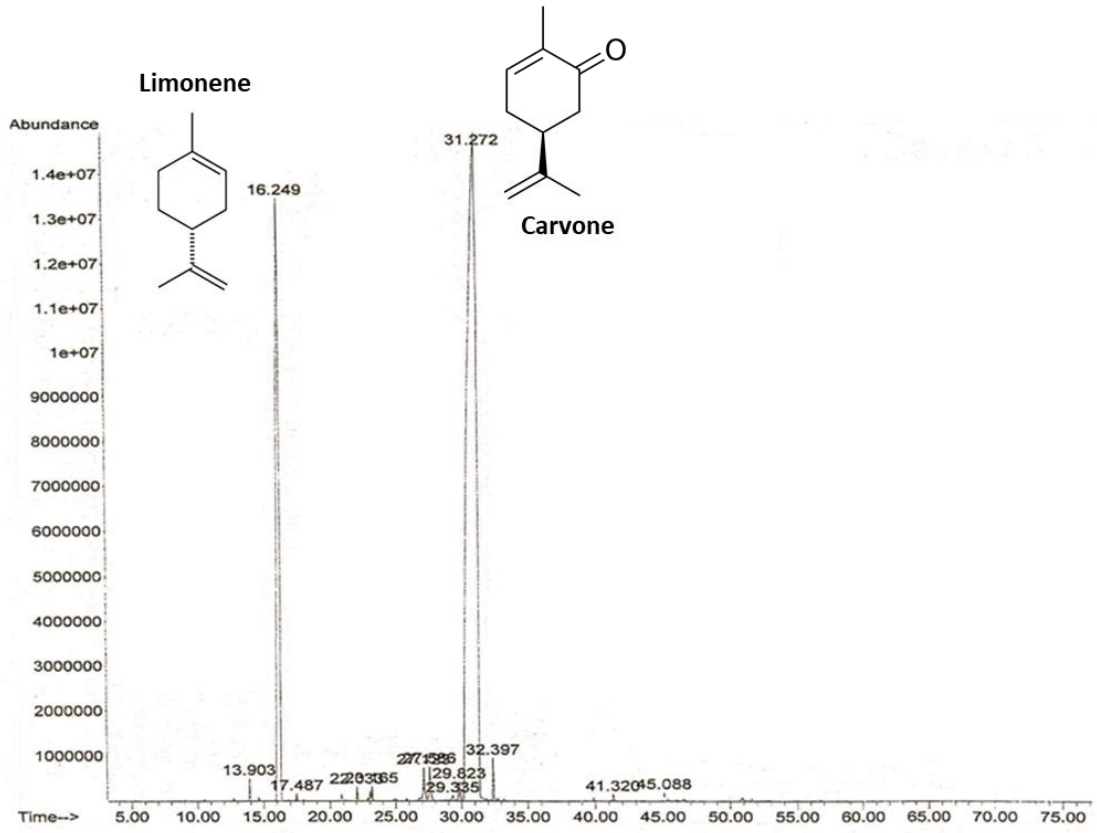

Figure 1. Chromatographic profile of the essential oil of *Carum carvi* L. seed

The two major components of this oil were carvone (75.64%) and limonene (20.70%), representing 96.34% of the essential oil (Table 1**)**. The other compounds were present in smaller percentages.

These results are in agreement with those of Assami et al. (2012) and Laribi et al. (2013) who reported that caraway seeds essential oil consists mainly of carvone and limonene. In addition to their fragrance, these compounds are also known for their antibacterial and antifungal properties (Zhang et al., 2014), antioxidant effects (Afify et al., 2012; De Almeida et al., 2014) as well as ability to inhibit the sprouting of potatoes (Hartmans et al., 1995).

Table 1. Chemical composition of the essential oil of *Carum carvi* L. seed

N	Compound[a]	RI[b]	RI[c]	Identification[e]	Percentage
1	β-Myrcene	991	991	RI, MS, CoI	0.22
2	D-Limonene	1012	1014	RI, MS, CoI	20.70
3	β-Ocimene	1101	1097	RI, MS, CoI	0.09
4	Oxyde de limonene	1132	1133	RI, MS	0.34
5	Cis-dihydrocarvone	1169	1172	RI, MS	0.75
6	Neodihydrocarveol	1170	1177	RI, MS	0.63
7	Trans-dihydrocarvone	1178	1175	RI, MS	0.15
8	Carveol	1203	1197	RI, MS	0.38
9	Carvone	1252	1240	RI, MS, CoI	75.64
10	Perillal	1287	1294	RI, MS	0.55
11	Caryophyllene	1411	1419	RI, MS, CoI	0.09
12	Germacrene D	1508	1477	RI, MS, CoI	0.20
				Monoterpene hydrocarbons	21.01
				Oxygenated monoterpene	78.44
				Sesquiterpenes	0.29
				Total	99.74

[a] Compounds listed in order of elution from HP-5MS column.

[b]Retention indices relative to C8 – C22 n-alkanes on HP-5MS column.

[c] Retention indices according to Adams (1995)

[d] Percentage (mean of three analyses) based on FID peak area

[e] RI: Retention indices relative to C8 – C22 n-alkanes on HP-5MS column, MS: mass spectrum, CoI: co-injection with authentic compounds (Fluka Chemika).

Identification of the spoilage microflora of potato

The identification of microorganisms from different samples of the healthy potatoes and those pigmented in pink allowed us to highlight two categories of microorganisms: bacteria and fungi. The characterization of this microflora made it possible to detect a difference between the samples of tested potatoes (Table 2). Among the isolated bacteria, *Enterobacter cloacae* was identified in the two types of potato but with different percentages: 100% (sound potato), 10% (infected potato). The genus *Citrobacter* was present only in the pigmented potato tubers with 80% relating to the species *Citrobacter freundii* and 10% to the species *Citrobacter braakii*.

Table 2. Sprouts isolated from samples of sound and pink pigmented potatoes.

Families	Sound potato	Pink pigmented potato
Enterobacteria	*Enterobacter cloacae* (100 %)	*Enterobacter cloacae* (10%) *Citrobacter braakii* (10%) *Citrobacter freundii* (80%)
Yeasts and molds	*Rhodotorula minuta*	*Aspergillus clavatus* *Phytophthora infestans* *Fusarium oxysporium*

With regard to yeasts and molds, *Rhodotorula minuta* species was identified only in sound potato tubers and three genera of molds were identified in pigmented potatoes: *Aspergillus*, *Phytophthora* and *Fusarium*. Microscopic analysis of the molds allowed us to identify mold species that corresponds to *Aspergillus clavatus*, *Phytophthora infestans* and *Fusarium oxysporum*. The presence of these pathogens in infected tubers during storage may be linked to the contamination of potato seeds and soil (Powelson and Rowe, 2008).

Antimicrobial activity of the essential oil of *Carum carvi* L. seed

The antimicrobial activity of the caraway essential oil was tested against two Gram-negative bacteria strains: *Citrobacter Freundii*, *Citrobacter braakii,* and three fungal species: *Aspergillus clavatus*, *Phytophthora infestans* and *Fusarium oxysporum*, isolated from the infected potatoes. The caraway essential oil shows notable inhibitory effects against all the studied microorganisms (Table 3). We note that this effect depends on the strain and the dose of used essential oil. According to Hassan et al. (2006) an inhibition zone diameter more than 10 mm means that an antimicrobial effect is proved.

Table 3. Diameters of inhibition zones (mm) for the different tested strains

	Volume of essential oil (µl)			
	10	**20**	**50**	**100**
Citrobacter freundii	12.0	14.0	18.0	22.0
Citrobacter braakii	6.0	6.0	10.0	14.0
Aspergillus clavatus	15.0	16.0	20.0	22.0
Phytophthora infestans	10.0	12.0	14.0	18.0
Fusarium oxysporium	6.0	8.0	9.0	13.0

The *Citrobacter freundii* strain shows the important inhibition zone diameters than those of *Citrobacter braakii.* In fact, *C. braakii* resisted to caraway essential oil action up to a dose of 50 µl (D = 10

mm), dissimilar to *C. freundii* which was inhibited from the lowest dose of EO which was 10 µl (D = 12 mm). The founded results are consistent with those of Roy et al. (2010) who showed that caraway EO has antibacterial activity against Gram- and Gram+ bacteria and more particularly against *enterobacteria.*

Among fungal species, *Aspergillus clavatus* was the most sensitive strain, followed by *Phytophthora infestans* and *Fusarium oxysporium* (Table 3). At a maximum dose of 100 µl caraway EO, the samples show inhibition zone diameters of 22, 18 and 13 mm, respectively.

This results confirm those obtained by Gómez-Castillo et al. (2013), who founded that the treatment of potato tubers with essential oils, including *Carum carvi* L. oil, reduce the proliferation of pathogenic microorganisms during storage, particularly molds. Moreover, this oil has been selected as a potent inhibitor of potatoes sprouts (Afify et al., 2012; Gómez-Castillo et al., 2013; Şanlı and Karadoğan, 2019).

The antimicrobial activity of caraway seed essential oil may be attributed to carvone and other monoterpenes, mainly limonene, which act as antiseptics, anti-inflammatories, antivirals, and antimicrobials. Many previous papers have shown that these two compounds have excellent antibacterial and antifungal properties (Roy et al. 2010 ; Esfandyari-Manesh et al., 2013). Notably, a degree of synergy between the majority and minority constituents of the caraway seed essential oil is possible.

Conclusion

The chemical composition analysis of caraway seeds essential oil, obtained with hydrodistillation, reveals that 99.74% of the constituents were identified. The main compound in this oil was carvone (75.64%), followed by limonene (20.70%). Due to its chemical composition, which is rich in monoterpene compounds, *Carum carvi* L. essential oil is effective against all strains of bacteria and molds isolated from infected potato (pink-pigmented), notably against *Citrobacter freundii* and *Aspergillus clavatus*. Thus, Caraway seeds essential oil can be used as a preservative to prevent contamination of potatoes due to the presence of enterobacteria and mold.

References

Abd El-Azeim, M. M., Sherif, M. A., Hussien, M. S., Tantawy, I. A. A., & Bashandy, S. O. (2020). Impacts of nano- and non-nanofertilizers on potato quality and productivity. Acta Ecologica Sinica, In press.

Afify AEMR, El-Beltagi HS, Aly AA, El-Ansary AE (2012) Antioxidant enzyme activities and lipid peroxidation as biomarker for potato tuber stored by two essential oils from caraway and clove and its main component carvone and eugenol. Asian Pacific Journal of Tropical Biomedicine, S772-S780.

Agrahari, P., & Singh, D. (2014). A review on the pharmacological aspects of *Carum carvi* L. Journal of Biology and Earth Sciences, 4(1), 1–13.

Al-Snafi, A. (2015). The chemical constituents and pharmacological effects of *Capparis spinosa*— an overview. Indian Journal of Pharmaceutical Sciences, 5(2)(7), 2–82.

Assami, K., Pingret, D., Chemat, S., Meklati, B. Y., & Chemat, F. (2012). Ultrasound induced intensification and selective extraction of essential oil from *Carum carvi* L. seeds. Chemical Engineering and Processing: Process Intensification, 62, 99–105.

Cushine, T.P.T, & Lamb, A J., (2005). Antimicrobial activity of flavonoids. International Journal of Antimicrobial Agents, 26, 343 – 356.

Esfandyari-Manesh, M., Ghaedi, Z., Asemi, M., Khanavi, M., Manayi, A., Jamalifar, H., Atyabi, F., & Dinarvand, R. (2013). Study of antimicrobial activity of anethole and carvone loaded PLGA nanoparticles. Journal of Pharmacy Research, 7(4), 290–295.

Essaidi, I., Ben Haj Koubaier, H., Snoussi, A., Casabianca, H., Chaabouni, M.M., & Bouzouita N. (2014). Chemical Composition of *Cyperus rotundus* L. Tubers essential oil from the South of Tunisia, antioxidant potentiality and antibacterial activity against foodborne pathogens. Journal of Essential Oil Bearing Plants, 17 (3), 522 – 532.

FAO (2016). Food and Agriculture Organization of the United Nations FAOSTAT. 2016. http://www.fao.org/faostat/en/#home.

Gómez-Castillo, D., Cruz, E., Iguaz, A., Arroqui, C., & Vírseda, P. (2013). Effects of essential oils on sprout suppression and quality of potato cultivars. Postharvest Biology and Technology, 82, 15–21.

Hartmans, K.J., Diepenhorst, P., Bakker, W., & Gorris, L. G. (1995). The use of carvone in agriculture: sprout suppression of potatoes and antifungal activity against potato tuber and other plant diseases. Industrial Crops and Products, 4(1), 3–13.

Hassan, S.W., Umar, R.A, Lawal, M., Biblis L.M., Muhammed, B.Y., Dabai, Y.U. (2006). Evaluation of antibacterial activity and phytochemical analysis of root extracts of *Boxia angustifolia*. African Journal of Biotechnology, 5 (18), 1602-1607.

Hwang, J.I., Zimmerman, A. R., & Kim, J.-E. (2018). Bioconcentration factor-based management of soil pesticide residues: Endosulfan uptake by carrot and potato plants. Science of the Total Environment, 627, 514–522.

Karameşe, M., & Özgür, D. (2020). The antibacterial and antifungal activities of commonly used herbal oils. International Journal of Clinical and Experimental Medicine, 37(2), 47-51

Kazemipoor, M., Hamzah, S., Hajifaraji M, Radzi, C., & Cordell, G. (2016). Slimming and Appetite-Suppressing Effects of Caraway Aqueous Extract as a Natural Therapy in Physically Active Women. Phytotherapy Research, 30(6), 981–987.

Larkin, R.P. (2016). Impacts of biocontrol products on *Rhizoctonia* disease of potato and soil microbial communities, and their persistence in soil. Crop Protection, 90, 96 – 105.

Laribi, B., Kouki, K., Bettaieb, T., Mougou, A., & Marzouk, B. (2013). Essential oils and fatty acids composition of Tunisian, German and Egyptian caraway (*Carum carvi* L.) seed ecotypes: A comparative study. Industrial Crops and Products, 41, 312–318

Lasram, S., Zemnia, H., Hamdia, Z,. Chenenaoui, S., Houissa, H., Tounsi, M. S., & Ghorbel, A. (2019). Antifungal and anti aflatoxinogenic activities of *Carum carvi* L., *Coriandrum sativum* L. seed essential oils and their major terpene component against *Aspergillus flavus*. Industrial Crops and Products, 134, 11–18.

Powelson, M. L., & Rowe, R. C. (2008). Managing diseases caused by seedborne and soilborne fungi and fungus-like pathogens. Potato Health Management, 2183-2195.

Robertson, T. M., Alzaabi, A. Z., Robertson, M. D., & Fielding, B. A. (2018). Starchy carbohydrates in a healthy diet: the role of the humble potato. Nutrients, 10(11), 1764.

Roy, S.D., Tharkur, S., Negi, A., Kumari, M., Sutar, N., & Jana, G.K. (2010). In vitro antibiotic activity of volatile oils of *Carum carvi* L. and *Coriandrum stavium*. International Journal of Chemical and Analytical Science, 1(7), 149-150

Saghir, M., Sadiq, S., Nayak, S., & Tahir, M. (2012). Hypolipidemic effect of aqueous extract of *Carum carvi* (black Zeera) seeds in diet induced hyperlipidemic rats. Pakistan Journal of Pharmaceutical Sciences, 25(2), 333–337.

Şanlı, A., & Karadoğan, T. (2019). Carvone containing essential oils as sprout suppressants in potato (*Solanum tuberosum* L.) tubers at different storage temperatures. Potato Research.

Sharma, N., Tiwari, D., & Singh, S. (2014). The efficiency appraisal for removal of malachite green by potato peel and neem bark: isotherm and kinetic studies. International Journal of Chemical and Environmental Engineering, 5(2), 83–88.

Zhang, Z., Vriesekoop, F., Yuan, Q., & Liang, H. (2014). Effects of nisin on the antimicrobial activity of d-limonene and its nanoemulsion. Food Chemistry, 150, 307-312.

In vitro anti-mikrobna aktivnost etarskog ulja semena *Carum carvi* L. protiv kvarenja ružičastog krompira

Ahmed Snusi[1,2], Hajet Ben Haj Kubajer [1,2], Susen Bikida[1,2], Ismahen Esaidi[3], Faten Kašuri[1] and Nabiha Buzuita [1,2]

1- Univerzitet u Kartagini, Viša škola industrije hrane Tunisa, 58 Alain Savary Avenue, Kartagina 1003, Tunis

2- Tunis El Manar Univerzitet, Fakultet prirodnih nauka u Tunisu, Laboratorija za strukturnu organsku hemiju: hemijska sinteza i fizičko-hemijska analiza, Tunis 2092, Tunis

3- Univerzitet u Susu, Viši agronomski Institut Čot Merijem, Sus 4042, Tunis

Sažetak

Tema našeg istraživanja je ispitivanje mogućnosti primene etarskog ulja iz semena *Carum carvi* L. kao biološke supstance za kontrolisanje rasta mikroba koji izazivaju kvarenje krompira u toku skladištenja. Hemijski sastav etarskog ulja semena kima, analiziranog GC-MS i gasnom hromatografijom korišćenjem FID detektora (engl. GC-MS), sadrži dvanaest jedinjenja, gde je karvon glavno jedinjenje (75.64% od ukupnog ulja). Upoređivanje mikrobnog profila različitih uzoraka krompira pokazalo je prisustvo roda *Citrobacter* i tri različita roda gljiva: *Aspergillus*, *Phytophthora* i *Fusarium* samo za kontaminirane krompirove krtole sa unutrašnjom roze pigmentacijom. Dakle antimikrobna aktivnost etarskog ulja semena kima ispitivana je na ove sojeve. Antimikrobna aktivnost ulja na izolovane sojeve procenjena je korišćenjem agar difuzne metode korišćenjem različitih zapremina (10, 20, 50 and 100 µl). Svi testirani sojevi inhibirani su etarskim uljem semena kima na način koji je zavisan od doze. Dobijeni rezultati sugerišu korišćenje *Carum carvi* L. kao obećavajuće prirodne supstance za očuvanje krompira metodom kontaktne pare.

Ključne reči: krompir, etarsko ulje, Carum carvi L., semenke, antimikrobna aktivnost, enterobakterije, gljive

Activité antimicrobienne *in vitro* de l'huile essentielle de graines de *Carum carvi* L. contre la flore d'altération de la pomme de terre rose

Ahmed Snoussi[1,2], Hayet Ben Haj Koubaier[1,2], Saoussen Bouacida[1,2], Ismahen Essaidi[3], Faten Kachouri1 et Nabiha Bouzouita[1,2]

1- Université de Carthage, École Supérieure des Industries Alimentaires de Tunisie, 58 avenue Alain Savary, Carthage 1003, Tunisie
2- Université Tunis El Manar, Faculté des Sciences de Tunis, Laboratoire de Chimie Organique Structurale: Synthèse Chimique et Analyse Physico-chimique, Tunis 2092, Tunisie
3- Université de Sousse, Institut Supérieur Agronomique de Chott Meriem, Sousse 4042, Tunisie

Résumé

Cette étude consiste à évaluer la capacité l'huile essentielle de graines de *Carum carvi* L. à être utilisée comme substance biologique pour contrôler la croissance des germes d'altération dans les pommes de terre pendant le stockage. La composition chimique de l'huile essentielle de graines de carvi, analysée par GC-MS et par chromatographie en phase gazeuse avec détecteur à ionisation de flamme (GC-FID), a conduit à l'identification de 12 composés, représentée essentiellement par le carvone avec un pourcentage de 75.64% de la composition totale. La comparaison des profils microbiens de différents échantillons de pommes de terre a montré la présence du genre Citrobacter et de trois genres de champignons distincts: *Aspergillus*, *Phytophthora* et *Fusarium* uniquement pour les échantillons de pomme de terre pigmentés en rose. Ainsi, l'activité antimicrobienne de l'huile essentielle de graines de carvi a été étudiée contre ces souches. L'activité antimicrobienne de l'huile contre les souches isolées a été évaluée par la méthode de diffusion sur gélose en utilisant différents volumes (10, 20, 50 et 100 µl). Toutes les souches testées ont été inhibées par l'huile essentielle de graines de carvi d'une manière dose-dépendante. Les résultats obtenus suggèrent l'utilisation de *Carum carvi* L. comme substance naturelle prometteuse pour la conservation des pommes de terre par la méthode de la vapeur de contact.

Mots clés : Pomme de terre, Huile essentielle, Graines Carum carvi L., Activité antimicrobienne, Enterobactéries, Champignons

Антимикробная активность эфирного масла семян *Carum carvi* L. *in vitro* в отношении порчи флоры розового картофеля

Ахмед Снусси[1,2], Хайет Бен Хадж Кубайер [1,2], Сауссен Буасида[1,2], Исмахен Эссайди[3], Фатен Качури1 и Набиха Бузуита [1,2]

1 – Карфагенский университет, Высшая школа пищевой промышленности Туниса, проспект Алена Савари, дом 58, Карфаген 1003, Тунис

2- Тунисский университет Эль-Манар, Тунисский факультет наук, Лаборатория структурной органической химии: химический синтез и физико-химический анализ, Тунис 2092, Тунис

3- Университет в Сусе, Высший агрономический институт Шотта Мериема, 4042, Сусс Тунис

Аннотация

Целью данного исследования является оценка возможности использования эфирного масла семян Carum carvi L. в качестве биологического вещества для контроля роста микробов порчи картофеля во время хранения. Химический состав эфирного масла семян тмина, проанализированный с помощью ГХ-МС и газовой хроматографии с пламенно-ионизационным детектором (ГХ-ПИД), привел к идентификации двенадцати соединений, из которых карвон был основным, с процентным содержанием 75.64% от общего содержания. Сравнение микробных профилей различных образцов картофеля показало присутствие рода Citrobacter и трех различных родов грибов: Aspergillus, Phytophthora и Fusarium только для загрязненных клубней картофеля с внутренней розовой пигментацией. Таким образом, была изучена антимикробная активность эфирного масла тмина в отношении этих штаммов. Антимикробную активность масла в отношении выделенных штаммов оценивали методом диффузии в агар с использованием различных объемов (10, 20, 50 и 100 мкл). Все испытанные штаммы дозозависимо подавляли эфирное масло тмина. Полученные результаты предполагают использование Carum carvi L. как перспективного природного вещества для консервирования картофеля контактным паровым методом.

Ключевые слова: картофель, эфирное масло, семена Carum carvi L., антимикробная активность, энтеробактерии, грибы

Antimikrobielle In-vitro-Wirksamkeit vom ätherischen Öl aus den Samen von *Carum carvi* L. gegen die Verderbnisflora von rosa Kartoffeln

Ahmed Snoussi[1,2], Hayet Ben Haj Koubaier[1,2], Saoussen Bouacida[1,2], Ismahen Essaidi[3], Faten Kachouri[1], Nabiha Bouzouita[1,2]

1- Universität Karthago, Hochschule für Lebensmittelindustrie in Tunesien, 58 Alain Savary Avenue, Karthago 1003, Tunesien

2- Universität Tunis El Manar, Fakultät für Naturwissenschaften, Labor für strukturelle organische Chemie: Chemische Synthese und physikalisch-chemische Analyse, Tunis 2092, Tunesien

3- Universität Sousse, Höheres Agronomisches Institut von Chott Meriem, Sousse 4042, Tunesien

ABSTRAKT

Das Ziel dieser Forschung ist es, die Möglichkeit zu untersuchen, das ätherische Öl aus den Samen von *Carum carvi L* als biologische Substanz dafür zu werwenden, das Wachstum von Verderbniskeimen in Kartoffeln während der Lagerung zu kontrollieren. Die chemische Zusammensetzung des ätherischen Öls aus Kümmelsamen, analysiert durch GC-MS und durch Gaschromatographie mit Flammenionisationsdetektor (GC-FID), führte zur Identifizierung von zwölf Verbindungen, wobei die Hauptverbindung Carvon war (mit einem Prozentsatz von 75.64% des Gesamtöls). Der Vergleich der mikrobiellen Profile verschiedener Kartoffelproben ergab das Vorhandensein der Gattung *Citrobacter* und drei verschiedene Pilzgattungen: *Aspergillus, Phytophthora* und *Fusarium* nur für kontaminierte Kartoffelknollen mit der inneren rosa Pigmentierung. Daher wurde die antimikrobielle Aktivität des ätherischen Kümmelöls gegen diese Stämme untersucht. Die antimikrobielle Aktivität des Öls gegen die isolierten Stämme wurde durch das Agardiffusionsverfahren unter Verwendung verschiedener Volumina (10, 20, 50 und 100 µl) bewertet. Alle getesteten Stämme wurden dosisabhängig durch ätherisches Kümmelöl inhibiert. Die erhaltenen Ergebnisse legen die Verwendung von *Carum carvi L.* als vielversprechende natürliche Substanz zur Konservierung von Kartoffeln nach der Kontaktdampf-Methode nahe.

Schlüsselwörter: Kartoffel, ätherisches Öl, Samen von Carum carvi L., antimikrobielle Aktivität, Enterobakterien, Pilze

Volatile Compounds of Homemade Grape Brandy Determined by GC-MS Analysis

Stamenković Jelena[1*], Stojanović Gordana[1]

1- University of Niš, Faculty of Science and Mathematics, Department of Chemistry, Višegradska 33, 18000 Niš, Serbia

Stamenković Jelena: jelena.stamenkovic@pmf.edu.rs
Stojanović Gordana: gocast@pmf.ni.ac.rs

ABSTRACT

The aim of this paper was to determine whether the addition of some ingredients to the same grape brandy after distillation affects the chemical composition of the volatile components by applying the gas chromatography coupled with mass spectrometry (GC-MS). Five samples were subjected to this study and a total of 57 compounds were identified. For all examined samples, esters were the most dominant class of compounds, but in different proportions. Ethyl decanoate was the most abundant compound in the sample L1 (grape brandy kept in an oak barrel) with the contribution of 29.1%, followed by ethyl octanoate (17.2%) and ethyl dodecanoate (14.8%). Sample L2 (grape brandy with summer truffles) was dominated by *n*-hexanol and ethyl lactate with similar contribution (18.1% and 17.8%, respectively). On the other hand, in the sample L3 (grape brandy with winter truffles) ethyl lactate was present with the contribution 44.8%. The dominant compounds in sample L4 (grape brandy with grains of coffee and dried grapes) were ethyl decanoate with contribution of 14.8% and phenyl ethyl alcohol (12.5%), while the two main volatiles of the sample L5 (grape brandy with young green walnuts) were diethyl succinate (22.9%) followed by ethyl lactate (21.9%). The results obtained in this study on volatile aromatic compounds in the analyzed grape brandies suggest that addition of some ingredients to the same grape brandy after distillation affects the chemical composition in both the number of aromatic compounds and their relative content.

Keywords: grape brandy, chemical composition, volatiles, GC-MS

* *Stamenković Jelena, jelena.stamenkovic@pmf.edu.rs, Department of Chemistry, Faculty of Sciences and Mathematics, University of Niš, Višegradska 33, 18000 Niš, Serbia*

Introduction

Fruit spirits are popular alcohol beverages due to their unique flavour and very often they represent the national drink of the country. *Rakija* is the collective term for fruit brandy popular in the Balkans and it can be made from all fruit species containing sugar from which alcohol is produced during alcoholic fermentation. The best fruits to produce *rakija* are plums, cherries, apples, pears, apricots and quinces. In some countries, as well as in Serbia, *rakija* can also be made from grapes; there are two different types of grape spirits: "*loza*" – obtained through fermentation and distillation of the whole non-strained mash of grapes and "*komova rakija*" – the spirits where the grape pomace (grape residues) that is left over from winemaking is used as base.

Normally, *rakija* is colourless, unless herbs or other ingredients are added. Some types of *rakija* are kept in wooden barrels (oak or mulberry) for extra aroma and a golden colour, while sometimes plum and grape *rakija* are mixed with other ingredients, such as herbs, honey, sour cherries and walnuts, during the fermentation process and during the distillation or after that.

The main ingredients of these beverages are water and ethanol, and they account around 99% of the total content of the spirits but there are hundreds of different compounds, so-called congeners, present in very low concentrations that are responsible for the differences between spirits obtained from different fruits. It is well known that the chemical composition depends on the cultivar used for the production (Biernacka and Wardencki, 2012; Coldea et al., 2011; Hernandez-Gomez et al., 2005), grape processing method (Radeka et al., 2008), fermentation procedure (Matijašević et al., 2019; Soufleros et al., 2005), distillation technique (Arrieta-Garay et al., 2013; Lukić et al., 2011a; Madrera and Alonso, 2012; Matias-Guiu et al., 2016; Spaho, 2017), use of post distillation processes and maturation of the spirits (Madrera et al., 2003; Tsakiris et al., 2014). The aim of this paper was to determine whether the addition of some ingredients to the same grape brandy after distillation affects the chemical composition of the volatile components by applying the gas chromatography coupled with mass spectrometry (GC-MS).

Experimental

Five samples were analyzed. All the analyzed samples were homemade grape brandies produced by traditional method. First sample (L1) was grape brandy kept in an oak barrel, the second sample (L2) being grape brandy kept in an oak barrel to which summer truffles (100 - 200 g truffles per liter of fresh brandy) were added and which stood in brandy for about 3 months, the third sample (L3) was grape brandy to which winter truffles (100 - 200 g truffles per liter of brandy) were added and which stood in brandy for about a month, the fourth sample (L4) was grape brandy kept in an oak barrel to which was then added 40 grains of coffee and 10 grains of dried grapes, per liter of brandy, and which stood in brandy for about 6

months and the fifth sample (L5) was grape brandy to which was then added 40 young green walnuts per liter of brandy and left in the dark for a month and then filtered.

Isolation of esters from *rakija*

Eighty milliliters of spirits were mixed with 80 mL of distilled water and 40 mL of CH_2Cl_2 in a 300 mL conical flask. Eight grams of NaCl was added and the mixture was stirred on a magnetic stirrer for 30 min. The layers were separated into a separating funnel and the organic layer was dried above of anhydrous $MgSO_4$. The extract was concentrated to 1 mL on a vacuum evaporator and directly analyzed by gas chromatography- mass spectrometry (GC-MS) (Tešević et al., 2005).

GC-MS analysis

GC-MS analyses were performed on an Agilent 7890 gas chromatograph with 7000B GC-MS-MS triple quadrupole system, operating in MS1 scan mode, and equipped with a fused-silica capillary column Agilent HP-5 MS (30 m × 0.25 mm i.d. × 0.25 μm film thickness). The chromatographic analyses were carried out in the following conditions: He as a carrier gas at a flow rate of 1.0 mL/min, GC oven temperature was kept at 50 °C for 2.25 min and programmed to 290 °C at a rate of 4 °C/min. One μL of the concentrated extract was injected at split ratio 40:1. The injector and interface operated at 250 and 300°C, respectively. Post run: back flash for 1.89 min, at 280 °C, with helium pressure of 50 psi. Ionization mode was electronic impact at 70 eV. Mass range was set from 40 to 440 Da.

The percentage amounts of the separated compounds were calculated from the total ion chromatogram.

Identification of volatile compounds

Components were identified by comparison of their mass spectra with those of Wiley 6, Adams (2007), NIST 11 and Essential oils libraries, applied on Agilent Mass Hunter Workstation (B.06.00) and AMDIS (2.1, DTRA/NIST, 2011) software and confirmed by comparing of calculated retention indexes (relative to C_8-C_{32} *n*-alkanes) with the literary values of the retention indices.

Results and Discussion

The individual and mean values for each volatile found in all four samples are presented in Table 1. In the samples that were subjected to this study a total of 57 compounds were identified that belong to different groups, eight of them were found to be common to all. For all examined samples, esters were the most dominant class of compounds, but in different proportions. Esters are formed during the alcoholic fermentation and they represent the most common class of compounds that contribute to the aroma in the

brandy (Ferrari et al., 2004; Silva and Malcata, 1999; Soufleros et al., 2001). The ethyl esters were the most dominant class of the esters identified in our samples and according to the literature they are produced during raw material fermentation and their content may increase or decrease during ageing (Genovese et al., 2013; Mamede et al., 2005; Tešević et al., 2005). Grape brandy that was kept in an oak barrel (L1) could be distinguished from the other samples by the highest relative amount of esters (89.1%). Among these, ethyl decanoate was the most abundant with the contribution of 29.1%, followed by ethyl octanoate (17.2%) and ethyl dodecanoate (14.8%). These compounds are produced during the raw material fermentation (Silva and Malcata, 1998) and they are contributing to the fruity and flowery smells at their relatively high levels (Madrera et al., 2013). Sample L2 was dominated by *n*-hexanol and ethyl lactate with similar contribution (18.1% and 17.8%, respectively). According to the literature, *n*-hexanol is originating only from raw material (Soufleros et al., 2004) and it is denominated as a rough indicator of the pressing degree (Lukić et al., 2011b) which presence can be associated with flower and herbaceous aromas. On the other hand, in the sample L3 ethyl lactate was present with the contribution 44.8% and it is considered to give the distillates a buttery flavour and smell of rancid butter and its presence can be linked to a malolactic fermentation (Léauté, 1990). The dominant compounds in sample L4 were ethyl decanoate with contribution of 14.8% and phenyl ethyl alcohol (12.5%) which is an aromatic alcohol and has a rose-like odour. Out of 28 compounds that were identified in the sample L4, 7 were exclusive to this sample. The most significant was caffeine which represented 7.1% of the sample. Caffeine is a purine alkaloid that occurs naturally in coffee beans. Alcoholic beverages (in our case-grape brandy) normally do not contain caffeine, so the presence of the caffeine in this sample is because it was extracted from the grains of coffee during the process of maceration. The two main volatiles of the sample L5 were diethyl succinate (22.9%) which gives a camphor-like character (Ferreira et al., 1999) and according to the literature derives mainly from bacterial spoilage (Karagiannis and Lanaridis, 2002), followed by ethyl lactate (21.9%). Among 27 components identified in this sample, five of them were detected only in this sample. Syringic acid (10.5%) is a phenol present in some distilled alcohol beverages and the presence of this compound only in sample L5 according to the previously published results (Colaric et al., 2005; Cosmulescu et al., 2010) lead us to the conclusion that it comes from young nuts that have been added. Another compound worth mentioning was juglone, which is a well-known component of walnut (Cosmulescu et al., 2010; Prasad, 2003; Stampar et al., 2006).

Table 1. Chemical composition of grape brandy volatiles.

				Content %				
No	RI	RN	Compound	L1	L2	L3	L4	L5

1	765	762	Pentanol	0.6	-	-	-	-
2	775	778	Ethyl butanoate	0.7	0.4	0.6	0.3	-
3	794	798	Ethyl lactate	4.3	17.8	44.8	-	21.9
4	805	827	3-Methylhexan-3-ol	-	3.5	-	-	-
5	810	815	Furfural	0.4	0.3	-	0.7	-
6	828	839	Ethyl 2-methylbutyrate	-	2.8	1.4	-	-
7	840	846	2-Methylbutanoic acid	-	2.8	2.1	-	-
8	852	858	*n*-Hexanol	0.8	18.1	8.5	1.7	-
9	861	867	Isopentyl acetate	0.4	2.1	0.9	0.3	2.2
10	948	955	1,1-Diethoxy-3-methyl-butane	-	0.6	-	-	0.3
11	954	959	Benzaldehyde	-	-	1.2	8.6	-
12	960	968	Ethyl 2-hydroxyisovalerate	-	-	0.5	-	-
13	968	977	1-(1-ethoxyethoxy)-Pentane	-	0.4	-	0.3	0.7
14	995	997	Ethyl hexanoate	2.3	0.4	0.9	0.8	1.0
15	1024	1024	Limonene	-	-	-	4.4	-
16	1030	1034	Benzyl alcohol	-	-	-	0.6	0.6
17	1054	1062	Ethyl 2-hydroxyhexanoate	-	0.4	1.1	-	0.5
18	1069	1067	*cis*-Linalool oxide	0.4	0.5	-	-	0.5
19	1085	1084	*trans*-Linalool oxide	-	-	-	0.4	0.3
20	1096	1095	Linalool	0.8	-	-	-	0.3
21	1100	1100	*n*-Nonanal	0.4	-	-	0.4	-
22	1110	1115	Phenyl ethyl alcohol	3.0	7.3	6.2	12.5	9.3
23	1164	1163	4-Ethyl-phenol	-	-	-	-	2.2
24	1167	1169	Ethyl benzoate	-	1.2	2.2	3.8	-
25	1175	1170	Octanoic acid	-	4.6	1.2	-	-
26	1177	1181	Diethyl succinate	3.0	-	2.7	-	22.9
27	1188	1186	α-Terpineol	0.5	-	-	0.2	-

28	1189	1188	2-Methoxy-*p*-cresol	-	0.3	-	-	-
29	1193	1194	Ethyl octanoate	17.2	1.9	4.2	5.7	4.1
30	1225	1246	Benzaldehyde diethylacetal	-	-	-	3.2	-
31	1241	1243	Benzene acetic acid, ethyl ester	-	0.8	0.5	-	-
32	1254	1254	2-Phenyl ethyl acetate	-	-	-	-	0.4
33	1276	1280	4-Ethyl-2-methoxy-phenol	-	-	-	-	1.0
34	1292	1295	Nonanoic acid, ethyl ester	0.4	-	-	0.3	-
35	1346	1347	Triacetin	-	-	1.0	-	-
36	1355	1356	Eugenol	-	-	-	0.5	-
37	1370	1364	Decanoic acid	2.1	4.0	0.9	-	2.4
38	1381	1381	*n*-Nonanal diethyl acetal	-	-	-	0.5	-
39	1392	1392	Ethyl decanoate	29.1	4.2	7.1	14.8	4.1
41	1396	1393	Vanillin	-	-	-	0.3	-
42	1465	1467	Ethyl-(2*E*,4*Z*)-decadienoate	-	2.3	1.4	-	-
43	1498		Juglone	-	-	-	-	1.8
44	1561	1565	Dodecanoic acid	0.3	0.2	-	-	0.4
45	1570	1569	γ-Undecalactone	-	-	-	-	-
46	1590	1593	Ethyl dodecanoate	14.8	1.1	2.1	7.6	1.0
47	1640	1641	Isoamyl decanoate	0.7	-	-	-	-
48	1657	1655	Syringaldehyde	-	-	-	1.1	-
50	1789	1795	Ethyl tetradecanoate	2.3	-	-	-	-
51	1817	1823	Syringic acid	-	-	-	-	10.5
52	1841	1842	Caffeine	-	-	-	7.1	-
53	1967	1977	Ethyl 9-hexadecenoate	0.9	-	-	0.2	-
54	1988	1193	Ethyl hexadecanoate	7.2	1.6	2.0	4.7	0.5
55	2156	2163	Ethyl linoleate	2.7	4.9	1.7	2.0	0.3
56	2162	2169	Ethyl oleate	-	1.7	1.2	-	-

57	2162	2173	Linolenic acid, ethyl ester	3.1	-	-	1.5	-
Number of constituents				25	27	24	28	24
Total identified				98.4	86.2	96.4	84.5	89.2
Alcohols				4.4	28.9	14.7	14.8	9.9
Esters				89.1	43.6	75.3	42.0	58.9
Others				4.9	13.7	6.4	27.7	20.4

Compounds listed in order of elution on a HP-5 MS column. RI: experimentally determined retention indices on the mentioned column by co-injection of a homologous series of *n*-alkanes C_8-C_{32}; RN: NIST Chemistry WebBook Retention indices; **-**: not detected. Samples: L1-grape brandy kept in an oak barrel; L2-grape brandy kept in an oak barrel with summer truffles; L3- grape brandy with winter truffles; L4-grape brandy kept in an oak barrel with coffee grains of dried grapes; L5-grape brandy with young green walnuts.

Conclusion

The results obtained in this study on volatile aromatic compounds in the analyzed grape brandies suggest that addition of some ingredients to the same grape brandy after distillation affects the chemical composition in both the number of aromatic compounds and their relative content. Ethyl esters from middle-chain fatty acids (octanoic, decanoic and dodecanoic) which make up over 60% of the samples L1 are contributing to the fruity and flowery smells of the sample. The volatile composition of the samples L2 and L3 was qualitatively rather similar, so their quite distinct organoleptic characteristics can be attributed to the differences between their volatile concentrations. The herbaceous odour of sample L2 can be explained by the domination of the *n*-hexanol. On the other hand, ethyl lactate which was the most abundant compound in the sample L3 is considered to give the distillates a buttery flavour and smell of rancid butter. Ethyl decanoate and phenyl ethyl alcohol are responsible for a fruity and rose-like odour of the sample L4, while the dominant presence of diethyl succinate gives a camphor-like character of the sample L5. Also, for samples L1, L2 and L4 it has been observed the presence of furfural which can be explained by the fact that these samples were kept in the oak barrel (while the samples L3 and L5 were not), since there are some studies that reports that volatile compounds extracted from the barrel wood are mainly furanic and phenolic compounds.

Acknowledgment

Financial support of the Ministry of Education, Science and Technological Development of Serbia (Project No. 451-03-68/2020-14/200124) is gratefully acknowledged.

Conflict-of-Interest Statement

All authors declare that they have no conflict of interest.

References

Arrieta-Garay, Y., García-Llobodanin, L., Pérez-Correa, J.R., López-Vázquez, C., Orriols, I., & López, F. (2013). Aromatically enhanced pear distillates from Blanquilla and conference varieties using a packed column. Journal of Agricultural and Food Chemistry, 61, 4936-4942.

Biernacka, P., & Wardenck, W. (2012). Volatile composition of raw spirits of different botanical origin. Journal of the Institute of Brewing, 118, 393400.

Colaric, M., Veberic, R., Solar, A., Hudina M., & Stampar F. (2005). Phenolic acids, syringaldehyde, and juglone in fruits of different cultivars of *Juglans regia* L. Journal of Agricultural and Food Chemistry, 53(16), 6390-6396.

Coldea, T. E. R., Socaicu, C., & Dan Vodnar, M. P. (2011). Gas-chromatographic analysis of major volatile compounds found in traditional fruit brandies from Transylvania, Romania. Notulae Botanicae Horti Agrobotanici Cluj-Napoca, 39, 109-116.

Cosmulescu, S. N., Trandafir, I., Achim, G., Botu, M., Baciu, A., & Gruia, M. (2010). Phenolics of green husk in mature walnut fruits. Notulae Botanicae Horti Agrobotanici Cluj-Napoca, 38(1), 53-56.

Ferrari, G., Lablanquie, O., Cantagrel, R., Ledauphin, J., Payot, T., Fournier, N., & Guichard, E. (2004). Determination of key odorant compounds in freshly distilled cognac using GC-O, GC- MS and sensory evaluation. Journal of Agricultural and Food Chemistry, 52, 5670-5676.

Ferreira, V., Hernandez-Orte, P., Escudero, A., Lopez, R., & Cacho, J. (1999). Semipreperative reversed-phase liquid chromatographic fractionation of aroma extracts from wine and other alcoholic beverages. Journal of Chromotography A, 864, 77-88.

Genovese, A., Lamorte, S. A., Gambuti, A., & Moio, L. (2013). Aroma of Aglianico and Uva di Troia grapes by aromatic series. Food Research International, 53, 15-23.

Hernandez-Gomez, L. F., Ubeda-Iranzo, J., Garcıa-Romero, E., & Briones-Perez, A. (2005). Comparative production of different melon distillates: chemical and sensory analyses. Food Chemistry, 90, 115-125.

Karagiannis, S., & Lanaridis, P. (2002). Insoluble grape material present in must affects the overall fermentation aroma of dry white wines made from three grape cultivars cultivated in Greece. Journal of Food Science, 67, 369-374.

Léauté, R. (1990). Distillation in Alembic. American Journal of Enology and Viticulture, 41, 90-103.

Lukić, I., Tomas, S., Miličević, B., Radeka, S., & Peršurić, Đ. (2011a). Behaviour of volatile compounds during traditional alembic distillation of fermented Muscat Blanc and Muskat Ruza Porecki grape marcs. Journal of the Institute of Brewing, 117, 440-450.

Lukić, I., Miličević, B., Banović, M., Tomas, S., Radeka, S., & Peršurić, Đ. (2011b). Secondary aroma compounds in fresh grape marc distillates as a result of variety and corresponding production technology. Food Technology and Biotechnology, 49, 214-227.

Madrera, R. R., Gomis, D. B., & Alonso, J. J. M. (2003). Characterization of cider brandy on the basis of aging time. Journal of Food Science, 68, 1958-1961.

Madrera, R. R., & Alonso, J. J. M. (2010). Distribution of the principal minor volatiles during cider distillation in 'alquitara'. Acta Alimentaria, 40, 262-269.

Madrera, R. R., Hevia, A. G., & Valles, B. S. (2013). Comparative study of two aging systems for cider brandy making. Changes in chemical composition. LWT-Food Science and Technology, 54, 513-520.

Mamede, E. O. M., Cardello, M. A. B. H., & Pastore, M. G. (2005). Evaluation of an aroma similar to that of sparkling wine: Sensory and gas chromatography analyses of fermented grape musts. Food Chemistry, 89, 63-68.

Matias-Guiu, P., Rodríguez-Bencomo, J. J., Orriols, I., Pérez-Correa, J. R., & López, F. (2016). Floral aroma improvement of Muscat spirits by packed column distillation with variable internal reflux. Food Chemistry, 213, 40-48.

Matijašević, S., Popović-Djordjević, J., Ristić, R., Ćirković, D., Ćirković, B., & Popović, T. (2019). Volatile aroma compounds of brandy 'Lozovača′ produced from muscat table grapevine cultivars (*Vitis vinifera* L.). Molecules, 24, 2485.

Prasad, R. B. N. (2003). Walnuts and pecans, pp. 6071-6079. In: B. Caballero, L. C. Trugo and P. M. Finglas (Eds.). Encyclopaedia of food sciences and nutrition, Academic Press, London.

Radeka, S., Herjavec, S., Peršurić, Đ., Lukić, I., & Sladonja, B. (2008). Effect of dfferent maceration treatments on free and bound varietal aroma compounds in wine of *Vitis vinifera* L. cv. Malvazija istarska bijela. Food Technology and Biotechnology, 46, 86-92.

Silva, M. L., & Malcata, F. X. (1998). Relationships between storage conditions of grape pomace and volatile composition of spirits obtained therefrom. American Journal of Enology and Viticulture, 49 (1), 56-64.

Silva, M. L., & Malcata, F. X. (1999). Effects of time of grape pomace fermentation and distillation cuts on the chemical composition of grape marcs. Zeitschrift fuer Lebensmittel-Untersuchung und-Forschung A, 208, 134-143.

Spaho, N. (2017). Distillation techniques in the fruit spirits production. In: Mendes, M.F. (Ed.), Distillation - Innovative Applications and Modeling. InTech, Rijeka.

Soufleros, H. E., Pissa, I., Petridis, D., Lygerakis, M., & Mermelas, K. (2001). Instrumental analysis at volatile and other compounds of Greek kiwi wine; sensory evaluation and optimization at its composition. Food Chemistry, 75, 487-500.

Soufleros, E. H., Mygdalia, A. S., & Natskoulis, P. (2004). Characterization and safety evaluation of the traditional Greek fruit distillate "Mouro" by flavor compounds and mineral analysis. Food Chemistry, 86, 625-636.

Soufleros, E. H., Mygdalia, S. A., & Natskoulis, P. (2005). Production process and characterization of the traditional Greek fruit distillate Koumaro by aromatic and mineral composition. Journal of Food Composition and Analysis, 18, 699-716.

Stampar, F., Solar, A., Hudina, M., Veberic R., & Colaric M. (2006). Traditional walnut liqueur-cocktail of phenolics. Food Chemistry, 95, 627-631.

Tešević, V., Nikičević, N., Jovanović, A., Djoković, D., Vujisić, Lj., Vučković, I., & Bonić, M. (2005). Volatile components from old plum brandies. Food Technology and Biotechnology, 43, 367-372.

Tsakiris, A., Kallithraka, S., & Kourkoutas, Y. (2014). Grape brandy production, composition and sensory evaluation. Journal of the Science of Food and Agriculture, 94, 404-414.

Isparljiva jedinjenja iz domaće rakije od grožđa određena GC-MS analizom

Stamenković Jelena[1*], Stojanović Gordana[1]

1- Univerzitet u Nišu, Prirodno-matematički fakultet, Departman za hemiju, Višegradska 33, 18000 Niš, Srbija

Stamenković Jelena: jelena.stamenkovic@pmf.edu.rs
Stojanović Gordana: gocast@pmf.ni.ac.rs

Sažetak

Cilj ovog rada bio je ispitivanje hemijskog sastava isparljivih komponenti rakije od grožđa kojoj su nakon destilacije dodati različiti sastojci primenom gasne hromatografije sa masenom spektrometrijom (GC-MS). U ovom istraživanju ispitivan je hemijski sastav pet uzoraka pri čemu je identifikovano ukupno 57 različitih jedinjenja. U svim ispitivanim uzorcima estri su bili najdominantnija klasa jedinjenja, ali u različitim procentima. Utvrđeno je da su etil-dekanoat (29.1%), etil-oktanoat (17.2%) i etil-dodekanoat (14.8%) bili glavni isparljivi sastojci uzorka L1 (rakija od grožđa koja je čuvana u hrastovom buretu). Kao glavni isparljivi sastojci uzorka L2 (rakija sa dodatkom letnjih tartufa) nađeni su *n*-heksanol i etil-laktat koji su u ovom uzorku identifikovani sa sličnim sadržajem (18.1%, odnosno 17.8%). Sa druge strane, uzorak L3 (rakija sa zimskim tartufima) bio je okarakterisan značajno većom zastupljenošću etil-laktata (44.8%). Glavne komponente identifikovane u uzorku L4 (rakija sa dodatkom zrna kafe i suvog grožđa) su bili etil-dekanoat (14.8%) i fenil etil-alkohol (12.5%), dok su dietil-sukcinat (22.9%) i etil-laktat (21.9%) dva glavna isparljiva sastojka identifikovana u uzorku L5 (rakija kojoj su dodati mladi zeleni orasi). Rezultati su pokazali da dodavanje različitih sastojaka istoj grožđanoj rakiji nakon destilacije utiče na hemijski sastav isparljivih komponenti, tj. da se broj aromatičnih jedinjenja i njihov relativni sadržaj razlikuju u zavisnosti od dodatih sastojaka.

Ključne reči: rakija od grožđa, hemijski sastav, isparljiva jedinjenja, GC-MS

* *Stamenković Jelena, jelena.stamenkovic@pmf.edu.rs, Departman za hemiju, Prirodno-matematički fakultet, Univerzitet u Nišu, Višegradska 33, 18000 Niš, Srbija*

Composés volatils de l'eau-de-vie de raisin fait maison déterminés par analyse GC-MS

Stamenković Jelena[1], Stojanović Gordana[1]

1- Université de Niš, Faculté des sciences naturelles et des mathématiques, Département de chimie, Višegradska 33, 18000 Niš, Serbie

Résumé

L'objectif de cet article était de déterminer si l'ajout de certains ingrédients à la même eau-de-vie de raisin après la distillation affecte la composition chimique des composants volatils en appliquant la chromatographie en phase gazeuse couplée à la spectrométrie de masse (GC-MS). Au cours de cette recherche, les cinq échantillons ont été soumis à cette étude et au total 57 composés ont été identifiés. Parmi tous les échantillons examinés, les esters constituaient la classe de composés la plus dominante, mais dans des proportions différentes. Le décanoate d'éthyle était le composé le plus abondant de l'échantillon L1 (eau-de-vie de raisin conservée en baril de chêne) avec un apport de 29.1%, suivi de l'octanoate d'éthyle (17.2%) et du dodécanoate d'éthyle (14.8%). L'échantillon L2 (eau-de-vie de raisin aux truffes d'été) était dominé par le *n*-hexanol et le lactate d'éthyle avec une contribution similaire (18.1% et 17.8%, respectivement). En revanche, dans l'échantillon L3 (eau-de-vie de raisin aux truffes d'hiver), le lactate d'éthyle était présent avec un apport important de 44.8%. Les composés dominants dans l'échantillon L4 (eau-de-vie de raisin avec grains de café et raisins secs) étaient le décanoate d'éthyle avec un apport de 14.8% et l'alcool phényl éthylique (12.5%), tandis que les deux principaux volatils de l'échantillon L5 (eau-de-vie de raisin avec de jeunes noix vertes) étaient du succinate de diéthyle (22.9%) suivi du lactate d'éthyle (21.9%). Les résultats obtenus dans cette étude sur les composés aromatiques volatils dans les eaux-de-vie de raisin analysées suggèrent que l'ajout de certains ingrédients à la même eau-de-vie de raisin après la distillation affecte la composition chimique à la fois du nombre de composés aromatiques et de leur teneur relative.

Mots-clés : eau-de-vie de raisin, composition chimique, volatils, GC-MS

Летучие соединения домашнего виноградного бренди, определенные методом ГХ-МС

Стаменкович Елена[1], Стоянович Гордана[1]

1 – Университет в Нише, Естественно-математический факультет, Кафедра химии, Вишеградска 33, 18000 Ниш, Сербия

Аннотация

Целью данной статьи было определить, влияет ли добавление некоторых ингредиентов к одному и тому же виноградному бренди после дистилляции на химический состав летучих компонентов с помощью газовой хроматографии в сочетании с масс-спектрометрией (ГХ-МС). Этому исследованию были подвергнуты пять образцов, и в общей сложности было идентифицировано 57 соединений. Для всех исследованных образцов преобладающим классом соединений были сложные эфиры, но в различных пропорциях. Этилдеканоат был самым распространенным соединением в образце L1 (виноградный бренди, выдержанный в дубовой бочке) с вкладом 29,1%, за ним следовали этилоктаноат (17.2%) и этилдодеканоат (14.8%). В пробе L2 (виноградный бренди с летними трюфелями) преобладали н-гексанол и этиллактат с аналогичным вкладом (18.1% и 17.8% соответственно). С другой стороны, в образце L3 (виноградный бренди с зимними трюфелями) присутствовал этиллактат с вкладом 44.8%. Доминирующими соединениями в образце L4 (виноградный бренди с зернами кофе и сушеным виноградом) были этилдеканоат с долей 14.8% и фенилэтиловый спирт (12.5%), а двумя основными летучими веществами образца L5 (виноградный бренди с молодыми зелеными грецкими орехами) были диэтилсукцинат (22.9%), а затем этиллактат (21.9%). Результаты, полученные в этом исследовании летучих ароматических соединений в проанализированных виноградных бренди, позволяют предположить, что добавление некоторых ингредиентов к одному и тому же виноградному бренди после дистилляции влияет на химический состав как количества ароматических соединений, так и их относительного содержания.

Ключевые слова: виноградный бренди, химический состав, летучие вещества, ГХ-МС

Flüchtige Verbindungen von hausgemachtem Traubenbrand, bestimmt durch die GC-MS-Analyse

Stamenković Jelena[1], Stojanović Gordana[1]

1-Department für Chemie, Fakultät für Naturwissenschaften und Mathematik, Universität Niš, Višegradska 33, 18000 Niš, Serbien

ABSTRAKT

Das Ziel dieser Arbeit war die Untersuchung der chemischen Zusammensetzung flüchtiger Bestandteile von Traubenbrand, dem verschiedene Zutaten nach der Destillation mittels Gaschromatographie mit Massenspektrometrie (GC-MS) zugegeben wurden. In dieser Studie wurde die chemische Zusammensetzung von fünf Proben untersucht und insgesamt 57 verschiedene Verbindungen identifiziert. Bei allen untersuchten Proben waren Ester die dominanteste Klasse der Verbindungen, jedoch in unterschiedlichen Anteilen. Es wurde festgestellt, dass Ethyldecanoat (29,1%), Ethyloctanoat (17,2%) und Ethyldodecanoat (14,8%) die am häufigsten vorkommenden flüchtigen Bestandteile der Probe L1 (der in einem Eichenfass gelagerte Traubenbrand) sind. Als flüchtige Hauptbestandteile der L2-Probe (Traubenbrand mit Sommertrüffelzusatz) wurden N-Hexanol und Ethyllactat gefunden, die in dieser Probe mit ähnlichem Gehalt identifiziert wurden (18.1/% beziehungsweise 17.8%). Andererseits war die L3-Probe (Traubenbrand mit Wintertrüffeln) durch eine signifikant höhere Anwesenheit von Ethyllactat (44.8%) gekennzeichnet. Die in der Probe L4 (Traubenbrand mit Kaffeebohnen und Rosinen) identifizierten Hauptkomponenten waren Ethyldecanoat (14.8%) und Phenylethylalkohol (12.5%), während Diethylsuccinat (22.9%) und Ethyllactat (21.9%) zwei identifizierte flüchtige Hauptbestandteile in der Probe L5 waren (Traubenbrand, dem junge grüne Walnüsse zugegegeben wurden). Die Ergebnisse zeigten, dass die Zugabe verschiedener Zutaten zu demselben Traubenbrand nach der Destillation die chemische Zusammensetzung der flüchtigen Bestandteile beeinflusst, dh. dass sich die Anzahl der aromatischen Verbindungen und ihr relativer Gehalt in Abhängigkeit von den zugegebenen Zutaten unterscheiden.

Schlüsselwörter: Traubenbrand, chemische Zusammensetzung, flüchtige Verbindungen, GC-MS

Antioxidant activity of *Micromeria croatica* (Pers.) Schott grown in plant tissue culture *in vitro* versus ones from the natural habitats

Svetlana M. Tošić[1*], Dragana D. Stojičić[1], Bojan K. Zlatković[1], Violeta D. Mitić[2], Marija D. Ilić[2], Marija S. Marković[1], Vesna P. Stankov Jovanović[2]

1- University of Niš, Faculty of Sciences and Mathematics, Department of Biology and Ecology, Višegradska 33, 18000 Niš, Serbia

2-University of Niš, Faculty of Sciences and Mathematics, Department of Chemistry, Višegradska 33, 18000 Niš, Serbia

Svetlana M. Tošić: tosicsvetlana59@yahoo.com
Dragana D. Stojičić: draganadstojicic@gmail.com
Bojan K. Zlatković: bojanzlat@pmf.ni.ac.rs
Violeta D. Mitić: violeta.mitic@pmf.pmf.edu.rs
Marija D. Ilić: marija.fertico@gmail.com
Vesna P. Stankov-Jovanović:sjvesna@yahoo.co.uk

ABSTRACT

Micromeria croatica, like many other species belonging to the Lamiaceae family, is characterized by good antioxidant activity. To avoid the exploitation of natural plant populations, it is recommended to grow them *in vitro* culture. The present study aimed to examine and compare the antioxidant potential of *M. croatica* obtain through nodal culture *in vitro* and collected from natural habitats. Different antioxidant methods were used: DPPH, ABTS, total reducing power, total phenol content, and flavonoid content. The obtained results indicate that the cultivation of plants by the *in vitro* culture technique stimulates the synthesis of secondary metabolites that promote antioxidant activity. It is increased in micropropagated plants primarily due to the increased phenol content by 136%. The possibility to test and then apply in practice the biological activity of the herb *M. croatica* is limited by the fact that the species is a local endemic.

Keywords: antioxidant activity, plant tissue culture in vitro, endemic, Micromeria croatica

[*]Svetlana Tošić
e-mail address: tosicsvetlana59@yahoo.com
address: Višegradska 33, PO Box 224 Niš, 18000 Serbia

Introduction

Rare, endemic or vulnerable species from the Lamiaceae family are really a challenge for various studies, especially in order to preserve the diversity of plant species and their natural population. Plant species of the genus *Micromeria* are relatively widespread. At the same time, many *Micromeria* taxa have a small limited geographical distribution or manifest local endemism. In the flora of Serbia, there are seven species of the genus *Micromeria*, which are classified into two sections, sects. *Micromeria* and sect. *Pseudomelisa*. This study refers to a *Micromeria croatica* belonging to a sect. *Micromeria*. Following the geographical criteria, such as the position and size of the range of the species, *M. croatica* is an endemic taxon limited to the western part of the Balkan Peninsula, including the easternmost enclave of in W. Serbia.

Endemic, endangered, and rare plant species with small populations and habitats near urban centers target negative anthropogenic actions. Many biotechnological methods are developing for biodiversity protection. One of them is a plant tissue cultured *in vitro* that has a prominent role as an *ex-situ* method.

Lamiaceae family representatives are a source of valuable bioactive molecules. Among the natural antioxidants belonging to secondary metabolites are mainly in the focus of interest. Phenols and flavonoids are the most prominent secondary metabolites in plants. Phenol compounds are very present in the Lamiaceae family. They have high antioxidant activity and the potential to catch free radicals and to chelate metals. Flavonoids enable different biological activities.

The main difficulty for the intensive use of species of the Lamiaceae family for pharmaceutical and phytochemical purposes is the tremendous individual variability due to genetic and biochemical heterogeneity. Overcoming this problem involves establishing an *in vitro* plant growing system (Saha et al., 2012). Quantitative and qualitative content of secondary metabolites may vary even among the plants of the same population. It is also under the seasonal influence. To avoid these differences, breeding plants by plant tissue culture *in vitro* has an advantage over other breeding methods. Except for this one, plant tissue culture has many other favorable features. A small amount of starting plant material is required for plant propagation by *in vitro* culture. In a short time, we can get many genetically uniform plantlets at the same ontogenetic stage. They all have the same origin, a little fragment of the parent plant, so-called explant. Just from one explant, several thousand plants can be obtained after a few weeks (Akin-Idowu et al., 2009).

Microcloned plants often grow better and faster than plants that grow *in vivo* because they are free of pathogens, bacterial, and fungal infections, and they often have better yields than conventionally grown plants (Debnath & Teixeira da Silva, 2007). The *in vitro* culture method also has excellent potential for mass production of natural secondary metabolites (Matkowski, 2008; Mulabagal & Tsay, 2004). Plant propagation *in vitro* is faster than *in vivo* propagation. A small space is required for plant propagation *in*

vitro culture. Thanks to controlled conditions, it is possible to predict the production time of individual plants.

A model system of growing *M. croatica in vitro* was established (Tošic et al., 2019; Kereša et al., 2018). To the best of authors' knowledge, there is no information concerning the antioxidant properties of micropropagated *M. croatica.* The *in vitro* culture method is widely used in the propagation of endemic and rare plants in danger of extinction to preserve the diversity of flora. Recent studies show that *M. croatica* exhibits promisingly suitable biological activities (antioxidant, antimicrobial, antiphytoviral, hepatoprotective). Despite functional biological activities, *M. croatica,* as endemic species, can not be exploited from natural habitats for commercial purposes. In line with that, the goal of the research is to evaluate the antioxidant potential of methanolic extracts of micropropagated *M. croatica* and compare it with the potential of naturally grown plants.

Experimental

Plant material

Above ground parts of *M. croatica* individuals at the vegetative stage of development were harvested from a natural population in May 2012. The location of the population was Beli Rzav gorge, W. Serbia (latitude 43° 46'26 "N and longitude 19° 27'44 "E) and the voucher specimen (Nº 6913) was deposited in the Herbarium collection of the Faculty of Science and Mathematics, University of Niš (HMN). *M. croatica* was already introduced into plant tissue culture *in vitro* (Tošic et al., 2019). For the analysis of the antioxidant activity of the extracts, micropropagated shoots that were growing on Murashige and Skoog (MS) media (1962) supplemented with 3% sucrose and 7% agar (Torlak, Belgrade) without the presence of phytohormones were used. Plant tissue cultures were growing at 25 ± 2 °C and under 16-h photoperiod in four weeks. After that, cultures were maintained by passages, which means replacing one-node stem segments on a new MS medium. The passages were done four times until we did not reach the desired amount of plant material.

Extracts preparation protocol

Both samples of plant material (natural and micropropagated) were dry and ground to powder. 1.0 g of dry weight was extracted with 10 ml methanol (Tosic at al. 2015). Obtained extracts were kept on cold (255 K) until analysis.

Antioxidant assays

All prepared extracts for antioxidant activity evaluation were of the initial concentration of 1 mg/mL. All measurements were done in triplicate, and results expressed as mean value ±standard deviation. Five different methods were used to assess the antioxidant activity of the extracts.

Determination of total reducing power using Fe(III)/Fe(II) redox pair and determination of Radical Scavenging Activity by DPPH radical was done according to the procedure described by Mitic (Mitic et al., 2011). BHT standard (butylated hydroxytoluene) solution of the same concentration as *M. croatica* extracts (1 mg/mL) was used as a reference. For the ABTS scavenging activity, we used the Trolox solution (final concentration 0–15 M) as a reference standard. The obtained results were expressed as μmol Trolox/g dry weight of extract (Li et al., 2007). Determination of Total Phenolic Content was quantified by Folin-Ciocalteu spectrophotometric method, and we used gallic acid as a reference standard while the absorbance values of the samples were read at 760 nm against a reagent blank (Mitic et al., 2011). Quantification of total flavonoid content was based on the calibration routine and is expressed as mg routine/g of dry extract (mg/g DE) (Mitic et al., 2011).

Results and Discussion

Numerous phenol compounds with antioxidant activities are identified in many plant species of the Lamiaceae family. Among the species of the genus, *Micromeria* has a noticed role. We analyzed the whole antioxidant activity of extract instead of particular compounds, because compounds may have additive, synergistic or antagonistic properties.

Whereas during *in vitro* cultivation, phytohormones added to the nutrient medium may inhibit certain enzymes involved in the biosynthetic pathways of secondary metabolites (Rothe et al., 2003). To assess the antioxidant activity of *Micromeria* shoots grown *in vitro*, only shoots cultivated in the absence of phytohormones were used.

All used methods for measuring antioxidant activities show that there are differences in obtained values among methanol extracts that originated from micropropagated and natural growing plants (Table 1).

Table 1. Antioxidant properties of *M. croatica* methanol extracts estimated by DPPH, ABTS, total reducing power, total phenolics, and total flavonoids assays

Extracts	**DPPH**%	**ABTS** (Trolox equivalents, μg/ml)	**TRP** (Ascorbate equivalentsμg/mg of dry extract)	**Total phenols** (gallic acid equivalents μg/mg of dry extract)	**Flavonoids** (rutin equivalents μg/mg of dry extract)
M. croatica nature	3.30±0.34	0.57±0.02	137.22±8.28	10.61±0.31	33.06±1.18
M. croatica in vitro	2.88±0.03	1.05±0.01	256.38±15	25.04±0.66	18.70±0.72

BHT 3.18±0.02% (RSD=0.65%) at concentration of 1 mg/ml

Due to the simple procedure and high reproducibility, the DPPH method is often used to measure antioxidant activity. There are small differences between plant samples from natural habitats and *in vitro* culture. Plantlets of *M. croatica* regenerated on the MS medium possess lower or closely similar DPPH antiradical scavenging capacities as naturally grown plants. The difference is the possibility to catch free DPPH radicals is the smallest, 12.73%.

The ABTS method is widely used to assess antioxidant activity. With this method, a large number of samples can be analyzed quickly, and a smaller number of interfering compounds occur during the measurement (Surveswaran et al., 2007). The value obtained by the ABTS method is 84.21% greater for the extract of shoots from plant tissue culture than value for the extract of nature originated plants.

The content of flavonoids in the plant extract decreases during cultivation *in vitro* culture. The content of flavonoids is 42.44% greater in shoots from natural habitats than in micropropagated plants.

The most apparent difference we got for the total phenols content. Shoots that were breeding in plant tissue culture *in vitro* have 136% higher phenol content compared with shoots of plants from natural habitat (Figure 1).

The total reducing power determined for shoots that have been developed and grown *in vitro* has a higher value than plants from natural habitats. This fact could be explained by the increased content of total polyphenols (136%) in the buds of *in vitro* grown plants. The total reducing power evaluated for *in vitro* cultivated shoots is bigger for 86.84% than for shoots collected from the natural population (Figure 1).

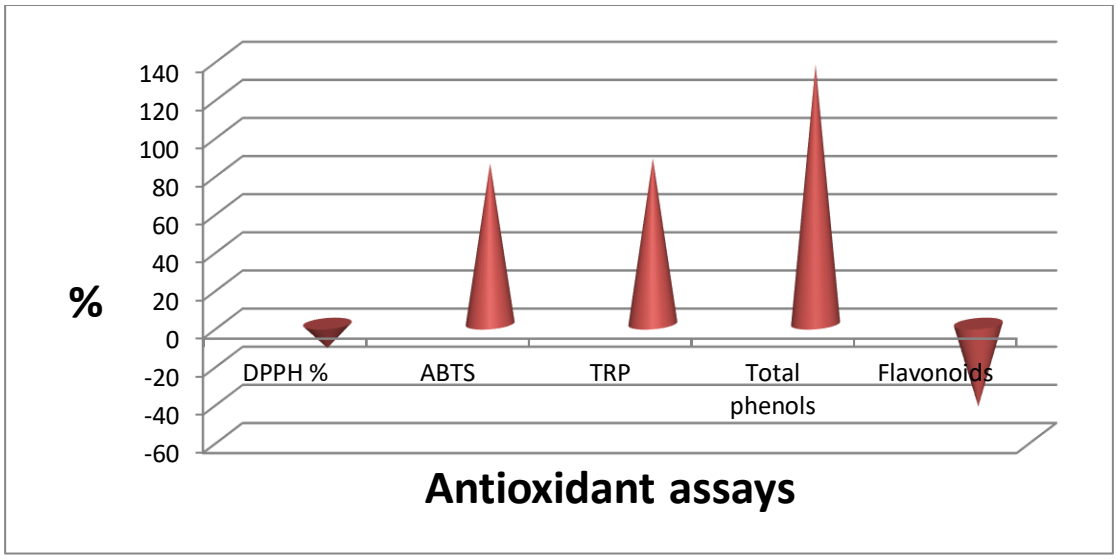

Figure 1. Degree of deviation (%) of antioxidant activities of *M. croatica* plants grown in plant tissue culture *in vitro* from the antioxidant activities obtained for plants growing in open field conditions

For different species of *Micromeria*, it has been confirmed that the total polyphenol content contributes to antioxidant activity (Vladimir-Knežević et al., 2011). The correlation between the antioxidant activity of the extracts and the polyphenol content was also confirmed in other Lamiaceae species (Tosun et al., 2009; Lopez, 2007).

We chose to use methanol for preparing extract as it is a useful solvent for phenol compounds extraction. It turned out that the most species belonging to genus *Micromeria* show better antioxidant activity in polar extracts. The methanol extract of *M. croatica* has antioxidant and pro-oxidant activity. It protects DNA and lipid molecules from damage. In low concentrations, it has an antioxidant effect on proteins, and, in high concentrations, it has a prooxidative effect. In high concentrations, methanol extract has a cytotoxic effect on HEp2 cells and leads to the formation of ROS species (Šamec et al., 2015).

Antioxidant properties are also characteristic of other species of *Micromeria*. Vladimir-Knežević et al. (2011) compared the antioxidant activity of ethanolic extracts of *M. croatica*, *M. juliana*, and *M. thymifolia*. Among them, *M. croatica* had the best antioxidant activity. The acetone extract of *M. cilicica* exhibits good antioxidant activity (Oeztuerk et al., 2011). The methanol extract of *M. fruticosa ssp. serpyllifolia* originating from Turkey has significant antioxidant activity measured by the DPPH method (Güllüce et al., 2004). The methanol extract of *M. myrtifolia* has good DPPH activity as well as reducing power, while essential oils and hexane extract do not show activity in free radical scavenging but have reducing potential. Also, the methanolic extract of *M. myrtifolia*, unlike chloroform and hexane, has a high content of polyphenols (Formisano et al., 2014).

The change in antioxidant activity of *M. croatica* shoots from the culture concerning shoots of plants from natural habitats follows the data obtained for *M pulegium*. We notice the similar data in earlier research, by comparing antioxidant activities of extracts prepared from micropropagated and nature growing plant of *M. pulegium* under the same experimental conditions (Tosic et al. 2015). Good antioxidant activity of micropropagated plant's extracts was recorded for different plant species. Extracts obtained from cultures of different organs of *Salvia officinalis* have good or even better antioxidant activity compared to extracts of the same plant organs from natural habitats (Grzegorczyk et al., 2007). Phenolic compounds with good antioxidant activity are present in the culture of *S. officinalis* shoots (Santos-Gomes et al., 2002). In experiments with different varieties of basil, it was observed that *in vitro* culture of tissues or cells accumulates more secondary metabolites than donor plants (Kiferle et al., 2011).

Good antioxidant activity due to polyphenol content has also been reported in endemic species of other families such as Rubiaceae and Myrtaceae (Angaji et al., 2012). Since endemic species cannot be exploited from natural habitats, it is recommended to grow them *in vitro*.

Conclusion

Plants are exposed to different and the altering environmental factors during their growth and development. The environmental factors may have impact on antioxidant activity of plants. Culture conditions appear to be stressful for plant tissues leading to increased antioxidant potential. The change of antioxidant potential represents an adaptation of plants on these conditions. During cultivation using *in vitro* culture, the antioxidant potential of *M. croatica* shoots is preserved or even better. Methanolic extracts of *M. croatica* shoots grown *in vitro* show higher antioxidant activity than extracts of plants from natural habitats. Higher antioxidant activity is attributed to the higher content of phenolic compounds in shoots grown *in vitro*. Plants grown *in vitro* do not lose their antioxidant potential and can serve as an alternative for production of active metabolites. According to the antioxidant activity, *Micromeria* species could be used to prevent or treat diseases caused by free radicals and oxidants. They can also be used as a source of additives in the food industry.

Acknowledgment

This research was financially supported by the Ministry of Education, Science and Technological Development ofthe Republic of Serbia, Grant Nos.
The Contract number is 451-03-68/2020-14.

Conflict-of-Interest Statement

The authors declare that they have no conflict of interest. All authors took part in experimental research, and they agree with publishing data.

References

Akin-Idowu, P. E., Ibitoye, D. O., & Ademoyegun, O. T. (2009). Tissue culture as a plant production technique for horticultural crops. African Journal of Biotechnology, 8(16), 3782-3788.

Angaji, S. A., Mousavi, S. F., & Babapour, E. (2012). Antioxidants: A few key points. Annals of Biological Research, 3 (8), 3968-3977.

Formisano, C., Oliviero, F., Rigano, D., Saabb, A. M., & Senatore, F. (2014). Chemical composition of essential oils and *in vitro* antioxidantproperties of extracts and essential oils of *Calamintha origanifolia* and *Micromeria myrtifolia*, two Lamiaceae from the Lebanon flora. Industrial Crops and Products, 62, 405–411.

Grzegorczyk, I., Matkowski, A., & Wysokin'ska, H. (2007). Antioxidant activity of extracts from *in vitro* cultures of *Salvia officinalis* L. Food Chemistry, 104, 536–541.

Güllüce, M., Sökmen, M., Şahin, F., Sökmen, A., Adigüzel, A., & Özer, H. (2004). Biological activities of the essential oil and methanolic extract of *Micromeria fruticosa* (L) Druce ssp *serpyllifolia* (Bieb) PH Davis plants from the eastern Anatolia region of Turkey. Journal of the Science of Food and Agriculture, 84(7), 735–741.

Kereša, S., Andrijanić, Z., Kremer, D., Habuš- Jerčić, I., Barić, M., Batelja- Lodeta, K., Bolarić, S., & Bošnjak- Mihovilović, A. (2018). Efficient micropropagation and rooting of *Micromeria croatica* (Pers.) Schott (Lamiaceae). Poljoprivreda, 24 (2), 27-33.

Kiferle, C., Lucchesini, M., Mensuali-Sodi, A., Maggini, R., Raffaelli, A., & Pardossi, A. (2011). Rosmarinic acid content in basil plants grown *in vitro* and in hydroponic. Central European Journal of Biology, 6, 946-957.

Li, H. B., Cheng, K. W., Wong, C. C., Fan, K. W., Chen, F., & Jiang, Y. (2007). Evaluation of antioxidant capacity and total phenolic content of different fractions of selected microalgae. Food Chemistry 102, 771–776.

Lopez, V., Akerreta, S., Casanova, E., Garcia-Mina, J. M., Cavero, R. Y., & Calvo, M. I. (2007). *In vitro* antioxidant antirhizopus activities of Lamiaceae herbal extracts. Plant Foods and Human Nutrition, 62, 151-155.

Matkowski, A. (2008). Plant *in vitro* culture for the production of antioxidants. A review, Biotechnology Advances, 26, 548–560.

Mitić, V., Stankov-Jovanović, V., Jovanović, O., Palić, I., Djordjević, A., & Stojanović G. (2011). Composition and antioxidant activity of hydrodistilled essential oil of Serbian *Ajuga chamaepitys* (L.) Schreber ssp chia (Schreber) Arcangeli. Journal of Essential Oil Research, 23(6), 70-74.

Mulabagal, V., & Tsay, H. S. (2004). Plant Cell Cultures - An alternative and efficient source for the production of biologically important secondary metabolites. International Journal of Applied Science and Engineering, 2 (1), 29-48.

Murashige, T., & Skoog F. (1962). A revised medium for rapid growth and bioassays with tobacco tissue cultures. Plant Physiology, 15, 473-497.

Oeztuerk, M., Kolak, U., Topcu, G., Oeksuez, S., & Choudhary, M. I. (2011). Antioxidant and anticholinesterase active constituents from *Micromeria cilicica* by radical-scavenging activity-guided fractionation. Food Chemistry, 126, 31–38.

Rothe, G., Hachiya, A., Yamada, Y., Hashimoto, T., & Dräger B. (2003). Alkaloids in plants and roots cultures of *Atropa belladonna* overexpressing putrescine *N*-methyltransferase. Journal of Experimental Botany, 54, 2065-2070.

Saha, S., Kader, A., Sengupta, C., & Ghosh, P. (2012). *In Vitro* propagation of *Ocimum gratissimum* L. (Lamiaceae) and its evaluation of genetic fidelity using RAPD marker. American Journal of Plant Sciences, 3, 64-74.

Debnath, C. S., & Teixeira da Silva, A. J. (2007). Strawberry culture *in vitro*: applications in genetic transformation and biotechnology. Fruit, Vegetable and Cereal Science and Biotechnology, 1(1), 1-12.

Santos-Gomes, P. C., Seabra, R. M., Andrade, P. B., & Fernandes-Ferreira, M. (2002). Phenolic antioxidant compounds produced by *in vitro* shoots of sage (*Salvia officinalis* L). Plant Science, 62, 981-987.

Surveswaran, S., Cai, Y. Z., Corke, H., & Sun, M. (2007). Systematic evaluation of natural phenolic antioxidants from 133 Indian medicinal plants. Food Chemistry, 102, 938–953.

Tosun, M., Ercisli, S., Sengul, M., Ozer, H., Pola, T., & Ozturk, E. (2009). Antioxidant properties and total phenolic content of eight *Salvia* species from Turkey. Biological Research, 42, 175-181.

Tošić, S., Stojičić, D., Stankov-Jovanović, V., Mitić, V., Mihajilov-Krstev, T., & Zlatković, B. (2015). Chemical composition, antioxidant and antimicrobial activities of micropropagated and native *Micromeria pulegium* (Lamiaceae) extracts. Oxidation Communications, 38, 55–66.

Tosic, S. M., Stojicic, D. D., Slavkovska, V. N., Mihajilov-Krstev, T. M., Zlatkovic, B. K., Budimir, S. M., & Uzelac, B. B. (2019). Phytochemical composition and biological activities of native and in vitro-propagated *Micromeria croatica* (Pers.) Schott (Lamiaceae). Planta, 249(5), 1365-1377.

Vladimir-Knežević, S., Blažeković, B., Bival -Štefan, M., Alegro, A., Köszegy, T., & Petrik, J. (2011). Antioxidant activities and polyphenolic contents of three selected *Micromeria* species from Croatia. Molecules, 16, 1454-1470.

Šamec, D., Gruz, J., Durgo, K., Kremer, D., Kosalec, I., Valek-Žulj, L., Martinez, S., Salopek-Sondi, B., & Piljac-Žegarac, J. (2015). Molecular and cellular approach in the study of antioxidant/pro-oxidant properties of *Micromeria croatica* (Pers.) Schott, Natural Product Research: Formerly Natural Product Letters, 29(18), 1770-1774.

Antioksidantna aktivnost *Micromeria croatica* (Pers.) Schott gajenih u kulturi biljnih tkiva *in vitro* i sa prirodnih staništa

Svetlana M. Tošić[1], Dragana D. Stojičić[1], Bojan K. Zlatković[1], Violeta D. Mitić[2], Marija D. Ilić[2], Marija S. Marković[1], Vesna P. Stankov Jovanović[2]

1- Univerzitet u Nišu, Prirodno-matematički fakultet, Departman za biologiju i ekologiju, Višegradska 33, 18000 Niš, Srbija
2- Univerzitet u Nišu, Prirodno-matematički fakultet, Departman za hemiju, Višegradska 33, 18000 Niš, Srbija

Sažetak

M. croatica kao i mnoge druge vrste koje pripadaju familiji Lamiaceae, odlikuje dobra antioksidativna aktivnost. Da bi se izbegla eksploatacija prirodnih populacija, preporučljivo je gajiti biljke metodom kulture *in vitro*. Istraživanje je imalo za cilj da se ispita i uporedi antioksidativni potenijal izdanaka *M. croatica* koji su gajeni metodom kulture biljnih tkiva *in vitro* i onih koji su sakupljeni iz prirode. Korišćene su različite metode: DPPH, ABTS, ukupna redukciona moć, ukupan sadržaj fenola i sadržaj flavonoida. Dobijeni rezultati ukazuju da se gajenjem biljaka tehnikom kulture *in vitro* stimuliše sinteza sekundarnih metabolita koji pospešuju antioksidativnu aktivnost. Ona je povećana kod mikropropagiranih izdanaka pre svega usled povećenog sadržaja fenola za 136%. Mogućnost da se ispituju a potom i primene u praksi biološke aktivnosti herbe *M. croatica* je limitirana činjenicom da je vrsta lokalni endemit.

Ključne reči: antioksidantna aktivnost, kultura biljnih tkiva in vitro, endemit, Micromeria croatica

Activité antioxydante de *Micromeria croatica* (Pers.) Schott cultivée en tissus végétaux *in vitro* par rapport à celles des habitats naturels

Svetlana M. Tošić[1], Dragana D. Stojičić[1], Bojan K. Zlatković[1], Violeta D. Mitić[2], Marija D. Ilić[2], Marija S. Marković[1], Vesna P. Stankov-Jovanović[2]

1- Université de Niš, Faculté des sciences naturelles et des mathématiques, Département de biologie et d'écologie, Višegradska 33,18000 Niš, Serbie
2-Université de Niš, Faculté des sciences naturelles et des mathématiques, Département de chimie, Višegradska 33,18000 Niš, Serbie

Résumé

M. croatica, comme de nombreuses autres espèces appartenant à la famille des Lamiaceae, se caractérise par une bonne activité antioxydante. Pour éviter l'exploitation des populations végétales naturelles, il est recommandé de les cultiver en culture *in vitro*. La présente étude visait à examiner et comparer le potentiel antioxydant des pousses de *M. croatica* cultivées en culture tissulaire végétale *in vitro* et prélevées dans la nature. Les différentes méthodes antioxydantes ont été utilisées : DPPH, ABTS, le pouvoir réducteur total, la teneur totale en phénol et la teneur en flavonoïdes. Les résultats obtenus indiquent que la culture de plantes par la technique de culture *in vitro* stimule la synthèse de métabolites secondaires qui favorisent l'activité antioxydante. Elle est augmentée dans les pousses micropropagées principalement en raison de l'augmentation de la teneur en phénol de 136%. La possibilité de tester, puis d'appliquer en pratique des activités biologiques de l'herbe *M. croatica* est limitée par le fait que l'espèce représente une endémie locale.

Mots-clés: activité antioxydante, culture de tissus végétaux in vitro, endémique, Micromeria croatica

Антиоксидантная активность *Micromeria croatica* (Pers.) Schott, выращенных в культуре тканей растений *in vitro*, по сравнению с культурами из естественных местообитаний

Светлана М. Тошич[1], Драгана Д. Стоичич[1], Боян К. Златкович[1], Виолета Д. Митич[2], Мария Д. Илич[2], Мария С. Маркович[1], Весна П. Станков Йованович[2]

1 – Университет в Нише, Естественно-математический факультет, Кафедра биологии и экологии, Вишеградска 33, 18000 Ниш, Сербия

2 – Университет в Нише, Естественно-математический факультет, Кафедра химии, Вишеградска 33, 18000 Ниш, Сербия

Аннотация

M. croatica, как и многие другие виды, относящиеся к семейству Lamiaceae, отличается хорошей антиоксидантной активностью. Чтобы избежать эксплуатации природных популяций растений, рекомендуется выращивать их в культуре *in vitro*. Настоящее исследование было направлено на изучение и сравнение антиоксидантного потенциала *M. croatica*, выращенных в культуре растительной ткани *in vitro* и собранных в природе. Были использованы различные антиоксидантные методы: DPPH, ABTS, общая восстанавливающая способность, общее содержание фенола и содержание флавоноидов. Полученные результаты свидетельствуют о том, что выращивание растений методом культивирования *in vitro* стимулирует синтез вторичных метаболитов, способствующих антиоксидантной активности. У микроразмножающихся растений он повышен в первую очередь за счет увеличения содержания фенола на 136%. Возможность протестировать, а затем применить на практике биологическую активность травы *M. croatica* ограничена тем фактом, что этот вид является местным эндемиком.

Ключевые слова: антиоксидантная активность, культура тканей растений in vitro, эндемик, Micromeria croatica

Antioxidative Aktivität von *Micromeria croatica* (Pers.) Schott, die *in vitro* mit Pflanzengewebekulturmethode gezüchtet wurde, im Vergleich zu solchen aus natürlichen Lebensräumen

Svetlana M. Tošić[1], Dragana D. Stojičić[1], Bojan K. Zlatković[1], Violeta D. Mitić[2], Marija D. Ilić[2], Marija S. Marković[1], Vesna P. Stankov-Jovanović[2]

1- Universität Niš, Fakultät für Naturwissenschaften und Mathematik, Institut für Biologie und Ökologie, Višegradska 33.18000 Niš, Serbien
2-Universität Niš, Fakultät für Naturwissenschaften und Mathematik, Fachbereich Chemie, Višegradska 33.18000 Niš, Serbien

ABSTRAKT

M. croatica zeichnet sich, wie viele andere Arten der Familie *Lamiaceae,* durch eine gute antioxidative Aktivität aus. Um die Ausbeutung natürlicher Pflanzenpopulationen zu vermeiden, wird empfohlen, diese Pflanzen *in vitro* zu züchten. Die vorliegende Studie zielte darauf ab, das Antioxidationspotential von Sprossen von *M. croatica* zu untersuchen und zu vergleichen, die *in vitro* mit Pflanzengewebekulturmethode gezüchtet und aus der Natur gesammelt wurden. Es wurden verschiedene Antioxidationsmethoden verwendet: DPPH, ABTS, Gesamtreduktionskraft, Gesamtphenolgehalt und Flavonoidgehalt. Die erhaltenen Ergebnisse zeigen, dass der *In-vitro*-Pflanzenanbau die Synthese von Sekundärmetaboliten stimuliert, die die antioxidative Aktivität fördern. Sie ist in mikropagierten Sprossen hauptsächlich aufgrund des um 136% erhöhten Phenolgehalts erhöht. Die Möglichkeit, die biologische Aktivität der Pflanze *M. croatica* zu prüfen und dann in der Praxis anzuwenden, wird durch die Tatsache begrenzt, dass die Spezies lokal endemisch ist.

Schlüsselwörter: *antioxidative Aktivität, Pflanzengewebekultur in vitro, endemisch, Micromeria croatica*

Analytical application of poly(vinyl chloride-co-vinyl acetate) electrode modified with silver for chloride ions determination in real systems

Dragana M. Sejmanović[1]*, Milana V. Budimir[1], Živana Ž. Radosavljević[1], Emilija T. Pecev[2]

1- University of Priština, Faculty of Natural Sciences and Mathematics, Kosovska Mitrovica, Serbia

2- University of Niš, Faculty of Natural Sciences and Mathematics, Niš, Serbia

*Dragana M. Sejmanović: dragana.sejmanovic@pr.ac.rs
Živana Ž. Radosavljević: zivana.radosavljevic30@gmail.com
Emilija T. Pecev: epecev@yahoo.com

ABSTRACT

Application possibility of new simple Ag-selective electrode for the determination of chloride ions, was investigated in this paper. The poly(vinyl chloride-co-vinyl acetate) electrode modified with silver (PVCAc/Ag) was prepared by simple immersion a glassy carbon rod coated with poly(vinyl chloride-co-vinyl acetate) polymer, which contained plasticizer and lipophilic additive, but without ionophore, into the silver nitrate solution. This simplicity of construction and extensive pH range through remarkable acidic media (pH 0.7 to 7.0), are the advantages of this modified electrode over many of reported silver selective electrodes based on a polymer matrix containing different ionophores. The response of the electrode was linear with a Nernstian slope of 60.25 mV/decade in the concentration range from 1.0×10^{-1} to 1.0×10^{-5} mol/dm^3 Ag^+ and with a detection limit of 4.25×10^{-6} mol/dm^3. Proposed PVCAc/Ag electrode was applied to the determination of chloride ions in the samples spring waters. The results of chloride ion determination in samples spring waters obtained by proposing electrode and comparative Ag/AgCl electrode were in satisfactory agreement.

Keywords: silver, electrodes, spring waters, vinyl chloride-co-vinyl acetate, chloride ions

Introduction

Silver is white, shiny metal of excellent conductivity of electricity and heat, long been known, and due to its characteristics has always attracted attention. It is widely used in electrical industry, electronics, photography, organic synthetic chemistry, and production of fungicides (Smith et al., 1977), batteries, in complex compounds, medicine and other fields. Silver is a non-toxic metal, but its role in physiological processes is not completely understood, so its appearance even in small amounts in the skin, hair (Barrera et al., 1998), gums, cornea, liver, kidneys (Kazuyuki et al., 2001; Wan et al., 1991) are harmful. Also, the presence of soluble silver in wastewater is a problem in many industries. Therefore, there is a need for a fast, sensitive and simple method of determining small amounts of silver ions in different samples. There are different sensitive methods for the determination of silver ions at low levels, such as spectrophotometry (El-Zawawy et al., 1995; Ohshita et al., 1982), atomic absorption spectrometry (Bermejo-Barrera et al., 1996; Chakrapni et al., 2001; Pu et al., 1998; Rahman et al., 2004; Sramkova et al., 1999), inductively coupled plasma mass spectrometry (Chiba et al., 1992), inductively coupled plasma atomic emission spectrometry (Argekar et al 1995), fluorimetry (Kabasakalis, 1994), stripping voltammetry (Damien, 1994).

All these methods require the preliminary preparation of samples, which involves separation from the matrix, preconcentration, and the use of reagents, which are generally expensive. Because of all these methods are complicated and time consuming.

On the other hand, potentiometric sensors, ion-selective electrodes (ISE) have found application as alternative analytical methods because of their precision, sensitivity, selectivity, easy available instruments and low cost.

Nowadays, the majority of ion-selective electrodes are comprised of an organic polymeric membrane into which sensor material based on different ionophores is incorporated. Silver selective electrodes based on crowns (Shamsipur et al., 2002), Schiff-bases (Gupta et al., 2009), calixarenes (Demirel et al., 2006; Lu et al., 2004), *o*-hydroxyacetophenone carbohydrazone (OHAC) (Chandra et al., 2012) as well as other ionophores have been developed.

Most ion-selective electrodes of this type use poly(vinyl chloride) (PVC), a suitable plasticizer as an organic matrix and ionophore as the active part of the sensor (Johnson and Bachas, 2003). Examining the influence of different cations on the PVC matrix, it was found that it is sensitive to concentration changes of some ions, including silver ions. This phenomenon has been elucidated and the possibility of using a simple silver(I) selective electrode based only on a polymeric matrix with a plasticizer and a lipophilic ionic additive, but without ionophores as an active component, has been investigated.

The possibility of applying the proposed PVCAc/Ag potentiometric sensor was tested by determining Ag^+ ions in ecological water samples and colloidal silver water (Sejmanović et al., 2011). In this study simple Ag- selective electrode was used for determination of Cl^- ions by potentiometric titrations in spring water samples.

Experimental

Reagents and Solutions

The following reagents were used to prepare the experimental solutions:

1. Silver(I) nitrate ($AgNO_3$), p.a. "Merck", Darmstadt, Germany.
2. Poly(vinyl chloride-co-vinyl acetate) (Pevikon C870, PVCAc), p.a. "Pevicon", Fostatbolaget, Sweden.
3. Dibutyl phthalate (DBP), p.a. "Fluka", Buchs, Switzerland.
4. Sodium tetraphenyl borate (NaTPB), p.a. "Merck", Darmstadt, Germany.
5. Tetrahydrofuran (C_4H_8O, THF), p.a. "Merck", Darmstadt, Germany.
6. Ammonium nitrate (NH_4NO_3), p.a. "Laphoma", Skopje, Macedonia.
7. Sodium chloride (NaCl), p.a. "Laphoma", Skopje, Macedonia.

High purity water (Millipore, 18M Ω cm resistivity) was used.

The ionic strength of the solution was adjusted using NH_4NO_3 solution, c (NH_4NO_3) =0. 05 mol/dm^3. Activities were calculated by the Debye-Hückel procedure.

A standard silver nitrate solution was prepared by measuring the required amount of silver nitrate for a solution of concentration 0.1 mol/dm^3. This amount (1.6897 g) was dissolved in high purity water and the solution diluted to 100 cm^3. The solution was standardized with 0.1 mol/dm^3 sodium chloride solution. The following standard silver nitrate solution, c ($AgNO_3$) = 10^{-2} mol/dm^3, was prepared by pipetting a 10 cm^3 solution of $AgNO_3$ concentration of 0.1 mol/dm^3 and diluted it with a solution of NH_4NO_3 (c (NH_4NO_3) = 0.05 mol/dm^3) in a volumetric flask (100 cm^3). Solutions of lower concentrations of 10^{-3} mol/dm^3 to 10^{-7} mol/dm^3 were prepared by tenfold successive dilution of a standard 0.01 mol/dm^3 solution of $AgNO_3$ with a solution of NH_4NO_3 (c (NH_4NO_3) = 0.05 mol/dm^3).

Apparatus

All potentiometric and pH measurements were performed using the pH meter (Hanna pH-211). The instrument covers an area from pH 2.00 to pH 16.00 (sensitivity ± 0.01 pH units). When using ion-selective electrodes, the measuring range of the instrument is in the range of +2.000 to -2.000 mV (sensitivity 0.1 mV);

- Magnetic mixer was a product of "VELP Scientifica", set at 4000 rpm;

- Potentiostat PAR Model 273;
- X-Y recorder Model 8033 was a product of "Philips".

Electrodes

PVCAc/Ag electrode of our own making, without internal solution and ionophore, is made by simply immersing a glassy carbon (GC) rod coated with a membrane of poly(vinyl chloride-co-vinyl acetate) polymer, plasticizer and lipophilic additive in silver nitrate solution. PVCAc/Ag electrode was used as a working electrode, an Ag(I) ion-selective electrode.

Ag/AgCl electrode was used as a comparative electrode for the determination of chloride in spring water samples. It is obtained by the process of coating a silver strip with melted sensory compound synthesized by pre-deposition from aqueous solutions of a homogeneous mixture (Jovanović et al., 1985).

A double junction saturated calomel electrode (SCEd.j.), produced by Hanna Instruments, with a salt bridge containing NH_4NO_3 (c (NH_4NO_3)=1 mol/dm^3), was used as a reference electrode in an electrochemical coupling:

SCEd.j. || standard solutions / sample solution | PVC membrane | GC

Preparation of PVCAc/Ag electrode

The polymeric membrane contained 39-48% PVCAc, 52-61% DBP and 0.2-1% NaTPB. A total mass of 0.270 g of these reagents was mixed with 2.5 cm^3 THF. A glassy carbon (GC) (Φ3 mm) (Sigardur-Sigri Electrographite, GmbH, Germany) was directly coated by dipping it several times in this mixture until a bead was formed coating the GC. Electrode prepared in this way was allowed to dry in the air about 12 h. Then, the bead on the glassy carbon was placed into a silver nitrate solution (c ($AgNO_3$) = 0.01 mol/dm^3) for about 30 min in order to condition it before use. This coated GC was used as Ag(I) ion-selective electrode and designated as a PVCAc/Ag electrode. Electrical contact with the instrument was made *via* a cable attached to the end of the undated portion of the glassy carbon.

The surface of the GC stick was washed with THF before being immersed in the mixture of substances, in order to remove traces of grease, carefully polished with 400 grit, then 1200 grit and finally with 2500 grit sandpaper, and afterwards washed with high purity water.

Sample preparation

For analytical confirmation of PVCAc/Ag ion-selective electrode by determination of chloride ions, the following water samples were used: spring waters sampled from Sjenica territory: source „Česmica", source „Bazeni", water from the „Vrelo", water from the „Jasen".

The samples of the spring waters were first treated by 1 cm^3 of HNO_3 c= 0.1 mol/dm^3 in a volumetric flask (50 cm^3) , since the working range of the electrode is in very acidic medium, and in

addition eliminates the possible presence of carbonate in the tested waters. The ionic strength in the samples was adjusted with a solution of NH_4NO_3 (c (NH_4NO_3) = 0.05 mol/dm^3).

Procedure

The potentials were measured by varying the concentration of $AgNO_3$ in the standard solution within the range from 1.0×10^{-7} to 1.0×10^{-1} mol/dm^3. All potentiometric and pH measurements were performed at a temperature of 25^0 C. The electrode was prepared as previously described, and placed into 0.01 mol/dm^3 $AgNO_3$ solution for 30 min.

After the preparation of the water sample, the PVCAc/Ag electrode along with the reference electrode was immersed into the sample and titrated with $AgNO_3$ solution. The concentrations of the $AgNO_3$ solution for potentiometric titration were: 1.0×10^{-3} mol/dm^3, 2.5×10^{-3} mol/dm^3, 1.0×10^{-4} mol/dm^3, and 5.0×10^{-4} mol/dm^3. The same increments of the $AgNO_3$ solution was added gently up to the end point and continued after it up to few readings. The value of three consecutive potential measurements is accepted as the ultimate. The end point and the amount of Cl^- ions in water samples were determined by extrapolation of the three linear portions of the titration plot. The concentrations of Cl^- ion in the different water samples were compared by direct potentiometric method, using standard chloride solutions, by Cl^- selective on a silver-deposited Ag/AgCl electrode.

Results and Discussion

Our previous experiments (Petković et al., 2010) where PVCAc was used as a sensor matrix revealed that this material was highly selective to Ag^+ with respect to many different cations, with the exception of Hg^{2+} and Fe^{3+} ions. The concept of sensor behavior of the PVC matrix without any ionophore, led us to the idea of the simplest construction of a polymer membrane electrode which certainly needed further attention. The similar attempt was performed before, but the analytical performance of the reported electrode was not satisfactory (Malinowska et al., 1994). In the research, a simple sensor was prepared by coating glassy carbon rod with a membrane of poly(vinyl chloride-co-vinyl acetate) polymer, plasticizer (DBP) and lipophilic additive (NaTPB) but without ionophores as the active component.

We showed earlier that GC as well as polypirrole (PPy) could be modified by silver simply by immersion of the electrode into the silver nitrate solution (Dekanski et al., 2001; Jovanović et al., 2005). The modified membrane was examined by cyclic voltammetry and it was found that cyclic voltammograms of the silver modified PVCAc electrode resemble the voltammograms for a pure silver electrode (Dirkse, 1989). Based on the CV recorded it was concluded that silver was deposited in the

elemental state on the surface and near surface layers of the membrane; similar results were reported for modified polypyrrole and glassy carbon (Figure 1). The operation mechanism of membranes with only PVCAc and DBP can be explained through the red-ox process of the Ag^{+} /Ag^{0} couple on the surface of the membrane.

In order to obtain the optimum potentiometric characteristics of the electrode, optimization of the membrane composition by changing the ratio of the membrane component was performed.

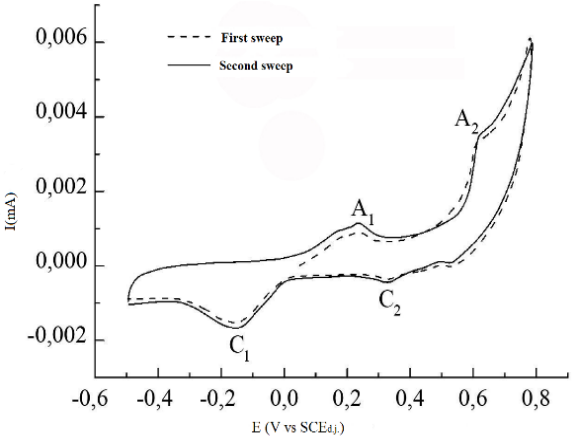

Figure 1. Cyclic voltammogram for the GC/PVCAc/Ag electrode in 0.1 mol/dm^3 NaOH solution (sweep rate 50 mV/s).

Characteristics of PVCAc/Ag electrodes

Linear range and limit of detection

The best performance was observed with the membrane optimized electrode composition 44.3%: 55.2%: 0.5% (PVCAc:DBP:NaTPB). The optimized electrode has a linear dependence in the concentration range from 1.0×10^{-1} mol/dm^3 to 1.0×10^{-5} mol/dm^3 of Ag(I) with an almost Nernstian slope of 60.25 mV/decade, slightly higher than the theoretical value (59.16 mV/decade), which means that the electrode is highly reproducible. The limit of detection is 4.25×10^{-6} mol/dm^3 (Figure 2). All the above characteristics make this electrode comparable with ionophore containing electrode reported in the literature (Demirel et al., 2006; Jeong et al., 2011; Shamsipur et al., 2002).

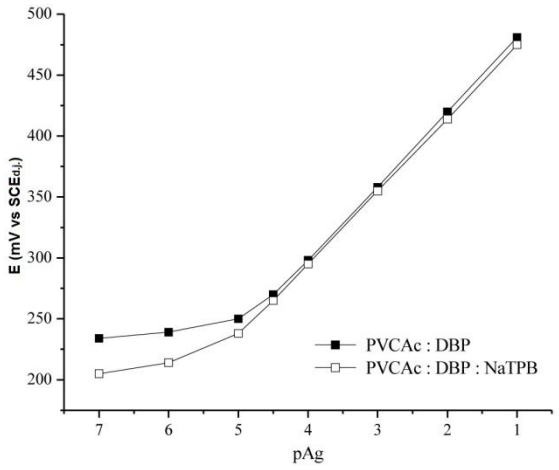

Figure 2. Calibration curve of the proposed Ag(I) selective electrode with NaTPB (○) and without NaTPB in its composition (▪).

Response time

The response time of this electrode was monitored depending on the electrode conditioning time. It was concluded that the shortest response time is 5 to 30 s for standard $AgNO_3$ solutions with concentrations of 1.0×10^{-1} mol/dm^3 to 1.0×10^{-7} mol/dm^3, and for the PVCAc/Ag electrode it is achieved after 30 min of conditioning in $AgNO_3$ (c ($AgNO_3$) = 0.01 mol/dm^3). After 30 min of conditioning in $AgNO_3$ (c ($AgNO_3$) = 0.01 mol/dm^3), the PVCAc/Ag electrode achieves the shortest response time (5 s to 30 s) for a standard $AgNO_3$ solution with concentrations of 1.0×10^{-1} mol/dm^3 to 1.0×10^{-7} mol/dm^3.

Response stability

The response stability of the PVCAc/Ag electrode was evaluated by constant current chronopotentiometry, which is a rapid experimental method and the electrode was found to exhibit a stable potential for a longer than two months.

Effect of pH

The effect of pH on the potentiometric response of the PVCAc/Ag electrode was studied in solutions with a constant concentration of silver ions (c ($AgNO_3$) = 0.01 mol/dm^3 and 0.001 mol/dm^3) in the range of pH 0.7 to 9.0. The pH values were adjusted by adding a solution of HNO_3 or NaOH at different concentrations. The potential is independent over the interval from very acidic to neutral medium, *i.e.* from pH 0.7 to 7.0 representing the working range of the sensor. Applicability in a highly

acidic media is a major advantage of this electrode. With increasing pH value, the potential response decreases, which is attributed to the hydroxylaton of silver ions. At lower pH value of 0.7 the electrode was not studied because of hydrogen error of the indicator electrode. The advantage of the proposed silver electrode is its applicability in very acidic media, where other electrodes which contain an ionophore in the polymer matrix do not function.

Selectivity

The selectivity of the PVCAc/Ag electrode was evaluated with fixed interference method and matched potential method (Umezawa et al., 1995). The results reveal that the electrode is highly selective for silver ions relative to other ions, and most of the cations tested do not interfere the determination of silver in the potential sample, with the exception of Hg^{2+} and Fe^{3+}, which strongly interfere even at 10^{-2} mol/dm^3 concentrations, and their removal from sample is necessary. These ions most likely exhibit their own interactions with the polymeric membrane and their potentiometric response often was not linear and steady under these conditions. The presence of most of the studied cations, such as Na^+, Ba^{2+}, Ca^{2+}, Mn^{2+}, Ni^{2+}, Co^{2+}, Cd^{2+}, Pb^{2+} and Zn^{2+}, would not cause any interference in the estimation of silver ions even if present in concentrations of 10^{-2} mol/dm^3. Cu^{2+}, Fe^{2+}, Cr^{3+} and Al^{3+} ions present at concentrations of 10^{-2} mol/dm^3 in solution have a slight interference.

Potentiometric titration with sodium chloride

Proposed optimized PVCAc/Ag electrode composition 44.3%: 55.2%: 0.5% (PVCAc: DBP: NaTPB) was applied as an indicator electrode in the potentiometric titration of silver(I) ions in sodium chloride solution (pH is about 5).

The following diagrams (Figures 3-7) show potentiometric curves when PVCAc/Ag electrode was used as the indicator electrode, with chlorides being titrated.

Potentiometric titration of 6 cm^3 solution of Ag(I) ($c=1.0\times10^{-1}$ mol/dm^3) diluted with deionized water to a volume of 50 cm^3 with a NaCl ($c=1.0\times10^{-1}$ mol/dm^3) yielded a sigmoidal (S - curve) curve (Figure 3). The end point of the titration and the amount of Ag^+ ions in the solution can be accurately determined on the basis of the potentiometric titration curve using the PVCAc/Ag electrode as the indicator electrode.

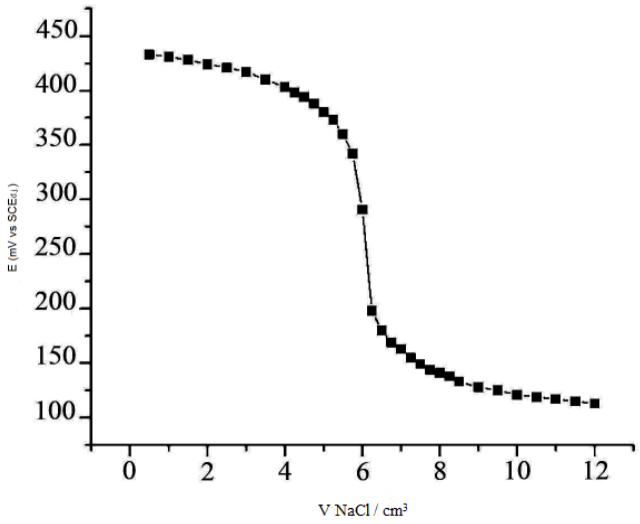

Figure 3. Potentiometric titration of 1.12×10^{-2} mol/dm^3 solution of Ag^+ ions with 1.0×10^{-1} mol/dm^3 solution of NaCl with indicator PVCAc/Ag electrode.

Analytical application in real systems

The following diagrams show potentiometric curves of titration of Ag^+ ions with chlorides when the PVCAc/Ag electrode was used as the indicator electrode. When all chlorides were precipitated, excess of Ag^+ ions caused the potential jump because the electrode is selective to silver ions.

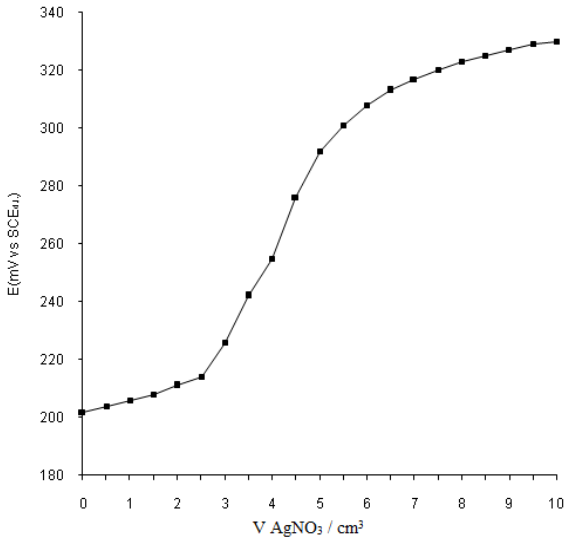

Figure 4. Potentiometric titration of Cl^- ions in a sample of spring water from „Jasen“, with a solution of $AgNO_3$ ($c = 2.5\times10^{-3}$ mol/dm^3), using PVCAc/Ag indicator electrode.

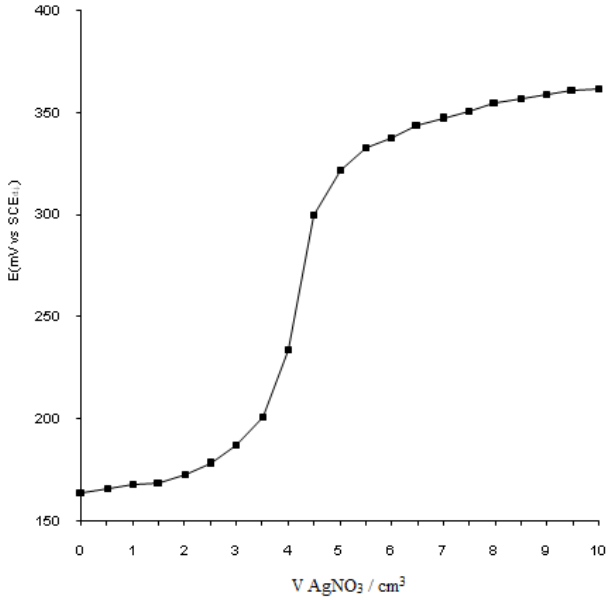

Figure 5. Potentiometric titration of Cl^- ions in a sample of spring water from „Česmica“, with a solution of $AgNO_3$ ($c = 1.0\times10^{-2}$ mol/dm^3), using PVCAc/Ag indicator electrode.

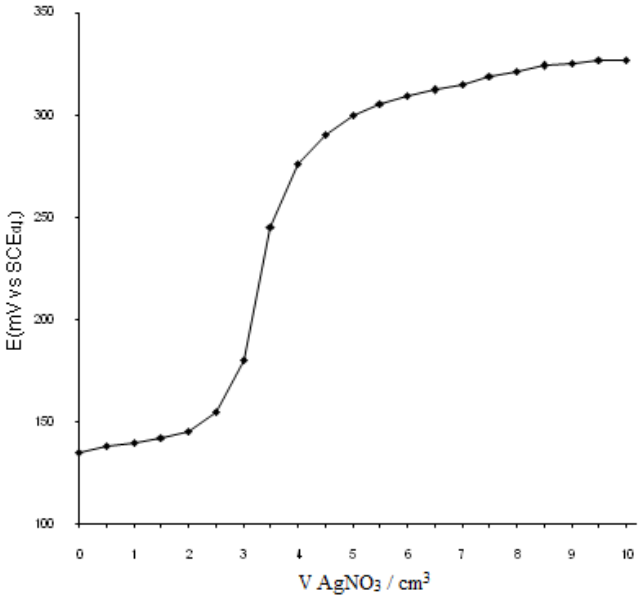

Figure 6. Potentiometric titration of Cl^- ions in a sample of spring water from „Vrelo", with a solution of $AgNO_3$ ($c = 1.0\times10^{-4}$ mol/dm^3), using PVCAc/Ag indicator electrode.

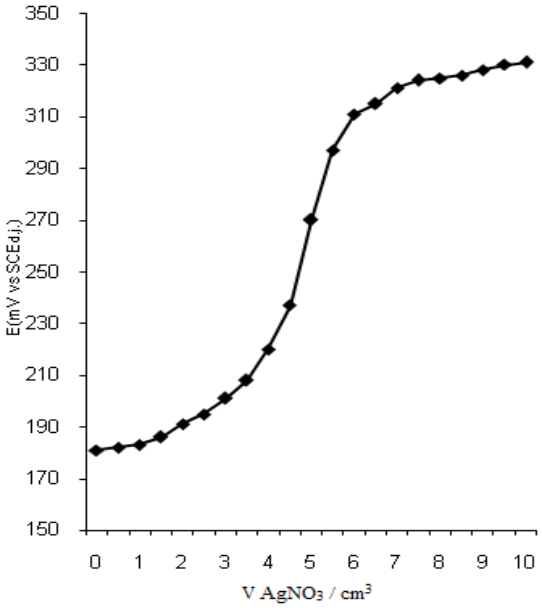

Figure 7. Potentiometric titration of Cl^- ions in a sample of water from „Bazeni", with a solution of $AgNO_3$ ($c = 5.0\times10^{-3}$ mol/dm^3), using PVCAc/Ag indicator electrode.

The potentiometric curve is sigmoidal in all cases, and the endpoint of the titration is sharp enough. Compare results are shown in Table 1, and it can be considered that the values obtained by the proposed sensor agree well with the results obtained by the comparative method. RSD values for chloride determination in different spring water samples range from 1.48-5.31%.

Table 1. Determination of chloride ion in spring water samples using the proposed PVCAc/Ag electrode and the comparative Ag/AgCl electrode.

Sample	Cl^- (mg/dm^3)		
Spring water from „Sjenica”	Found by PVCAc/Ag electrode (n=3)	Found by comparative Ag/AgCl electrode	RSD %
„Jasen”	7.028±0.2	6.987±0.2	3.22
„Česmica”	27.509±0.4	27.787±0.4	1.48
„Vrelo”	0.232±0.1	0.301±0.2	5.31
„Bazeni”	15.399±0.3	15.612±0.3	1.86

The results reported, our previous studies as well as the results reveal that proposed PVCAc/Ag electrode has been used for the determination of chloride ion concentration in the range of 1.0 to 25.0 mg/dm^3. At higher concentrations of Cl^- ions, the water sample solution was used to dilute beginning of the reaction. Water samples that contain lower concentrations of Cl^- ions than 1.0 mg/dm^3 were concentrated (sample “Vrelo” was concentrated on 1/10 V), because applicability of the proposed method is in the concentration range of 1.0-25.0 mg/dm^3 of chloride ions. The presence of cations in environmental water samples do not interfere the determination of chloride ions by the proposed electrode. Therefore, on the basis of all the above, it can be concluded that the chloride concentration was

successfully determined in spring water samples by potentiometric titration with standard solutions of $AgNO_3$ of appropriate concentrations when using the PVCAc/Ag electrode as indicator electrode.

Conclusion

The potentiometric titration curve in all cases is of the typical S-shape, and the end point of the titration is sharp enough. The values obtained agree well with those obtained by the comparative direct potentiometric method. Precision is satisfactory as indicated by the standard deviation values (1.48-5.31%).

Analytical application of poly(vinyl chloride-co-vinyl acetate) electrode modified with silver, without ionophores, of simple construction, is wide because of its characteristics. It is comparable or even better than silver selective electrodes based on a polymer membrane containing different ionophores which are already widely accepted.

Given that the electrode is proven to be reliable throughout this work, a wide concentration and pH range can be used in the analysis of real samples if the interfering ions of Hg^{2+} and Fe^{3+} are not present.

Conflict-of-Interest Statement

Authors declare no conflict of interest.

References

Argekar, A.A., Kulkarni, M.J., Mathur, J.N., Page, A.G., & Iyer, R.H. (1995). ICP-AES determination of silver after chemical separation from uranium matrix. Talanta, 42, 1937-1942.

Bermejo-Barrera, P., Moredo-Pineiro, A., & Moredo-Pineiro, J., & Bermejo-Barrera, A. (1998). Determination of traces of silver in human scalp hair slurries by electrothermal atomic absorption spectrometry. Microchimica Acta, 129, 71-76.

Bermejo-Barrera, P., Moreda-Pineiro, J., Moreda-Pineiro, A., & Bermejo-Berrera, A. (1996). Study of chemical modifiers for direct determination of silver in sea water by ETA-AAS with deuterium background correction. Talanta, 43, 35-44.

Chakrapani, G., Mahanta, P.L., Murty, D.S., & Gomathy, B. (2001). Preconcentration of traces of gold, silver and palladium on activated carbon and its determination in geological samples by flame AAS after wet ashing. Talanta, 53, 1139-1147.

Chandra, S., Deepshikha, & Sarkar, A. (2012). Selective electrochemical sensor for silver(I) ion based on chelating ionophore *o*-hydroxyacetophenone carbohydrazone (OHAC). Analytical & Bioanalitical Electrochemistry, 4, 45-60.

Chiba, K., Inamoto, I., & Saeki, M. (1992). Application of isotope dilution analysis—inductively coupled plasma mass spectrometry to the precise determination of silver and antimony in pure copper. Journal of Analytical Atomic Spectrometry, 7, 115-119.

Damien, W. M. A. (1994). Tutorial review. Voltammetric determination of trace metals and organics after accumulation at modified electrodes. *Analyst, 119, 1953-1966.*

Daniel Johnson, R., & Bachas, L.G. (2003). Ionophore-based ion-selective potentiometric and optical sensors. Analytical and Bioanalytical Chemistry, 376, 328-341.

Dekanski, A., Stevanović, J., Stevanović, R., & Jovanović, V. M. (2001). Glassy carbon electrodes II. Modification by immersion in $AgNO_3$. Carbon, 39, 1207-1216.

Demirel, A., Dogan, A., Akkus, G., Yilmaz, M., & Kilic, E. (2006). Silver(I)-selective PVC membrane potentiometric sensor based on a recently synthesized calix[4]arene. Electroanalysis, 18, 1019-1027.

Dirkse, T.P. (1989). A potentiodynamic study of the electrolytic formation of AgO. Electrochimica Acta, 34, 647-650.

El-Zawawy, F.M., El-Shahat, M.F., Mohamed, A.A., & Zaki, M.T.M. (1995). Spectrophotometric determination of silver and gold with 5-(2,4-dihydroxybenzylidene)rhodanine and cationic surfactants. Analyst, 120, 549-554.

Gupta, V.K., Pal, M.K., & Singh, A.K. (2009). Comparative study of Ag(I) selective poly(vinyl chloride) membrane sensors based on newly developed Schiff-base Lariat ethers derived from 4,13-diaza-18-crown-6. Analytica Chimica Acta, 631, 161-169.

Jeong, E., Ahmed, M.S., Jeong, H., Lee, E., & Jeon, S. (2011). Novel silver(I) ion selective PVC membrane electrode based on the Schiff base ($N^2E,N^{2'}E$)-$N^2,N^{2'}$-bis(thiophen-2-ylmethylene)-1,1'-binaphthyl-2,2'-diamine. Bulletin of the Korean Chemical Society, 32, 800-804.

Jovanović, V.M., Radovanović, M., & Jovanović, M.S. (1985). Ion-Selective electrodes 4. Budapest: Akademiai Kiado, p. 489.

Jovanović, V.M., Terzić, S., & Dekanski, A. (2005). Characterization and electrocatalytic application of silver modified polypyrrole electrodes. Journal of the Serbian Chemical Society, 70, 41-49.

Kabasakalis, V. (1994). Fluorimetric determination of silver with brilliant green in aqueous systems and its application in photographic fixing solutions. *Analytical Letters,* 27, 2789-2796.

Matsuda, K., Hiratsuka, N., Koyama, T., Kurihara, Y., Hotta, O., Itoh, Y. & Shida, K. (2001). Sensitive method for detection and semiquantification of Bence Jones protein by cellulose acetate membrane electrophoresis using colloidal silver staining. Clinical Chemistry, 47, 763-766.

Lu, J.-Q., Pang, D.-W., Zeng, X.-S., & He, X.-W. (2004). A new solid-state silver ion-selective electrode based on a novel tweezer-type calixarene derivative. Journal of Electroanalytical Chemistry, 568, 37-43.

Malinowska, E., Brzozka, Z., Kasiura, K., Egberink, R.J.M., & Reinhoudt, D. N. (1994). Silver selective electrodes based on thioether functionalized calix [4] arenes as ionophores. Analytica Chimica Acta, 298, 245-251.

Ohshita, K., Wada, H., & Nakasawa, G. (1986). Spectrophotometric determination of silver with 4-(3,5-dibromo-2-pyridylazo)-*N,N*-diethylaniline in the presence of sodium dodecylsulfate. Analytica Chemica Acta, 182, 157-162.

Petković, B.B., Sovilj, S.P., Budimir, M.V., Simonović, R.M., & Jovanović, V.M. (2010). A copper(II) ion-selective potentiometric sensor based on *N* ,*N* ′,*N* ″,*N* ‴-tetrakis(2-pyridylmethyl)-1,4,8,11-tetraazacyclotetradecane in PVC matrix. Electroanalysis, 22, 1894-1900.

Pu, Q., & Sun, Q. (1998). Application of 2-mercaptobenzothiazole-modified silica gel to on-line preconcentration and separation of silver for its atomic absorption spectrometric determination. Analyst, 123, 239-243.

Rahman, M.A., Kaneco, S., Amin, M.N., Suzuki, T., & Ohta, K. (2004). Determination of silver in environmental samples by tungsten wirepreconcentration method–electrothermal atomic absorption spectrometry. Talanta, 62, 1047-1050.

Sang, S., Yu, C., Li, N., Ji, Y., & Zhang, J. (2012). Characterization of a new Ag^{+} -selective electrode with lower detection limit. International Journal of Electrochemical Science, 7, 3306-3313.

Sejmanović, D.M., Petković, B.B., Budimir, M.V., Sovilj, S.P., & Jovanović, V.M. (2011). Characterization of a silver modified PVCAc electrode and its application as a Ag(I)-selective potentiometric sensor. Electroanalysis, 23 (8), 1849-1855.

Shamsipur, M., Javanbakht, M., Ganjali, M.R., Mousavi, M.F., Lippolis, V., & Garau, A. (2002). Mixed aza-thioether crowns containing a 1,10-phenanthroline sub-unit as neutral ionophores for silver ion. Electroanalysis, 14, 1691-1691.

Smith, I.C., & Carson, B.L. (1977). Trace metals in the environment. Michigan: Ann Arbor Science Publ., Ann Arbor.

Sramkova, J., Kotrly S., & Peknicova, M. (1999). Determination of silver in layered monocrystals of thermoelectric tellurides by graphite furnace atomic absorption spectrometry. Analusis, 27, 839-846.

Umezawa, Y., Umezawa, K., & Sato, H. (1995). Selectivity coefficients for ion-selective electrodes: recommended methods for reporting $K_{A,B}^{pot}$ values. Pure and Applied Chemistry, 67, 507-518.

Wan, A.T., Conyers, R.A., Coombs, C.J., & Masterton, J.P. (1991). Determination of silver in blood, urine, and tissues of volunteers and burn patients. Clinical Chemistry, 37, 1683-1687.

Analitička primena poli(vinil hlorid-ko-vinil acetat) elektrode modifikovane sa srebrom za određivanje hloridnih jona u realnim sistemima

Dragana M. Sejmanović[1], Milana V. Budimir[1], Živana Ž. Radosavljević[1], Emilija T. Pecev[2]

1- Univerzitet u Prištini, Prirodno-matematički fakultet, Kosovska Mitrovica, Srbija

2- Univerzitet u Nišu, Prirodno-matematički fakultet, Niš, Srbija

Sažetak

Mogućnost primene nove jednostavne Ag-selektivne elektrode za određivanje hloridnih jona, izučavana je u ovom radu. Poli (vinil hlorid-ko-vinil acetat modifikovana elektroda sa srebrom (PVCAc/Ag) pripremljena je jednostavnim uranjanjem staklene ugljene electrode prekrivene poli(vinil hlorid-ko-vinil acetat) polimerom, koji sadrži plastifikator i lipofilni aditiv, ali bez jonofore, u rastvor srebro-nitrata. Ova jednostavnost pripreme i veliki pH opseg kroz prilično kiselu sredinu (pH 0.7 do 7.0), prednosti su ove modifikovane elektrode nad mnogobrojnim prethodnim srebrnim selektivnim elektrodama baziranim na polimernom matriksu koji sadrži različite jonofore. Odgovor elektrode bio je linearan sa Nernst-ovim nagibom 60.25 mV/dekada u koncentracionom opsegu od 1.0×10^{-1} do 1.0×10^{-5} mol/dm^3 Ag^+ I sa granicom detekcije 4.25×10^{-6} mol/dm^3. Predložena PVCAc/Ag elektroda je primenjena za određivanje hloridnih jona u uzorcima izvorskih voda. Rezultati određivanja hloridnih jona u uzorcima izvorskih voda dobijeni predloženom metodom i komparativnom Ag/AgCl elektrodom bili su u zadovoljavajućoj saglasnosti.

Ključne reči: srebro, elektrode, izvorske vode, vinil hlorid-ko-vinil acetat, hloridni joni

Application analytique d'une électrode en poly (chlorure de vinyle-co-acétate de vinyle) modifiée avec de l'argent pour la détermination des ions chlorure dans des systèmes réels

Dragana M. Sejmanović[1], Milana V. Budimir[1], Živana Ž. Radosavljević[1], Emilija T. Pecev[2]

1- Université de Priština, Faculté des sciences naturelles et des mathématiques, Kosovska Mitrovica, Serbie

2- Université de Niš, Faculté des sciences naturelles et des mathématiques, Niš, Serbie

Résumé

Dans cet article a été étudiée la possibilité d'application d'une nouvelle et simple Ag-électrode sélective pour la détermination des ions chlorure. L'électrode de poly (chlorure de vinyle-co-acétate de vinyle modifiée avec de l'argent – PVCAc/Ag) a été préparée par une simple immersion d'une électrode de carbone vitreux revêtue de polymère de poly (chlorure de vinyle-co-acétate de vinyle), qui contenait un plastifiant et un additif lipophile, mais sans ionophore, dans la solution de nitrate d'argent. Cette simplicité de construction et la gamme étendue de pH à travers des milieux acides remarquables (pH 0.7 à 7.0) sont les avantages de cette électrode modifiée par rapport à de nombreuses électrodes sélectives d'argent antérieures qui sont basées sur une matrice polymère contenant des différents ionophores. La réponse de l'électrode était linéaire avec une pente de Nernstian de 60.25 mV/décade dans l'étendu de concentration de 1.0×10^{-1} à 1.0×10^{-5} mol/dm^3 Ag^+ et avec une limite de détection de 4.25×10^{-6} mol/dm^3. L'électrode PVCAc/Ag proposée a été appliquée à la détermination des ions chlorure dans les échantillons d'eaux de source. Les résultats de la détermination des ions chlorure dans les échantillons d'eaux de source obtenus à l'aide de la méthode proposée et de l'électrode comparative Ag/AgCl étaient en accord satisfaisant.

Mots-clés: *argent, électrodes, eaux de source, chlorure de vinyle-co-acétate de vinyle, ions chlorure*

Аналитическое применение электрода из поливинилхлорида-винилацетата, модифицированного серебром, для определения хлорид-ионов в реальных системах

Драгана М. Сеймановић[1], Милана В. Будимир[1], Живана Ж. Радосављевић[1], Емилия Т. Печев[2]

1- Университет в Приштине, Естественно-математический факультет, Косовска-Митровица, Сербия

2- Университет в Нише, Естественно-математический факультет, Кафедра химии, Вишеградска 33, 18000 Ниш, Сербия

Аннотация

В работе исследована возможность применения нового простого Ag-селективного электрода для определения хлорид-ионов. Электрод из сополимера винилхлорида и винилацетата, модифицированного серебром (PVCAc/Ag), был приготовлен простым погружением стеклоуглеродного стержня, покрытого полимером сополимера винилхлорида и винилацетата, который содержал пластификатор и липофильную добавку, но без ионофора, в раствор нитрата серебра. Простота подготовки и широкий диапазон pH в довольно кислой среде (pH 0.7–7.0) являются преимуществами этого модифицированного электрода по сравнению со многими предыдущими сереброселективными электродами на основе полимерной матрицы, содержащей различные ионофоры. Отклик электрода был линейным с наклоном Нернста 60,25 мВ / декаду в диапазоне концентраций от 1.0×10^{-1} до 1.0×10^{-5} моль/дм^3 Ag + I с пределом обнаружения 4.25×10^{-6} моль/дм^3. Предложенный электрод PVCAc / Ag был использован для определения ионов хлора в образцах родниковой воды. Результаты определения хлорид-ионов в образцах родниковой воды, полученные предлагаемым методом, и сравнительным Ag/AgCl электродом удовлетворительно согласуются.

Ключевые слова: серебро, электроды, родниковые воды, винилхлорид-винилацетат, хлорид

Analytische Anwendung einer mit Silber modifizierten Poly(vinylchlorid-Co-Vinylazetat)-Elektrode zur Bestimmung von Chloridionen in realen Systemen

Dragana M. Sejmanović[1], Milana V. Budimir[1], Živana Ž. Radosavljević[1], Emilija T. Pecev[2]

1- Universität Priština, Fakultät für Naturwissenschaften und Mathematik, Kosovska Mitrovica, Serbien

2- Universität Niš, Fakultät für Naturwissenschaften und Mathematik, Višegradska 33, Niš, Serbien

ABSTRAKT

In dieser Arbeit wurde die Anwendungsmöglichkeit einer neuen einfachen Ag-selektiven Elektrode zur Bestimmung von Chloridionen untersucht. Eine mit Silber modifizierte Poly(vinylchlorid-Co-Vinylazetat)-Elektrode (PVCAc/Ag) wurde einfach hergestellt, indem eine Glaskohlenstoffelektrode, die mit Poly(vinylchlorid-Co-Vinylazetat)-Polymer beschichtet wurde, der Weichmacher und lipophiles Additiv enthielt, jedoch ohne Ionophor, in die Silbernitratlösung getaucht wurde. Diese einfache Herstellung und der breite pH-Bereich durch ziemlich saure Umgebung (pH 0.7 bis 7.0) sind Vorteile dieser modifizierten Elektrode gegenüber vielen bisherigen silbernen selektiven Elektroden, die auf einer Polymermatrix basieren, die verschiedene Ionophore enthält. Die Reaktion der Elektrode war linear mit einer Nernst-Steigung von 60.25 mV/Dekade im Konzentrationsbereich von 1.0×10^{-5} bis 1.0×10^{-5} mol/dm^3 Ag^+ und mit einer Nachweisgrenze von 4.25×10^{-6} mol/dm^3. Die vorgeschlagene PVCAc/Ag-Elektrode wurde zur Bestimmung von Chloridionen in den Proben von Quellwässern verwendet. Die Ergebnisse der Chloridionenbestimmung in Quellwasserproben, die durch die vorschlagene Methode und die komparative Ag/AgCl-Elektrode erhalten wurden, stimmten zufriedenstellend überein.

Schlüsselwörter: Silber, Elektroden, Quellwässer, Vinylchlorid-Co-Vinylazetat, Chloridionen

Molecular dynamics simulations of ASC09, ritonavir, lopinavir and darunavir with the COVID-19 protease

Budimir S. Ilić[1]*

1- University of Niš, Faculty of Medicine, Department of Chemistry, 18000 Niš, Serbia

ABSTRACT

Given the novelty of SARS-CoV-2 infection (COVID-19), and the lack of proven therapies, a wide variety of strategies are being employed to combat COVID-19 pandemic. Many of these emerging strategies rely on repurposing existing drugs and their mechanistic approaches that are effective against either similar viral infections or the serious symptoms that are caused by COVID-19. The recently solved issue of the crystal structure of the COVID-19 protease has made elucidating the structure–activity relationship feasible. The interaction of ASC09, ritonavir, lopinavir and darunavir with COVID-19 protease was simulated using the Site Finder module, molecular docking and molecular dynamics (MD). Analysis of the MD trajectories has provided the ligand/receptor interaction fingerprints, combining information on the crucial receptor residues and frequency of the ligand/residue contacts. The contact frequencies and the contact maps suggest that for all studied antiviral drugs, the interactions with Gln 107, Pro 108, Gln 110 and His 246 are an important factor for drugs affinities toward the COVID-19 protease. However, the leading interactions with Arg 105, Phe 134, Glu 240, Thr 243, Asp 245 or Phe 294 also significantly contribute to the ligand/receptor interplay and, in particular, differentiate their binding affinities toward COVID-19 protease.

Keywords: COVID-19, Molecular dynamics, ASC09, Ritonavir, Lopinavir, Darunavir

*Budimir S. Ilić, Department of Chemistry, Faculty of Medicine, University of Niš, 18000 Niš, Serbia, bucabule@yahoo.com (or budimir.ilic@medfak.ni.ac.rs)

Introduction

At the time of this writing, the SARS-CoV-2 infection has sickened more than 11 million people globally and killed more than half a million of them (Worldometer, 2020). No vaccine or direct treatment currently exists (Ahmed et al., 2020; Robson, 2020). The most promising vaccine clinical trials at this moment include an adenovirus-based candidate that is in a phase IIb/III trial and an mRNA vaccine that is in a phase II trial (Mullard, 2020). As the SARS-CoV-2 infection continues to spread worldwide and more people become critically ill, scientists are racing to find a treatment that will reverse the course (Ren et al., 2020; Robson, 2020; Wang et al., 2020;). Dozens of medicines are in clinical trials in China and the United States to treat the disease, officially named COVID-19 (Harrison 2020; Zhang et al., 2020;). More than 240 clinical trials being conducted involve antiviral drugs that were developed to treat illnesses such as HIV/AIDS, malaria, *etc.* (ClinicalTrials, 2020).

Protease inhibitors are a class of antiviral drugs that are widely used to treat HIV, hepatitis C, SARS-CoV and MERS-CoV (Feng et al., 2019; Pillaiyar et al., 2016; Sheahan et al., 2020). They prevent SARS-CoV replication by selectively binding to viral proteases and blocking proteolytic cleavage of protein precursors that are necessary for the production of infectious viral particles (Haagmans and Osterhaus, 2006). Last five months, at least 50 different trials for SARS-CoV-2 registered in the Clinical Trial Registry (*e.g.*, NCT04251871, NCT04255017, NCT04261270, NCT04261907, NCT04275388, NCT04276688, NCT04286503, NCT04291729, NCT04295551, NCT04303299, NCT04306497, NCT04307693, NCT04315948) proposed the use of protease inhibitors (ASC09, ritonavir, lopinavir and darunavir) in the treatment of COVID-19 (ClinicalTrials, 2020).

A key aspect of the inhibitor discovery process is to determinate the three-dimensional structure of the inhibitor/protein complex. Therefore, elucidating the binding mode of viral protease inhibitors with COVID-19 protease could provide some clues to the design of more promising COVID-19 protease inhibitors. This paper presents and discuss the results of molecular dynamics (MD) simulations of ASC09, ritonavir, lopinavir and darunavir with recently reported, high-resolution crystal structure of COVID-19 protease. The Site Finder module of the Molecular Operating Environment (MOE) software (MOE, 2019), was utilized to define and rank potential ligand-binding sites according to their propensity for ligand binding, which was based on the amino acid composition of the pocket (Soga et al., 2007). Furthermore, molecular docking and molecular dynamics simulations methods were applied as a powerful computational strategy to investigate the detailed interactions of protease inhibitors with COVID-19 protease. The aim is to sketch the mechanism of inducing distinct responses of the COVID-19 protease to the chosen ligands. The study includes independent MD simulations for the top-ranked poses of each ligand and examines frequency of contacts and patterns between viral protease inhibitors and the COVID-19 protease residues.

Experimental

Examined viral protease inhibitors have been generated using the builder panel in the MOE software. Using the MOE LigX module, partial atomic charges were ascribed and possible ionization states were generated at a pH of 7.0. The MMFF94x force field was used for optimization and the resulting structures were used for modeling studies (Halgren, 1996). Conformational search was carried out by MOE LowModelMD method which performs molecular dynamic perturbations along with low frequency vibrational modes with energy window of 7 kcal mol^{-1}, and conformational limits of 1000.

Several X-ray crystallographic structures of COVID-19 protease (PDB: 6Y84, 6Y2E, 5R84, 6Y2F, 6M03, 6LU7 and 6Y2G) have been recently published (Protein Data Bank, 2020). Considering the receptor resolution (King, 1958), the crystallographic structure (PDB: 6Y84) was elected as the top structure for further molecular modeling (Owen et al., 2020). The inaccuracy of COVID-19 protease was corrected by the Structure Preparation process in MOE. After the correction, hydrogens were added and partial charges (Gasteiger methodology) were calculated. Energy minimization (AMBER14:EHT, RMS gradient: 0.100) was performed.

The Site Finder module of the MOE was used to identify possible ligand-binding sites within the optimized structure of COVID-19 protease. Hydrophobic or hydrophilic alpha spheres served as probes denoting zones of tight atom packing. These alpha spheres were utilized to define and rank potential ligand-binding sites according to their propensity for ligand binding (PLB) score, which was based on the amino acid composition of the pocket (Soga et al., 2007).

The molecular docking study was performed using the MOE to understand the ligand protein interactions in detail. The default Triangle Matcher placement method was used for the induced fit docking (MOE, 2019). GBVI/WSA dG scoring function which estimates the free energy of binding of the ligand from a given pose was used to rank the final poses (Corbeil et al., 2012). Each ligand/protein complex with lowest relative binding free energy (ΔG) score was selected.

The molecular dynamics simulation of selected viral protease inhibitors on COVID-19 protease was carried out using the Desmond (Desmond, 2018). The structure of the added water was based on the simple point charge (SPC) solvent model. The system was neutralized with Na^+ ions to balance the net charge of the whole simulation box to neutral. The final system contained approximately 36800 atoms. The system was passed through a 6-step relaxation protocol before molecular dynamics simulations. The relaxed system was simulated for 10 ns, using a normal pressure temperature (NPT) ensemble with a Nosé–Hoover thermostat at 300 K and Martyna–Tobias–Klein barostat at 1.01325 bar pressure. Atomic coordinate data and system energies were recorded every 1 ps. The root mean square deviation (RMSD) and root mean square fluctuation (RMSF) of the inhibitor/COVID-19 protease complexes were analyzed with respect to simulation time.

Results and Discussion

The binding site residues in the COVID-19 protease have been identified using the Site Finder module implemented in the MOE software. The results from the analysis highlighted that amino acid residues like Phe 3, Arg 4, Lys 5, Met 6, Ala 7, Phe 8, Pro 9, Lys 102, Val 104, Arg 105, Ile 106, Gln 107, Pro 108, Gly 109, Gln 110, Thr 111, Gln 127, Pro 132, Phe 134, Phe 150, Asn 151, Ile 152, Asp 153, Tyr 154, Cys 156, Val 157, Ser 158, Phe 159, Cys 160, Gly 183, Ile 200, Thr 201, Val 202, Asn 203, Glu 240, Pro 241, Thr 243, Asp 245, His 246, Ile 249, Phe 291, Thr 292, Pro 293, Phe 294, Asp 295, Val 296, Arg 298, Gln 299, Gly 302, Val 303 and Thr 304 constituted the top binding pocket of the COVID-19 protease (Table 1).

The intermolecular contacts between four representative viral protease inhibitors and COVID-19 protease were analyzed using the ligand interaction diagram of MOE suite. According to binding free energy, it was predicted that ASC09 (-7.83 kcal mol^{-1}) could inhibit COVID-19 protease better than ritonavir (-7.42 kcal mol^{-1}), lopinavir (-6.98 kcal mol^{-1}) and darunavir (-6.56 kcal mol^{-1}).

The study was further extended to assess the stability of inhibitor/COVID-19 protease complexes through the molecular dynamics simulations. The RMSD and RMSF plots for COVID-19 protease showed that docking complexes were stable during entire simulation period (Figure 1). The RMSD and RMSF values for Cα, side chains and heavy atoms remained within the limit of 2 Å (Figure 1). The obtained results indicated small structural rearrangements, less conformational changes and confirmed stability of inhibitor/COVID-19 protease complexes (Liu and Kokubo, 2017). The interactions observed during 10 ns molecular simulation confirmed the importance of Arg 105, Gln 107, Pro 108, Gln 110, Phe 134, Glu 240, Thr 243, Asp 245, His 246 and Phe 294 in the formation of inhibitor/COVID-19 protease complexes (Figures 2 and 3).

Table 1. Summary of the possible inhibitor-binding sites in the COVID-19 protease.

Site	Size	PLB	Hyd	Side	Residues
1	193	4.5	61	112	Phe 3, Arg 4, Lys 5, Met 6, Ala 7, Phe 8, Pro 9, Lys 102, Val 104, Arg 105, Ile 106, Gln 107, Pro 108, Gly 109, Gln 110, Thr 111, Gln 127, Pro 132, Phe 134, Phe 150, Asn 151, Ile 152, Asp 153, Tyr 154, Cys 156, Val 157, Ser 158, Phe 159, Cys 160, Gly 183, Ile 200, Thr 201, Val 202, Asn 203, Glu 240, Pro 241, Thr 243, Asp 245, His 246, Ile 249, Phe 291, Thr 292, Pro 293, Phe 294, Asp 295, Val 296, Arg 298, Gln 299, Gly 302, Val 303, Thr 304
2	21	0.68	14	22	Trp 218, Phe 219, Leu 220, Asn 221, Phe 223, Ser 267, Glu 270, Leu 271, Asn 274, Gly 275, Met 276, Asn 277
3	18	0.33	11	18	Leu 220, Asn 221, Phe 223, Ile 259, Asp 263, Met 264, Ser 267
4	54	0.33	13	34	His 41, Met 49, Asn 142, His 164, Met 165, Glu 166, Leu 167, Pro 168, Thr 169, Gly 170, Arg 188, Gln 189, Thr 190, Ala 191, Gln192

5	13	0.16	8	11	Asn 63, His 64, Phe 66, Leu 67, Val 68, Gln 74, Leu 75, Arg 76, Val 77
6	13	0.15	8	19	Arg 40, Asn 84, Cys 85, Arg 105, Gly 179, Asn 180, Phe 181, Gly 183, Phe 185, Val 186, Asp 187
7	25	0.11	4	17	Phe 140, Leu 141, Asn 142, Gly 143, Ser 144, Cys 145, His 163, Met 165, Glu 166
8	28	-0.01	12	18	Thr 199, Tyr 237, Tyr 239, Leu 271, Leu 272, Gly 275, Met 276, Asn 277, Gly 278, Arg 279, Ala 285, Leu 286, Leu 287
9	15	-0.01	6	8	Glu 14, Gly 15, Cys 16, Met 17, Val 18, Trp 31, Ala 70, Gly 71, Gly 120, Pro 122
10	31	-0.07	7	24	Lys 5, Arg 131, Lys 137, Asp 197, Thr 198, Thr 199, Leu 286, Leu 287, Glu 288, Asp 289, Glu 290

Examined inhibitor/COVID-19 protease complexes, throughout the molecular dynamics simulation exhibited four types of interactions: hydrophobic, ionic, water-bridged and hydrogen bonds (Figures 2 and 3). The molecular dynamics simulations of ASC09/COVID-19 protease (Figure 2A and 2B), revealed firm ionic/water-bridged interactions with Glu 240 (72 % of the simulation time) and water-bridged interactions with Thr 243 (44 % of the simulation time), Asp 245 (35 % of the simulation time) and Gln 110 (16 % of the simulation time). In addition, the ASC09/COVID-19 protease complex uncovered H-bonding/water-bridged interactions with Gln 107 (37 % of the simulation time), as well as hydrophobic/water-bridged interactions with His 246 (35 % of the simulation time) and Pro 108 (22 % of the simulation time). The interaction profile of ritonavir/COVID-19 protease revealed slightly different results (Figure 2C and 2D). The molecular dynamics showed stable water-bridged interactions with Asp 245 (78 % of the simulation time) as well as forceful H-bonding/water-bridged interactions with Gln 110 (76 % of the simulation time) and Gln 107 (62 % of the simulation time). Furthermore, examined complex showed substantial H-bonding/hydrophobic interactions with Pro 108 (65 % of the simulation time) and His 246 (52 % of the simulation time) (Figure 2C and 2D).

The molecular dynamics simulations of lopinavir and darunavir with COVID-19 protease (Figure 3), revealed prevalent H-bonding/water-bridged interactions with Gln 107 (exceeding 116 % of the simulation time). In addition, lopinavir and darunavir exhibited modest interactions with previously discussed Pro 108, Gln 110 and His 246 (Figure 3). The contact frequencies and the contact maps suggest that for all studied antiviral drugs, the interactions with Gln 107, Pro 108, Gln 110 and His 246 are an important factor for drugs affinities toward the COVID-19 protease. Highlighted residues of COVID-19 protease are comparable with structural features and catalytic residues of SARS-CoV $3CL^{pro}$ which inhibition by peptidomimetics and small molecule inhibitors is well documented (Pillaiyar et al., 2016). Of note, the importance of Gln (as Gln 189 or Gln 192) and His (as His 41) in the anti-SARS-CoV $3CL^{pro}$ chemotherapies is clearly established in Pillayiar et al. (2016) and references therein. However, the

molecular dynamics simulations of examined complexes reveal that leading interactions with Arg 105, Phe 134, Glu 240, Thr 243, Asp 245 or Phe 294 also significantly contribute to the ligand/receptor interplay and, in particular, differentiate their binding affinities toward COVID-19 protease (Figures 2 and 3).

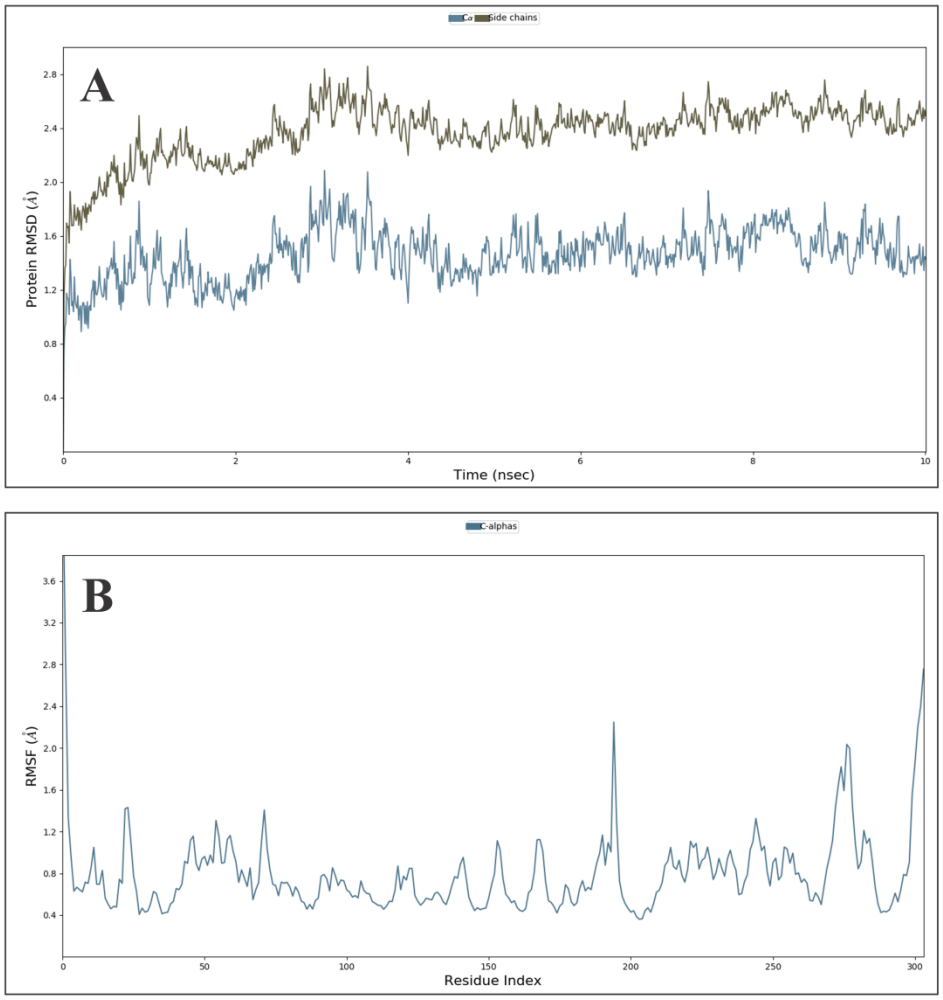

Figure 1. RMSD (**A**) and RMSF (**B**) plot of COVID-19 protease, during the course of 10 ns molecular dynamics simulation.

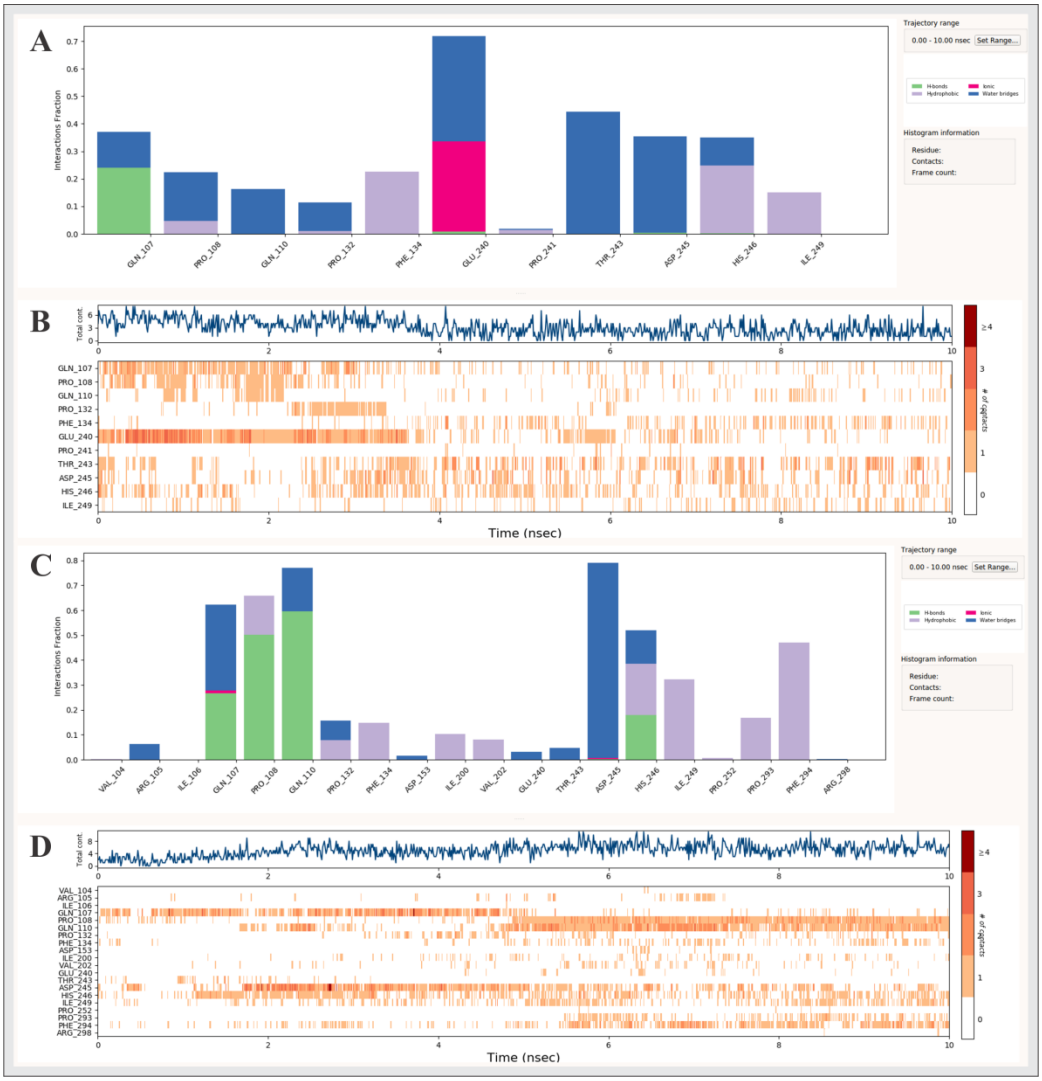

Figure 2. Normalized stacked bar chart representation and timeline representation of interactions and contacts between COVID-19 protease and antiviral drugs ASC09 (**A**, **B**) and ritonavir (**C**, **D**), during the course of 10 ns molecular dynamics simulation.

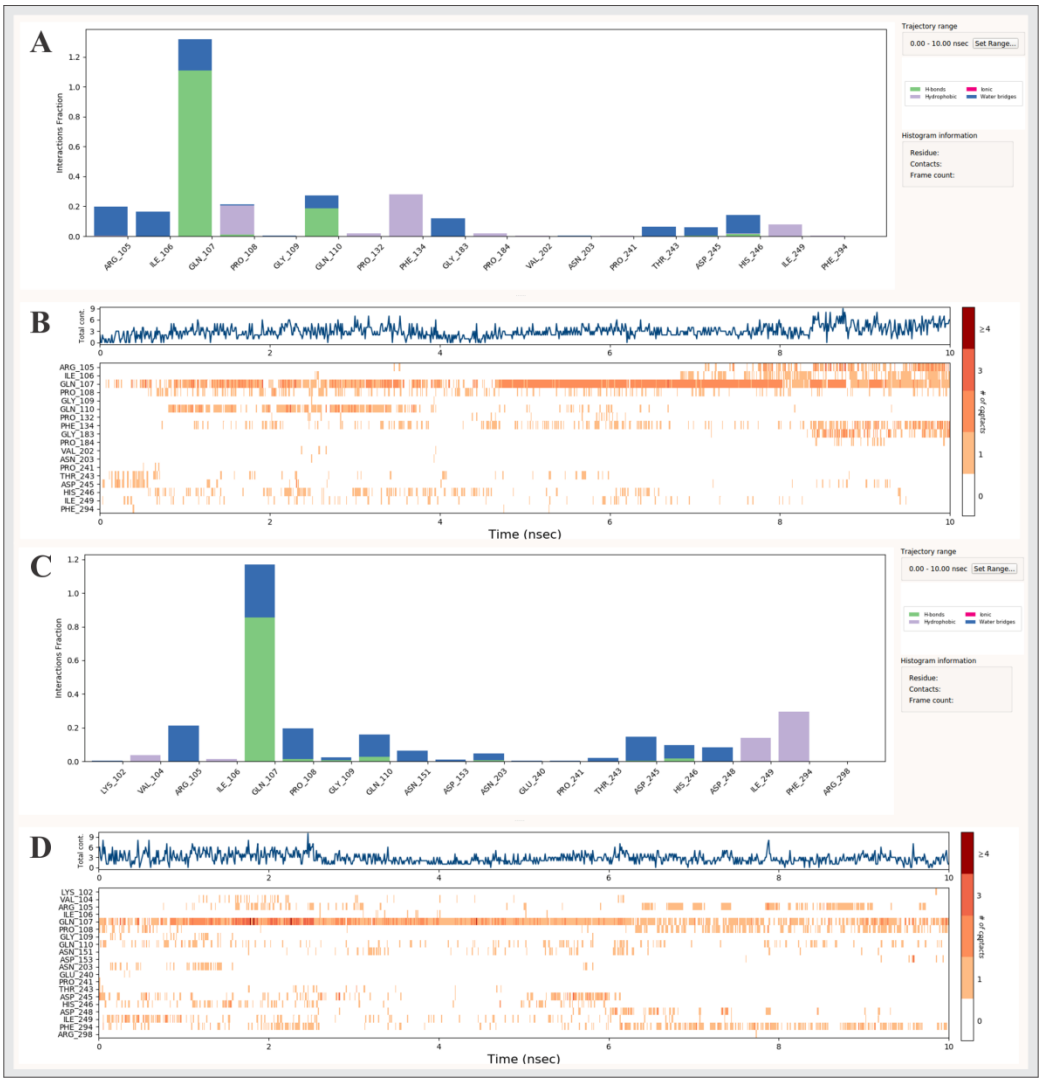

Figure 3. Normalized stacked bar chart representation and timeline representation of interactions and contacts between COVID-19 protease and antiviral drugs lopinavir (**A**, **B**) and darunavir (**C**, **D**), during the course of 10 ns molecular dynamics simulation.

Conclusion

In summary, given the novelty of SARS-CoV-2 infection, and the lack of proven therapies, a wide variety of strategies are being employed to combat COVID-19 pandemic. The results presented herein provide dynamic insight into the binding of ASC09, ritonavir, lopinavir and darunavir with COVID-19 protease through the computational modeling approaches. Analysis of the observed intermolecular contact frequencies together with the contact maps indicates that the interactions with Gln 107, Pro 108, Gln 110 and His 246, retained by all of the studied ligands, are a contributing factor to the affinity of the ligand/COVID-19 protease interaction. However, the leading interactions with Arg 105, Phe 134, Glu 240,

Thr 243, Asp 245 or Phe 294 also significantly contribute to the ligand/receptor interplay and, in particular, differentiate their binding affinities toward COVID-19 protease. I anticipate that the results presented herein will open the way for a deeper understanding of inhibitor/COVID-19 protease interactions, especially for peptidomimetics that have recently been included in the treatment of COVID-19.

Acknowledgment

I would like to thank D. E. Shaw Research, for providing me the Desmond software package free of cost for this study.

Conflict-of-Interest Statement

Declarations of interest: none.

Informed Consent Statement

Informed consent was obtained from all individual participants included in the study.

Human and Animal Rights Statement

This article does not contain any studies with human participants or animals performed by any of the authors.

References

Ahmed, S. F., Quadeer, A. A., & McKay, M. R. (2020). Preliminary identification of potential vaccine targets for the COVID-19 coronavirus (SARS-CoV-2) based on SARS-CoV immunological studies. Viruses, 12(3), 254.

ClinicalTrials (2020, July 4). U. S. National Library of Medicine, ClinicalTrials.gov. Retrieved from https://clinicaltrials.gov/ct2/results?term=Antiviral&cond=covid-19

Corbeil, C. R., Williams C. I., & Labute, P. (2012). Variability in docking success rates due to dataset preparation. Journal of Computer-Aided Molecular Design, 26, 775–786.

Desmond (2020, May 16). Desmond Molecular Dynamics System, version 2018.4, (D. E. Shaw Research, New York, NY). Retrieved from https://www.deshawresearch.com/index.html

Feng, H.-P., Caro, L., Fandozzi, C., Chu, X., Guo, Z., Talaty, J., Panebianco, D., Dunnington, K., Du, L., Hanley, W. D., Fraser, I. P., Mitselos, A., Denef, J.-F., Lepeleire, I. D., de Hoon, J. N., Vandermeulen, C., Marshall, W. L., Jumes, P., Huang, X., Martinho, M., Valesky, R., Butterton, J. R., Iwamoto, M., & Yeh, W. W. (2019). Pharmacokinetic interactions between the Hepatitis C virus inhibitors elbasvir and

grazoprevir and HIV protease inhibitors ritonavir, atazanavir, lopinavir, and darunavir in healthy volunteers. Antimicrobial Agents and Chemotherapy, 63(e02142-18), 1–14.

Haagmans, B. L., & Osterhaus, A. D. M. E. (2006). Coronaviruses and their therapy. Antiviral Research, 71, 397–403.

Halgren T. A. (1996). Merck molecular force field. I. Basis, form, scope, parameterization, and performance of MMFF94. Journal of Computational Chemistry, 17(5-6), 490–519.

Harrison, C. (2020). Coronavirus puts drug repurposing on the fast track. Nature Biotechnology, 38, 379–381.

King, M. V. (1958). Improved resolution of X-ray diffraction patterns of protein crystals at low temperature. Nature, 181, 263–264.

Liu, K., & Kokubo, H. (2017). Exploring the stability of ligand binding modes to proteins by molecular dynamics simulations: A cross-docking study. Journal of Chemical Information and Modeling, 57, 2514–2522.

MOE (2020, May 16). Molecular Operating Environment (MOE) 2019.0101, (Chemical Computing Group ULC, Montreal, QC, Canada). Retrieved from https://www.chemcomp.com/index.htm

Mullard, A. (2020). COVID-19 vaccines start moving into advanced trials. Nature Reviews Drug Discovery, 19, 435.

Owen, C. D., Lukacik, P., Strain-Damerell, C. M., Douangamath, A., Powell, A. J., Fearon, D., Brandao-Neto, J., Crawshaw, A. D., Aragao, D., Williams, M., Flaig, R., Hall, D. , McAuley, K. , Stuart, D. I., von Delft, F., & Walsh, M. A. (2020). COVID-19 main protease with unliganded active site.. RCSB Protein Data Bank (PDB) ID, 6Y84. Retrieved from https://www.rcsb.org/structure/6y84

Pillaiyar, T., Manickam, M., Namasivayam, V., Hayashi, Y., & Yung, S.-H. (2016). An overview of severe acute respiratory syndome-coronavirus (SARS-CoV) 3CL protease inhibitors: Peptidomimetics and small molecule chemotherapy. Journal of Medicinal Chemistry, 59, 6595–6628.

Protein Data Bank (2020, May 16). Retrieved from https://www.rcsb.org/

Ren, J.-l., Zhang, A.-H., & Wang, X.-J. (2020). Traditional Chinese medicine for COVID-19 treatment. Pharmacological Research, 155(104743), 1–2.

Robson, B. (2020). Computers and viral diseases. Preliminary bioinformatics studies on the design of a synthetic vaccine and a preventative peptidomimetic antagonist against the SARS-CoV-2 (2019-nCoV, COVID-19) coronavirus. Computers in Biology and Medicine, 119(103670), 1–19.

Sheahan, T. P., Sims, A. C., Leist, S. R., Schäfer, A., Won, J., Brown, A. J., Montgomery, S. A., Hogg, A., Babusis, D., Clarke, M. O., Spahn, J. E., Bauer, L., Sellers, S., Porter, D., Feng, J. Y., Cihlar, T., Jordan, R., Denison, M. R., & Baric, R. S. (2020). Comparative therapeutic efficacy of remdesivir and combination lopinavir, ritonavir, and interferon beta against MERS-CoV. Nature Communications, 11(222), 1–14.

Soga, S., Shirai, H., Kobori, M., & Hirayama, N. (2007). Use of amino acid composition to predict ligand-binding sites. Journal of Chemical Information and Modeling, 47, 400–406.

Wang, M., Cao, R., Zhang, L., Yang, X., Liu, J., Xu, M., Shi, Z., Hu, Z., Zhong, W., & Xiao, G. (2020). Remdesivir and chloroquine effectively inhibit the recently emerged novel coronavirus (2019-nCoV) in vitro. Cell Research, 30, 269–271.

Worldometer (2020, July 4). COVID-19 coronavirus pandemic. Retrieved from https://www.worldometers.info/coronavirus/

Zhang, T., He, Y., Xu, W., Ma, A., Yang, Y., & Xu, K.-F. (2020). Clinical trials for the treatment of Coronavirus disease 2019 (COVID-19): A rapid response to urgent need. Science China Life Sciences, 63, 774-776.

Molekularna dinamika ASC09, ritonavira, lopinavira i darunavira sa COVID-19 proteazom

Budimir S. Ilić[1]

1- Univerzitet u Nišu, Medicinski fakultet, Departman za hemiju, 18000 Niš, Srbija

Sažetak

Usled pojave nove infekcije SARS-CoV-2 (COVID-19) kao i nedostatka dokazane terapije, danas se koriste različite metode u pokušaju borbe protiv pandemije COVID-19. Mnoge od ovih metoda oslanjaju se na primenu već postojećih lekova koji su efikasni protiv sličnih virusnih infekcija ili ozbiljnih simptoma sličnih COVID-19. Nedavno određena kristalna struktura COVID-19 proteaze omogućila je povezivanje strukture proteaze sa aktivnostima supstanci. Interakcija ASC09, ritonavira, lopinavira i darunavira sa COVID-19 proteazom simulirana je korišćenjem modula Site Finder, molekularnog dokinga i molekularne dinamike (MD). Analiza MD trajektorija obezbedila je uvid u interakcije ligand/receptor, pružajući informacije o ključnim aminokiselinama receptora i frekvenciji kontakata ligand/receptor. Frekvencije kontakta i mape kontakata sugerišu da su za proučavane antivirusne lekove interakcije sa Gln 107, Pro 108, Gln 110 i His 246 odlučujući faktor u vezivanju lekova za proteazu COVID-19. Takođe, vodeće interakcije sa Arg 105, Phe 134, Glu 240, Thr 243, Asp 245 ili Phe 294 značajno doprinose različitom afinitetu vezivanja ispitanih lekova za COVID-19 proteazu.

Ključne reči: *COVID-19, molekularna dinamika, ASC09, ritonavir, lopinavir, darunavir*

Simulations de la dynamique moléculaire de l'ASC09, du ritonavir, du lopinavir et du darunavir avec la protéase COVID-19

Budimir S. Ilić[1]

1- Université de Niš, Faculté de médecine, Département de chimie18000 Niš, Serbie

Résumé

En raison de l'apparition de la nouvelle infection SARS-CoV-2 (COVID-19), ainsi que du manque de thérapie éprouvée, aujourd'hui s'emploient les diverses stratégies dans la lutte contre la pandémie de COVID-19. De nombreuses stratégies reposent sur l'usage des médicaments existants et sur leur mécanisme de fonctionnement, qui sont efficaces contre des infections virales similaires ou des symptômes graves ressemblants au COVID-19. La structure cristalline de la protéase du COVID-19 récemment déterminée a rendu possible une liaison entre la structure de la protéase et les activités des substances. L'interaction de l'ASC09, du ritonavir, du lopinavir et du darunavir avec la protéase COVID-19 a été simulée à l'aide du module Site Finder, de l'ancrage moléculaire et de la dynamique moléculaire (MD). L'analyse des trajectoires MD a fourni les empreintes digitales d'interaction ligand/récepteur, en donnant des informations sur les aminoacides cruciaux des récepteurs et la fréquence des contacts ligand/récepteur. Les fréquences des contacts et les cartes de contacts suggèrent que pour les médicaments antiviraux étudiés, les interactions avec Gln 107, Pro 108, Gln 110 et His 246 sont un facteur décisif dans l'affinité de liaison des médicaments pour la protéase COVID-19. De même, les interactions principales avec Arg 105, Phe 134, Glu 240, Thr 243, Asp 245 ou Phe 294 contribuent d'une manière significative à l'affinité de liaison différente des médicaments examinés pour la protéase COVID-19.

Mots-clés: COVID-19, dynamique moléculaire, ASC09, ritonavir, lopinavir, darunavir

Моделирование молекулярной динамики ASC09, ритонавира, лопинавира и дарунавира с протеазой COVID-19

Будимир С. Илич[1]

1-Университет в Нише, Медицинский факультет, Кафедра химии, г. Ниш, Сербия

Аннотация

В связи с появлением новой инфекции SARS-CoV-2 (COVID-19), а также из-за отсутствия проверенных методов лечения, в попытке борьбы с пандемией используются самые разные стратегии. Многие из этих методов основаны на использовании существующих лекарств и механизма их действия, которые эффективны либо против аналогичных вирусных инфекций, либо против серьезных симптомов, подобных COVID-19. Недавно определенная кристаллическая структура протеазы COVID-19 позволила выяснить взаимосвязи между структурой протеазы и активности веществ. Взаимодействие ASC09, ритонавира, лопинавира и дарунавира с протеазой COVID-19 моделировалось с помощью модуля Site Finder, молекулярной стыковки и молекулярной динамики (MD). Анализ траекторий МД предоставил представление о взаимодействиях лиганд / рецептор, объединив информацию о ключевых аминокислотах рецептора и частоте контактов лиганд/рецептор. Частота контактов и карты контактов предполагают, что взаимодействия с Gln 107, Pro 108, Gln 110 и His 246 являются решающим фактором в связывании лекарств и протеазы COVID-19, для исследуемых противовирусных препаратов. Однако ведущие взаимодействия с Arg 105, Phe 134, Glu 240, Thr 243, Asp 245 или Phe 294 также вносят значительный вклад во взаимодействие лиганд/рецептор и, в частности, дифференцируют их аффинность связывания с протеазой COVID-19.

Ключевые слова: COVID-19, Молекулярная динамика, ASC09, Ритонавир, Лопинавир, Дарунавир

Molekulardynamische Simulationen von ASC09, Ritonavir, Lopinavir und Darunavir mit der COVID-19-Protease

Budimir S. Ilić[1]

1- Universität Niš, Medizinische Fakultät, Department für Chemie, 18000 Niš, Serbien

ABSTRAKT

Aufgrund des Auftretens einer neuen SARS-CoV-2-Infektion (COVID-19) und des Mangels an einer bewährten Therapie werden unterschiedliche Methoden zur Bekämpfung der COVID-19-Pandemie eingesetzt. Viele dieser Methoden beruhen auf der Verwendung der schon bestehenden Medikamente und dem Mechanismus ihrer Wirkung, die gegen ähnliche Virusinfektionen oder schwerwiegende, dem COVID-19 ähnliche, Symptome wirksam sind. Die kürzlich aufgeklärte Kristallstruktur der COVID-19-Protease ermöglichte es, die Struktur der Protease mit den Aktivitäten von Substanzen zu verknüpfen. Die Wechselwirkung von ASC09, Ritonavir, Lopinavir und Darunavir mit COVID-19-Protease wurde unter Verwendung des *Site Finder*-Moduls, des molekularen Andockens und der Molekulardynamik (MD) simuliert. Die Analyse der MD-Trajektorien hat Einblicke in die Ligand/Rezeptor-Interaktion ermöglicht und Informationen über die wichtigsten Aminosäuren von Rezeptoren und die Häufigkeit der Ligand/Rest-Kontakte geliefert. Die Kontaktfrequenzen und die Kontaktmappen legen nahe, dass die Wechselwirkungen mit Gln 107, Pro 108, Gln 110 und His 246 der entscheidende Faktor bei der Bindung der Arzneimittel an die COVID-19-Protease für alle untersuchten antiviralen Arzneimittel sind. Die führenden Wechselwirkungen mit Arg 105, Phe 134, Glu 240, Thr 243, Asp 245 oder Phe 294 tragen ebenfalls wesentlich zu unterschiedlichen Bindungsaffinitäten der untersuchten Arzneimittel an die COVID-19-Protease bei.

Schlüsselwörter: COVID-19, Molekulardynamik, ASC09, Ritonavir, Lopinavir, Darunavir

Chemia Naissensis, Vol 3, Issue 1, POPULAR SCIENTIFIC ARTICLE, 171-177

Lipinski's rule of five, famous extensions and famous exceptions

Violeta Ivanović[1], Miroslav Rančić[1], Biljana Arsić[1*], Aleksandra Pavlović[1]

1- University of Niš, Faculty of Science and Mathematics, Department of Chemistry, Višegradska 33, 18000 Niš, Republic of Serbia

Violeta Ivanović: violeta.ivanovic@pmf.edu.rs
Miroslav Rančić: miroslav.rancic@pmf.edu.rs
[*]Biljana Arsić: biljana.arsic@pmf.edu.rs
Aleksandra Pavlović: petra1974@yahoo.com

ABSTRACT

Mathematical models show qualitative and quantitative dependencies between the structure, physico-chemical properties and activities of the investigated compounds. There are different rules for the prediction of good bioavailability, and one of the most well-known is the Lipinski rule. The rule is related to the molecular properties important for a drug's pharmacokinetics in the human body: absorption, distribution, metabolism, and excretion (ADME). In addition to the Lipinski rule, there are reported different combinations of criteria that are important predictors of permeability. An additional rule was proposed by Veber. He compared the oral bioavailability of the compound and the permeability of the compound with the molecular flexibility.

Keywords: absorption, acceptors, biological activity, donors, exceptions

Introduction

Most scientific studies today are focused on the discovery and synthesis of biologically active compounds, the study of their action, efficiency and possible toxicity to the environment. In order to save time and money, before the synthesis of a new bioactive compound, the application of various mathematical models establishes qualitative and quantitative dependencies between its structure, physico-chemical properties and activities. The molecular descriptor most commonly used to predict the potential of a compound as bioactive is lipophilicity. According to IUPAC, lipophilicity represents the affinity of molecules or parts of molecules towards the lipophilic environment. In addition to lipophilicity, the rules of good bioavailability are applied for the theoretical assessment of the existence of biological activity of compounds, among which the most well-known is the Lipinski rule (Apostolov and Vastag, 2017).

Once in the body, the pathway of a biologically active compound is determined by its absorption, distribution, metabolism, excretion and toxicity (ADMET). To evaluate and optimize the action and efficiency of a bioactive compound, it is necessary to know its pharmacokinetics. Since most bioactive substances are not administered intravenously, the pharmacokinetic predictor that may indicate the level of intestinal absorption is the human effective permeability in the jejunum. Molecules with higher lipophilicity have better permeability through the phospholipid bilayer of enterocytes, so the level of permeability is directly conditioned by the lipophilicity of the molecules.

The activity of the compound in the central nervous system is conditioned by its passage through the blood-brain barrier. The blood-brain barrier (BBB) is a mechanism that controls the passage of substances from the blood into the cerebrospinal fluid, and thus into the brain and spinal cord. The value of the pharmacokinetic parameter, log BBB, indicates the possibility of using a molecule as neurologically active. The early stages of modern design of a biologically active compound require the study of its impact on the environment, which is most often reflected in the assessment of its danger to various test organisms (Apostolov and Vastag, 2017).

Lipinski rule of five

In order to advance the discovery and development of new drugs, great efforts are being made to evaluate the similar ‘drug-like’ properties of molecules in the early stages of the discovery-research process. There are different approaches to solve this problem, but the simplest and most used approach is developed by Chris Lipinski and his colleagues at Pfizer, which is generally referred either as the Lipinski Rules or the Rule of Five (ROF) (Petit et al., 2012).

Rule of five (ROF) is a rule of thumb to evaluate drug likeness or determine if a chemical compound with a certain pharmacological or biological activity has properties that would make it a likely orally active drug in humans(Lipinski et al., 1997).

The biologically active molecule must implement five conditions to be potentially used as a drug for oral administration. Poor absorption or permeation are most likely if:

- Molar mass >500,
- Number of H-bond acceptors >10,
- Number of H-bond donors > 5,
- LogP> 5 (or MlogP>4.15)

(Lipinski et al.,1997).

Based on the ROF, the rating of an orally active drug is between „0“ and „4“ which means that a potential drug has no more than one violation of the exposed criteria. However, Lipinski points out that such molecules should not be completely removed from further consideration; it is known that many drugs do not undergo ROF (Petit et al., 2012).

Although the rule of five has a wide application, there are certain deficiencies. The two major weaknesses are the equal weight given to each of the rules and the sharp boundary that marks the violation of a given rule. Another disadvantage of this rule is that it does not include natural and biological compounds. ROF does not incorporate criteria relevant to metabolism.

Lipophilicity

Lipophilicity, a description of the ability of a molecule to partition into octanol versus water, is a physicochemical property commonly considered to be highly relevant to the rate of absorption. Lipophilicity is defined as the logarithm of the ratio of drug that partitions into organic phase to that in aqueous phase, and is referred as logP. While this property can be physically measured in various ways, numerous methods for computation of logP exist, each of which has its own advantages and shortcomings. For example, clogP is a method that computes the lipophilicity of a molecule by computing the sum of the logP of the fragments that comprise it. These fragmentary values were generated by least-squares fitting to a training set, and include correction factors for electronic and steric effects. The cLogP method works well for molecules that possess typical drug-like functional groups, and fragments that are closely related to the training set. An atomic-based prediction of logP (AlogP, MlogP) utilizes the atomic contributions of each atom in the molecule, also fit to a training set with experimentally determined partition coefficients. During the development of the Rule of Five, Lipinski compared the use of the fragment-based cLogP computation to that of the atomic-based MlogP parameter. While the cLogP method produced highly accurate results in classes of compounds where all the fragments of a given compound were defined within the training set,

the rule-based Moriguchi method always provided an answer, even at the expense of accuracy. Therefore, within a series of related compounds (generated within a medicinal chemistry optimization program), the more-accurate cLogP is typically used, and, for assessment of lipophilicity of large collections, the more general MlogP computation was applied.

M log P: log P by the method of Moriguchi

The calculation of log P *via* the method of Moriguchi begins with a straightforward counting of lipophilic atoms (all carbons and halogens with a multiplier rule for normalizing their contributions) and hydrophilic atoms (all nitrogen and oxygen atoms). The Moriguchi method applies 11 correction factors: four that describe the hydrophobicity and seven that describe the lipophilicity (Lipinski et al., 1997).

The correction factors that describe hydrophobicity are:

1. UB (the number of unsaturated bonds except those in nitro groups);
2. AMP (the correction factor for amphoteric compounds): an α amino acid structure adds 1.0 to the AMP parameter, while each amino-benzoic acid and each pyridine carboxylic acid adds 0.5;
3. RNG: it has the value of 1.0 if the compound has any rings other than benzene-based with hetero-aromatic, or hydrocarbon rings;
4. QN (the number of quaternary nitrogen atoms).
5. The seven correction factors that describe lipophilicity are:
6. PRX (a proximity correction factor for nitrogen and oxygen atoms that are close to one another topologically): 1) addition of 2.0 for each two atoms directly connected and also for each two atoms connected *via* a carbon, sulfur, or phosphorus atom, 2) addition of 1.0 unless one of the two bonds connecting the two atoms is a double bond; 3) addition of an extra 1.0 for each carboxamide group, and for each sulfonamide group2.0;
7. HB: 1.0 if there are structural features that will make an internal hydrogen bond;
8. POL (the number of heteroatoms connected to an aromatic ring by only one bond or the number of carbon atoms attached to two or more heteroatoms which are also attached to an aromatic ring by only one bond);
9. ALK: 1.0 if the molecule contains only carbon and hydrogen atoms and not more than one double bond;
10. NO_2 (the number of nitro groups);
11. NCS: 1.0 for each isothiocyanate group and 0.5 for each thiocyanate group;
12. BLM: 1.0 if there is a beta lactam ring in the molecule (Lipinski et al., 1997).

Hydrogen-Bond Donors

In addition to high molecular weight and lipophilicity, large numbers of hydrogen-bond donor groups in a compound can reduce the ability of a molecule to permeate a membrane bilayer. Compounds that possess a large number of hydrogen-bond donors will partition into a strongly hydrogen-bonding solvent (such as water) rather than into the lipophilic environment present in a cellular membrane. The hydrogen bonding ability of functional groups in a molecule might be measured by simple accounting of N-H and O-H bonds in a molecule (Lipinski et al., 1997).

Hydrogen-Bond Acceptors

For the same reason that hydrogen-bond donors reduce the permeability of compounds into lipophilic environments, hydrogen-bond acceptors affect permeability by interacting favorably with a strongly hydrogen bonding solvents such as water. Again, while hydrogen-bonding parameters can be computed, Lipinski and coworkers observed that simply summing the numbers of nitrogen and oxygen atoms in the molecule serves as a good surrogate to correlate to oral bioavailability (Lipinski et al., 1997).

Variations of the rule of five

Recognizing the value of such retrospective analyses of drug candidates as originally performed and formalized by Lipinski, others have reported different combinations of criteria that are important predictors of permeability. An additional rule was proposed by Veber. He compared the oral bioavailability of the compound and compared the permeability of the compound with the molecular flexibility, which can be described in terms of the number of rotatable bonds. Estimation of the number of rotatable bonds allows correlation of permeability properties without consideration of molecular weight. It has been concluded that compounds with more than ten rotatable bonds generally have poor permeability. Also, Veber concluded that the high polar surface area affects the reduction of permeability (Pollastri, 2010).

Veber's flexibility rules complement the rule of five:

- The product must have no more than 5 hydrogen bond donor sites,
- It must have no more than 10 hydrogen bond acceptor sites,
- Its molecular mass must be less than 500 Daltons,
- Its molecules must contain between 20 and 70 atoms (50 on average),
- Its polar surface area must be smaller than 140 $Å^2$.

These criteria can predict intestinal absorption of a product and its ability to pass through the blood–brain barrier.

Linking computed molecular descriptors to central nervous system (CNS) permeability was proposed by Ajay. Computed properties, including molecular weight, molecular branching, hydrogen bonding, aromatic density and logP, were evaluated and compared to lists of drugs for which data about CNS activity were available. Molecular weight, degree of branching, number of rotatable bonds, and number of hydrogen bonds showed the highest correlation to CNS permeability, such that if these values are increased, CNS exposure is decreased. Similarly, increasing aromatic density, numbers of H-bond donors, or cLogP values predicted compounds are with higher CNS permeability (Pollastri, 2010).

A variation of ROF known as rule three, is used to display small fragments and for screening set design, that desirable fragments possess a:

- molecular weight <300,
- fewer than 3 hydrogen bond donors and acceptors,
- cLogP$\leq$ 3.

The rule three also contains a variation of the Veber's criterion, so that the desirable fragments have three or less rotating bonds and a polar surface area $\leq$ 60 $Å^2$. These data imply that a rule of three could be useful when constructing fragment libraries for efficient lead discovery (Congreve et al., 2003).

The rule of five exceptions

The 'rule of 5' is based on a distribution of calculated properties among several thousand drugs. Therefore, by definition, some drugs will lie outside the parameter cutoffs in the rule. Very small number of therapeutic categories account for most of the USAN (United States Adopted Name) drugs with properties falling outside Lipinski rule. These orally active therapeutic classes are:

- antibiotics,
- antifungals,
- vitamins,
- cardiac glycosides.

These compounds have structural features that allow the drugs to act as substrates for naturally occurring transporters. If such classes are excluded from the USAN library, there are very few examples of compounds remaining that violate the ROF (Lipinski et al., 2001).

References

Apostolov S., & Vastag D. (2017). Proučavanje lipofilnosti potencijalno biološki aktivnih derivata cijanoacetamida. Journal of Engineering & Processing Management, 9 (1), 01-09.

Congreve, M., Carr, R., Murray, C., & Jhoti, H. (2003). A "rule of three" for fragment-based lead discovery? Drug Discovery Today, 8, 876-877.

Lipinski, C. A., Lombardo F., Dominy B. W., & Feeney P. J. (1997). Experimental and computational approaches to estimate solubility and permeability in drug discovery and development settings. Advanced Drug Delivery Reviews, 23, 3-25.

Lipinski, C. A., Lombardo, F., Dominy, B. W., & Feeney, P. J. (2001). Experimental and computational approaches to estimate solubility and permeability in drug discovery and development settings. Advanced Drug Delivery Reviews, 46, 3–26.

Petit, J., Meurice, N., Kaiser, C., & Maggiora, G. (2012). Softening the Rule of Five—where to draw the line? Bioorganic and Medicinal Chemistry, 20,5343–5351.

Pollastri, M. (2010). Overview on the Rule of Five. Department of Chemical Biology, Northeastern University, Boston, Massachusetts, 49:9.12.1-9.12.8.

Lipinski pravilo pet, poznata proširenja i poznati izuzeci

Violeta Ivanović[1], Miroslav Rančić[1], Biljana Arsić[1], Aleksandra Pavlović[1]

1- University u Nišu, Prirodno-matematički fakultet, Departman za hemiju, Višegradska 33, 18000 Niš, Republic of Serbia

Sažetak

Matematički modeli pokazuju kvalitativne i kvantitativne zavisnosti između strukture, fizičko-hemijskih osobina i aktivnosti ispitivanih jedinjenja. Postoje različita pravila za predviđanje dobre biodostupnosti, i jedno od najpoznatijih je Lipinski pravilo. Pravilo se odnosi na molekulske osobine važne za farmakokinetiku leka u ljudskom telu: apsorpcija, raspodela, metabolizam i ekskrecija (engl. ADME). Pored pravila Lipinskog, postoje različite kombinacije kriterijuma koje su važni prediktori propustljivosti. Jedno dodatno pravilo je predloženo od strane Vebera. On je upoređivao oralnu biodostupnost jedinjenja i propustljivost jedinjenja sa molekulskom fleksibilnošću.

Ključne reči: apsorpcija, akceptori, biološka aktivnost, donori, izuzeci

La règle des cinq de Lipinski, des extensions célèbres et des exceptions célèbres

Violeta Ivanović[1], Miroslav Rančić[1], Biljana Arsić[1], Aleksandra Pavlović[1]

1- Université de Niš, Faculté des sciences naturelles et des mathématiques, Département de chimie, Višegradska 33, 18000 Niš, République de Serbie

Résumé

Les modèles mathématiques montrent des dépendances qualitatives et quantitatives entre la structure, les propriétés physico-chimiques et les activités des composés étudiés. Il existe de différentes règles pour prédire une bonne biodisponibilité et l'une des plus connues est la règle de Lipinski. La règle se rapporte aux propriétés moléculaires importantes pour la pharmacocinétique du médicament dans le corps humain, à savoir : absorption, distribution, métabolisme et excrétion (angl. ADME). À part de la règle de Lipinski, il y a des combinaisons variées des critères qui sont des prédicteurs importants de la perméabilité. Une règle supplémentaire a été proposée par Veber qui comparait la biodisponibilité orale du composé et la perméabilité du composé à la flexibilité moléculaire.

Mots-clés: absorption, accepteurs, activité biologique, donateurs, exceptions

Правило пяти Липинского, известные расширения и известные исключения

Виолета Иванович[1], Мирослав Ранчич[1], Биляна Арсич[1], Александра Павлович[1]

1- *Университет в Нише, Естественно-математический факультет, Кафедра химии, Вишеградска 33, 18000 Ниш, Сербия*

Аннотация

Математические модели показывают качественные и количественные зависимости между структурой, физико-химическими свойствами и активностью исследуемых соединений. Существуют разные правила для прогнозирования хорошей биодоступности, среди которых как одно из самых известных выделяется правило Липинского. Правило относится к молекулярным свойствам, важным для фармакокинетики лекарственного средства в организме человека: абсорбция, распределение, метаболизм и экскреция (англ. ADME). В дополнение к правилу Липинского существуют различные комбинации критериев, являющиеся важными предикторами проницаемости. Дополнительное правило было предложено Вебером. Он сравнил пероральную биодоступность соединения и проницаемость соединения с молекулярной гибкостью.

Ключевые слова: абсорбция, акцепторы, биологическая активность, доноры, исключения

Lipinskis Fünferregel, berühmte Erweiterungen und berühmte Ausnahmen

Violeta Ivanović[1], Miroslav Rančić[1], Biljana Arsić[1], Aleksandra Pavlović[1]

1- Universität Niš, Fakultät für Naturwissenschaften und Mathematik, Abteilung für Chemie, Višegradska 33, 18000 Niš, Republik Serbien

ABSTRAKT

Mathematische Modelle zeigen qualitative und quantitative Abhängigkeiten zwischen Struktur, physikalisch-chemischen Eigenschaften und Aktivitäten der untersuchten Verbindungen. Es gibt verschiedene Regeln für die Vorhersage einer guten Bioverfügbarkeit, und eine der bekanntesten ist die Lipinski-Regel. Die Regel bezieht sich auf die molekularen Eigenschaften, die für die Pharmakokinetik eines Arzneimittels im menschlichen Körper wichtig sind: Absorption, Distribution, Metabolismus und Elimination (ADME). Zusätzlich zur Lipinski-Regel gibt es verschiedene Kriterienkombinationen, die wichtige Prädiktoren für die Permeabilität sind. Eine zusätzliche Regel wurde von Veber vorgeschlagen. Er verglich die orale Bioverfügbarkeit der Verbindung und die Permeabilität der Verbindung mit der molekularen Flexibilität.

Schlüsselwörter: Absorption, Akzeptoren, biologische Aktivität, Donatoren, Ausnahmen